HEADQUARTERS

AIR FORCE SPECIAL WEAPONS CENTER

AIR RESEARCH AND DEVELOPMENT COMMAND

KIRTLAND AIR FORCE BASE, NEW MEXICO

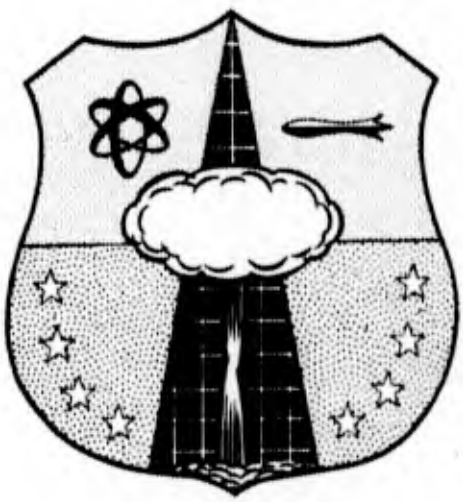

Technical Report

LUNAR RESEARCH FLIGHT STUDIES

ASTROPHYSICAL MEASUREMENTS
Vol I

Montgomery H. Johnson
Irving H. Blifford, Jr.
Thor A. Bergstralh
Ralph Havens
Dinsmore Alter

AERONUTRONIC
A Division of Ford Motor Company
Newport Beach, California

15 July 1959

HEADQUARTERS
AIR FORCE SPECIAL WEAPONS CENTER
Air Research and Development Command
Kirtland Air Force Base, New Mexico

Major General Charles M. McCorkle
Commander

Colonel Carey L. O'Bryan, Jr.
Deputy Commander

Colonel Leonard A. Eddy
Director, Research Directorate

SWC
TR-
59-37
Vol. I

LUNAR RESEARCH FLIGHT STUDIES

ASTROPHYSICAL MEASUREMENTS

Montgomery H. Johnson Thor A. Bergstralh
Irving H. Blifford, Jr. Ralph Havens
Dinsmore Alter

AERONUTRONIC
A Division of Ford Motor Company
Newport Beach, California

15 July 1959

Research Directorate
AIR FORCE SPECIAL WEAPONS CENTER
Air Research and Development Command
Kirtland Air Force Base
New Mexico

Approved:

DAVID R. JONES
Lt Col USAF
Chief, Physics Division

LEONARD A. EDDY
Colonel USAF
Director, Research Directorate

Project Number 7811
Task Number 78046

ABSTRACT

The astrophysical measurements which can be carried out in lunar probes and satellites are considered. The background information available as to lunar surface characteristics and composition is discussed.

The areas covered in some detail include plastic reflectors for tracking, magnetic field measurements, infra-red measurements, lunar radioactivity, lunar fluorescence, lunar atmosphere, and solar winds. Background information on possible gaseous emission from the moon, and photography of the moon are covered in appendices.

PUBLICATION REVIEW

This report has been reviewed and is approved.

CAREY L. O'BRYAN, JR.
Colonel USAF
Deputy Commander

TABLE OF CONTENTS

LIST OF ILLUSTRATIONS

LIST OF TABLES

SUMMARY

LUNAR RESEARCH FLIGHT STUDIES

ASTROPHYSICAL MEASUREMENTS

A. PURPOSE

The development of ballistic missiles has reached the stage where research flights to the moon can be considered practicable. This imminent capability warrants a detailed consideration of the reasons for attempting such research and the nature of the experimental studies which would be most rewarding. The primary purpose of this study has been to outline in a general way the basic scientific problems and questions concerning the moon and particularly to indicate how a lunar research vehicle may be applied to such investigations. It has been our intention also to attempt to outline such areas of research requiring additional study or where increased emphasis may be desirable. A number of specific experiments are discussed with the hope of showing in some detail the scientific problems involved.

B. CONCLUSIONS

The general conclusion of this study is that the use of lunar satellite and impacting research vehicles can provide valuable data as to lunar characteristics and cis-lunar environment with existing instrumental techniques. Only a restricted number of investigation areas have been considered in any detail. These studies lead to the following conclusions

1. An optical system for tracking a lunar research vehicle in flight can provide valuable information for the flights themselves and for improving our present knowledge of the astronomical and geophysical constants. The use of reflectorized plastic balloons inflated and launched in sequence during the cis-lunar flight appears to be a practicable method for making such measurements. A 30 foot diameter balloon, reflectorized with a 2000 Å coating of aluminum will be visible at lunar distances with a 12 inch telescope. Survival of the balloons in the cis-lunar environment for adequate time periods appears likely (Section 2).

2. The measurement of the magnetic field existing between the earth and the moon will provide valuable data with reference to magnetic field sources, and as to the sources and behavior of cosmic ray particles. A measurement of the magnetic field of the moon will provide information as to terrestrial and lunar origins. Instrumentation capable of accurate measurements is available in the art. (Section 3).

3. Measurement of lunar infra-red radiation by means of lunar satellites can provide information as to the lunar surface temperatures, sub-surface temperatures, dust layer thickness, and surface characteristics. Measurement in the infra-red from the earth is difficult, and for nighttime temperatures probably impossible. Instrumentation designs based on presently available equipment appear feasible (Section 4).

4. The measurement of the lunar radioactivity can provide valuable information about the composition of the moon's crust. Comparison of the measured activity with that of terrestrial and meteoritic sources can shed light on the questions of lunar origin. Measurements of sufficient sensitivity for the weakest known sources (stony meteorite) appear feasible (Section 5).

5. There is a possibility of detecting fluorescence of lunar crust materials from research vehicles if additional background information can be obtained from earth-based observations. Fluorescence measurements can aid in identification of the surface materials and if specific areas exhibit fluorescence may possibly be useful for guidance (Section 6).

6. There are theoretical and experimental reasons for believing that the moon possesses a very tenuous atmosphere consisting mainly of argon atoms from the radioactive decay of potassium. Another source

of lunar atmosphere may be atoms sputtered from the surface by high energy particles. These possibilities are discussed in Section 7. A method for detection of argon in the lunar atmosphere is discussed in Section 4 of Volume II.

7. Evidence has been accumulating as to the existence in interplanetary space of a highly ionized gas which represents an extension of the solar corona. There are possible destructive effects of such "solar winds" on thin films and instrumentation now contemplated for use in space research. The values of solar wind particle densities and velocities are in dispute. Without additional data as to these quantities and additional experimental information as to the sputtering of surfaces by particles of the postulated energies, the probable damage effects cannot be assessed. Some seemingly paradoxical effects of solar winds on meteorites are discussed. (Section 8).

8. Laboratory experiments may have a place in the simulation of various structural features apparent from lunar observation. Mechanisms responsible for the creation of lunar surface features such as craters, domes, terraces, etc., may be studied in this way (Section 9). Additional observation of the moon from the earth using the best of photographic and spectrographic techniques will provide valuable background information for future lunar exploration. The techniques, background and some of the results of such programs are discussed in Appendices A and B.

C. RECOMMENDATIONS

On the basis of the conclusions stated above it is recommended that measurements of the magnetic fields, radioactivity and infra-red characteristics of the moon be carried out in any lunar probes or satellites. A tracking system incorporating the balloon reflectors warrants serious consideration for the improvement of future landing potential, and for improvement of astrophysical and geophysical constants. Increased emphasis should be placed on observational astronomy from the earth for the purpose of obtaining additional spectrographic, absolute brightness, and possible fluorescence data.

D. BACKGROUND

The moon has for centuries excited the interest of man. Knowledge relating to its surface and sub-surface materials, information and origins can be of extreme importance in relation to the origins of the earth and other planets. As the nearest space station, exploration of the moon provides an ideal development of techniques for space exploration.

E. DISCUSSION

The body of this report, Sections 1 through 9 which follow, comprises the discussion

SECTION 1

INTRODUCTION

1.1 GENERAL BACKCROUND

In order to place in perspective the discussion of lunar experimentation it may be of value to discuss very briefly the information presently available concerning the moon Except for knowledge derived from planetary motion, most of the ideas concerning the lunar surface have been deduced from telescopic observation and include a fair measure of subjective reasoning

The available information of a factual nature is listed in Table 1-1.

The lunar surface has generally been considered to be very old and essentially unchanging However, recent observations have raised questions as to the correctness of these beliefs The scientific literature contains references to changes which have taken place and within the last few years photographic and spectrographic measurements have indicated the possibility of the evolution of gas and possibly volcanic activity. The present status of knowledge on this subject is reviewed in Appendix A

There is no evidence of water, although water may be an internal constituent of the rocks From the moments of inertia it may be concluded that the moon has been "rigid" since formation The chemical composition of the crust is unknown

TABLE 1.1

LUNAR DATA

Air Density	10^{-6} - 10^{-13} *	
Length of day	29.53 *	Mean solar day
Percent of surface visible from earth	41	always
	18	sometimes
	41	never
Gravitational attraction	1/6 *	
Surface Temperature	101° C	Subsolar point
	-140° C	Night
Mean diameter	3476 km	
Distance from earth	221,463 miles	Minimum
	252,710 miles	Maximum
	238,860 miles	Mean
Mass	0.01226 *	
Velocity of escape	2.38 km/sec	
Mean density	3.33	
Albedo	0.07 (Avg)	
Color	None	
Position of earth in lunar sky	± 8° from mean	

* Values are compared with those for earth.

Various aspects of the lunar surface are discussed very briefly in the following. A fairly detailed discussion of lunar surface characteristics can be obtained from references 1, and 3 through 7 inclusive at the end of the section.

1.1.1 Surface Features of the Moon

Maria

The maria[1] are great comparatively smooth areas which appear to have been molten rock. They are smooth only by comparison to other areas and commonly are bounded by high cliffs. They are much darker than the general surface and have an albedo of about 0.04 to 0.05 The maria comprise about one-third of the lunar surface and are covered by dust. Although most students believe the layer to be thin, perhaps less than one cm., Gold[2] has proposed a theory which predicts dust hundreds of meters thick. Some craters are observed of which a few appear to be older than the maria, as for example Archimedes in the Mare Imbrium. Others like Aristillus, also Imbrium, are newer than the mare. Many "ghosts" of earlier features are apparent.

There has been some controversy regarding the formation of the maria. Some authors believe that the rock was melted by asteroidal impact; an explanation which seems probable for the central third of Mare Imbrium. Very likely others are collapse phenomena possibly resulting from triggering impacts.

Rough Surface

In general the rough surface has an albedo two or three times that of the maria although there are a few dark areas. It exhibits bombardment, volcanic, subsidence and mixed features, with much of the area covered by crater-like formations.

Peculiar Features

These are the features[3] which do not fit well into general categories, and perhaps only the valleys are important. The broad valleys are probably graben-like. There are thousands of very narrow ones usually moderately deep with steep walls with lengths of 200 miles or more. They are not found in the central parts of the maria or very rough areas but are very common near shorelines. These rills and clefts will interfere seriously with surface travel.

Mountain Walled Plains

The typical walled plains[4] are 50 to 150 miles in diameter and characteristically have little or no external wall. Their internal walls however are not circular but tend toward square, rectangular or especially hexagonal shape and are discontinuous. Such plains are found only in mountainous areas. Their floors tend toward smoothness; the large ones resembling small maria. They have no system of rays and seldom have central peaks. Scarps and lines of small craters sometimes are common boundaries for adjoining plains with many on a rather smooth floor. They become almost invisible under a high sun and only the shadows make them conspicuous. The rock inside and on the walls is similar to that outside. They appear to be the result of graben-like collapse perhaps triggered by impact, rather than of explosive origin.

The Explosion Craters

The explosion craters[5] have definite external walls and some brighten very much under a high sun. Others, such as Eratosthenes, almost disappear when shadows are short. In some instances, the inner walls exhibit terraces, and craterlets commonly are found around the rims of all except the smaller craters. Unlike the typical mountain walled plains, which are found only in mountainous areas, these craters exist in all sorts of terrain. Many lines of craterlets exist on their outer walls and in the neighboring areas and often form numerous rills or clefts. Most commonly the clefts tend to be radial to the great explosion, although some clefts are found to point in other directions or even to follow curved loci. Some of the outer slopes of explosion craters exhibit valleys which give at least a casual impression of having been formed by erosion. Aristillus is an excellent example. Central mountains or groups of hills are common to the craters although rare within the typical walled plains. The explosion craters exhibit an approach toward circularity while the rims of the mountain walled plains definitely are polygons.

The largest craters that brighten under a high sun probably were initially of meteoritic or asteroidal origin, but assumed their present form from subsequent volcanic action, and the small craters that so brighten were apparently formed by meteoritic impact. Quite a number of nonbrightening craters, which exhibit bright craterlets, seem to be volcanic, but the action may have been initiated by meteoritic shock. The large nonbrightening explosion craters

probably are mostly volcanic, although it is at present impossible to be certain in the case of any particular example. The craters found on the Iridum Highlands, the Alps, the Caucasus, and the Apennines are mostly volcanic.

The Domes and Small Craters

Many, perhaps all, of the craterlets[6] have external walls and lines of craterlets are common. Some are composed both of craters and of domes. Sometimes the lines are curved and form complex patterns. Craterlets in these lines do not brighten to a starlike appearance under a high sun. Isolated craterlets are common on the mare floors. They exhibit, in general at least, an appearance of having floors deeper than the surrounding mare. The typical isolated mare floor craterlets have the same general appearance as have the domes, except for the opening in the top and seem to be collapsed domes. Small craters are common around the rims of large craters and of mountain walled plains.

More than a thousand craterlets exist in the Copernicus area and at least hundreds near Tycho. Some of these craterlets brighten very much under a high sun and become starlike, a phenomenon that is observed in the cases of Tycho, Copernicus, and others of the larger craterlike formations. Other craterlets tend to disappear, and many of them brighten moderately. In many cases lines of craterlets have coalesced to form valleys. Careful examination with large instruments reveals signs of craterlets in many, perhaps in the majority, of the rills or clefts. Occasionally even fairly large craters form a line, a beautiful example being the north-and-south line that touches the western wall of Pitatus. An arc of craterlets may enclose a partially sunken area. Excellent examples may be found south of Hell Plain and in the northwestern part of Lexell. Craterlets are also found in the mountain regions. Many small craters can be observed on the Apennines under favorable conditions; larger craterlets are observable on the Sinus Iridum Highlands, and others can be seen in the Alps and the Caucasus regions.

The Lunar Rays

Lunar rays[7] are brightish streaks which can be seen in connection with craters that brighten under a high sun and which reappear at the same phase each month. Long rays are complex and often are observed to progress from one crater to another. In systems connected with the larger rings there is a tendency for the longer rays

to be tangent to the rings. At first glance, Kepler would appear to be an exception to the rule, but careful observation shows that some of the radial spokes are composed of two converging tangential rays from opposite sides of the ring. In other instances, a single ray can be traced back to tangency. As in the system of Furnerius, rays often issue from small, intensely bright rings on, or near, large ones.

Usually rays are seen only at the general level of the surface. This may not necessarily describe the whole situation because elevations are apt to be brighter than the surrounding country. Large rays are composite and are composed of small, dagger-like rays, radial to the associated crater, while short rays are associated directly with crater-like formations which brighten under a high sun. Frequently craters that brighten have tiny ray systems, and some of these ray systems combine to form the complex principal rays of such craters as Tycho and Copernicus. The rays appear to be a type of surface marking and lie along cracks which themselves are not visible. The rays may be due to dust from gases that have escaped from the cracks or a staining of the rocks by such gases.

1.1.2 Origin and Evolution

It appears most probable that the moon was formed as a separate planet and that it was rigid when it first approached the earth. This origin is indicated by its moments of inertia, its orbital and equatorial constants and the mixed character of its surface features.

Probably as it approached close to the earth tidal forces disrupted its surface badly and heated it a great deal but did little to the deep volume. This tidal friction was sufficient to change its orbit with respect to the earth from hyperbolic to a stable ellipse. Since that time tidal forces have followed classical theory and forced the two bodies farther apart.

1.2 LUNAR RESEARCH PROGRAM

1.2.1 General Program

Lunar research can be carried out in three broad phases:

1) from the earth,

2) through the use of research vehicles and lunar satellites,

3) by landing instruments on the moon, and finally,

4) by manned landings.

In addition to experiments directed specifically toward the moon itself, lunar research vehicles can perform a number of investigations of a geophysical or astrophysical nature.

Greenfield has presented at a meeting of the Lunar and Planetary Exploration Colloquium a list of possible experiments to be performed in a program of lunar measurements. Obviously not all of the investigations were of equal merit and therefore some criteria for determining the time sequence and desirability were necessary. In a subsequent meeting of the Colloquium the experiments were arranged in three categories which were based mainly on contamination, and requirement for knowledge gained from prior experiments. A somewhat different grouping has been adopted for the purpose of this report.

In any experiment involving contact with the lunar surface there always will be the risk of contamination. Either radioactive or biological contamination is undesirable, at least until certain preliminary investigations can be carried out. However the surface area of the moon is very great and an inordinate fear of contamination should not be allowed to inhibit unreasonably all lunar experimentation, particularly where the possibility of wide-spread distribution of the contaminant is negligible. The state of the art will no doubt be the determining factor in many of the suggested investigations.

1.2.2 Experimentation from the Earth

Table 1.2-1 lists several areas in which experimentation can be profitably carried out from the earth.

TABLE 1.2-1

EXPERIMENTS TO BE PERFORMED FROM THE EARTH

A. Photographic and photometric observation in different wavelength regions

B. Laboratory experiments on hypothetical lunar materials

C. Studies of terrestrial geology as applied to lunar features

D. Laboratory studies of closed ecological cycles as applied to man as well as other biological studies

E. Spectrographic and polarigraphic measurements

Although the moon has been studied by observational techniques for many years, there are important regions where information is lacking or out-dated. Therefore an intensive program of experimentation from terrestrial locations is desirable and may even be a necessary preliminary to vehicular research. Some of the more important investigations are described in the following.

Direct Photography

This program will involve a long detailed search with a large telescope at all possible phases. Instead of pairs, as have been obtained (1-7), three plates in different parts of the spectrum should be secured at each observation. Photographs should be made also in polarized light. One complete observation will require from three to nine exposures. Use of a blink type scanner will allow studies in extreme detail.

Appendix B contains a comprehensive survey of the problem of lunar photography including historical notes.

Photometry

There is no satisfactory scale of brightness for lunar features. Accurate knowledge of relative brightnesses is essential in any program to determine possible lunar changes. A photometric program also will have much value in general studies of the nature of the surface. It would be desirable to measure by modern photometric equipment at least

one hundred of the most important areas. Observations should be made at small intervals of colatitude throughout the month and curves of albedo established. For features near the limb, corrections for libration will be necessary.

Spectrographic Program

All intensely bright and intensely black craterlets should be investigated spectrographically throughout the month. Such ring plains as Plato need to be studied carefully. Only through a comprehensive program does there appear to be much chance of gaining needed data concerning outgassings such as occurred in Alphonsus[8,9]. Such a program should discover any strong luminescence which may exist.

Surface Temperatures

The work of Pettit and Nicholson[10,11,12] should be repeated, using one of the largest telescopes and the more sensitive techniques now available. It will be desirable to include separate measurements on areas as small as the floor of plato and sections of the floor of Alphonsus. The problem of measuring lunar surface temperatures with earth based equipment is discussed in some detail in Section 4 of this report.

1.2.3 Experimentation Using Research Vehicles and Satellites

Experiments which may be performed from research rockets are described in the main body of the report. Some of the possible experiments are listed in Table 1.2-2.

TABLE 1.2-2

EXPERIMENTATION THROUGH USE OF
RESEARCH VEHICLES AND LUNAR SATELLITES

A. Astrophysical experiments bearing on the cis-lunar environment

B. Radioactivity of the surface

C. Lunar gravity and geodesy

D. Measurement of basic astrometric constants

E. Thermal mapping (infra-red)

F. Magnetic field measurements

G. Measurement of lunar atmospheric parameters

A lunar satellite should provide opportunity for making measurements which require longer flight times than are available in a probe vehicle. Accurate measurements of the lunar magnetic field as well as determination of the moon's shape and possible lack of isostacy may be made from study of satellite motions.

The selenography of the far side of the moon, knowledge of heights of mountains, craters, rims, etc., would be extremely valuable since present information regarding lunar elevations is notoriously poor. Stereoscopic photographic maps of special areas of the moon as well as detailed photographs of sites considered for landings of men and instruments are worthwhile objectives of a lunar reconnaissance satellite. However the resolution obtainable will, of course, determine the usefulness of the information obtained. High resolution is desirable in order to see impacts and resulting dust clouds, to obtain better resolution of the moon as a whole, and to obtain better resolution of limited areas, such as the craters Tycho and Copernicus or the walled plains Alphonsus and Plato.

1.2.4 Experimentation by Landing Men and Instruments on the Moon

Table 1.2-3 lists some of the possible experiments that either require contact or would be most conveniently performed right at the surface.

TABLE 1.2-3

EXPERIMENTATION BY LANDING INSTRUMENTS ON THE MOON

A. Magnetic measurements

B. Determination of chemical composition

C. Search for sub-life forms and macromolecules

D. Determination of surface consistency, electrification, dust thickness, electrical conductivity and temperature profile of soil.

E. Bomb experiments

F. Atmospheric measurements

G. Marking by impact

H. Photographic and astronomical observations

I. Seismic and gravitational measurements

J. Ground exploration by controlled vehicles

K. Meteorite bombardment rate

L. Return of lunar sample

The fourth category, manned landings, offers such a wide range of possible experiments that no listing was attempted. A brief discussion of landing sites has been included below and may serve to outline in a general way some of the problems involved.

Landing Sites

Although preliminary measurements can be made using instrumental techniques, perhaps by so-called hard and soft landings, it is likely that manned landings will be attempted eventually and with it the question of the landing site will arise. Urey[13] has suggested that an initial landing be made near the boundary of the western Mare Serenitatis. In this way samples of both the black and grey materials there as well as specimens from the nearby mountains could be obtained. Tombaugh[14] recommends a landing on the south edge of Mare Frigoris between Aristoteles and the western end of the Alpine Valley. The selection is made mainly on the basis of variety of features and the presence of a smooth landing area. The same author quotes Ryan as selecting Sinus Roris and exploration of the crater Harpolus, a choice apparently dictated by the same considerations.

Estimates of landing sites are uncertain primarily for two reasons. First, there are many still unknown conditions of the lunar surface and, secondly, the accuracy of the guidance system is not known.

With low accuracy guidance a large mare floor tends to be favored. The comparatively featureless surface of such a floor will make it easier to find equipment. Also, rills have not been observed across the central parts of mare floors. The presence of rills is exceptionally important if there is to be movement from one place to another.

The maria are believed to be covered by dust but whether it is hundreds of feet thick or only a few centimeters is not known. A guess however, is not sufficient to select such a site for a landing that perhaps would be rendered useless by deep dust. The second section of the general problem has to do with the purposes of the landing. Hard landings to locate transmitting instruments probably could be made almost any place on the surface. Soft landings could be made more easily in the mare-like areas. In the temporary landing of men a site could be chosen that was entirely different from that for a permanent landing. In a temporary landing it would not be necessary to construct permanent dwelling shelters. Probably there would be little travel and therefore rills would be a minor problem. If the question of deep dust does not disqualify them, mare-like plains would appear to be best for temporary landings.

The permanent landing of men is complicated by the lack of shelter sites and the presence of rills will make travel from one place to another difficult. Permanent shelters on the moon perhaps could be small craterlets covered over. The advantages are:

1. A great deal of the construction work already has been done

2. Such shelters are less vulnerable to meteorites

3. With the small weight of objects on the moon the covering problem should not be too serious

If men are to work permanently on the moon, it is essential that they gain from it water, air, and metals. Very likely it will not be practicable to carry such things except for short-lived expeditions of a very few men. A chain of craterlets such as those near Copernicus and near Tycho would appear to be the most suitable for shelter purposes. Copernicus however is much nearer the lunar equator than Tycho. If the sun passes almost directly overhead the problem of protecting such a craterlet shelter from heat radiation is formidable. At high latitudes the inner surface that is subject to direct solar radiation is much smaller and the problem is simplified a great deal. One would guess from analogy to terrestrial conditions that usable mineral sources most likely would be found in mountainous areas.

In the location of a site the ability to travel of personnel who are left on the moon is exceedingly important. Today more than 1,000 rills on the moon are known. A rill is a narrow, rather deep valley which may be as long as perhaps 200 miles. The narrowest rills we may observe under the best conditions perhaps are between 1/8 and 1/4 mile wide. Crossing them would have to be either by bridging or by using a sophisticated "pogo stick". There may well be 100 rills for every one observable from earth. Final observations must be from photographs made rather near the lunar surface. Another question of site is that of observation optically from the earth. If this is very important, it favors mare-like areas.

If there is any way by which the depth of the dust can be determined from the earth it must be done. If it is deep over the maria there certainly will be some mountainous areas where it will be shallow. For example, if guidance is good enough it might be possible to land on the rather wide rim of Copernicus without much fear of serious dust difficulties. The question of outgassing in some of the craterlets is important. From the few data which are available it might be well to avoid craterlets which were excessively black or excessively white.

The question of lunar latitude of the site will not be important for a temporary landing where shelter has been carried from the earth. However, as mentioned above, it becomes very important if craterlets are to be the basis of habitation. The question of latitude scarcely enters into the problem of optical observation of the earth from the moon. Because of the lack of atmosphere, the earth can be observed as accurately only a few degrees above the lunar horizon as at any other altitude. It may be however that some other types of observations would be handicapped if the earth were too close to the horizon. If astronomical observations are to be made, high latitudes should of course be avoided, unless stations were established in both the northern and southern hemispheres.

REFERENCES

1. D. Alter, Pub. Ast. Soc. Pac.; 68, No. 400, Feb. 1956
2. T. Gold, M.N.; 115, 585 (1955)
3. D. Alter, Pub. Ast. Soc. Pac.; 70, No. 146, Oct. 1958
4. D. Alter, Pub. Ast. Soc. Pac.; 68, No. 404, Oct. 1956
5. D. Alter, Pub. Ast. Soc. Pac.; 69, No. 411, Dec. 1957
6. D. Alter, Pub. Ast. Soc. Pac.; 69, No. 408, June 1957
7. D. Alter, Pub. Ast. Soc. Pac.; 67, No. 367, August 1957
8. D. Alter, Pub. Ast. Soc. Pac.; 69, No. 407, April 1957
9. D. Alter, Griffith Observer XXIII No. 3 March 1959
10. E. Pettit and S. B. Nicholson, A. J. LXXI 21 (1930)
11. E. Pettit, A. J. 81 483 (1935)
12. E. Pettit, A.J. 91 165 (1940)
13. H. C. Urey, Observatory, 76/77, p. 232 (1956/57)
14. C. Tombaugh, Proc. Lunar and Planetary Exploration Coll. 1, No. 3, p. 15 (1958)

SECTION 2

TRACKING REFLECTORS

2.1 INTRODUCTION

Accurate observations and measurements of the trajectories of lunar flights will constitute an experiment of major scientific importance. The information to be obtained is needed for predicting the time and place of impact, or for the activation of retro-rockets to establish the probe as a lunar satellite. The trajectory observations are also of prime importance for improving our knowledge of the astronomical and geophysical constants, including the mass of the moon. Our present knowledge of these constants is not sufficiently exact for high precision orbit prediction. For example, a landing on the moon by means of a ballistic trajectory based upon present values would be uncertain by more than 1000 miles, a landing on Mars, by some 50,000 miles. It follows, that high precision in observation of the trajectory and especially the point of impact of several lunar flights will serve to significantly improve our knowledge of these constants. As a consequence, our potential for future landings on the moon will be improved, which is essential to the establishment of depots or supplying future expeditions to the moon.

Prediction of time and point of impact requires that corrections to the orbit be made and consequently that good observational data be available within a few hours after launch. These observations must be reduced as carefully and accurately as is consistent with the time available. Post-impact revisions of the

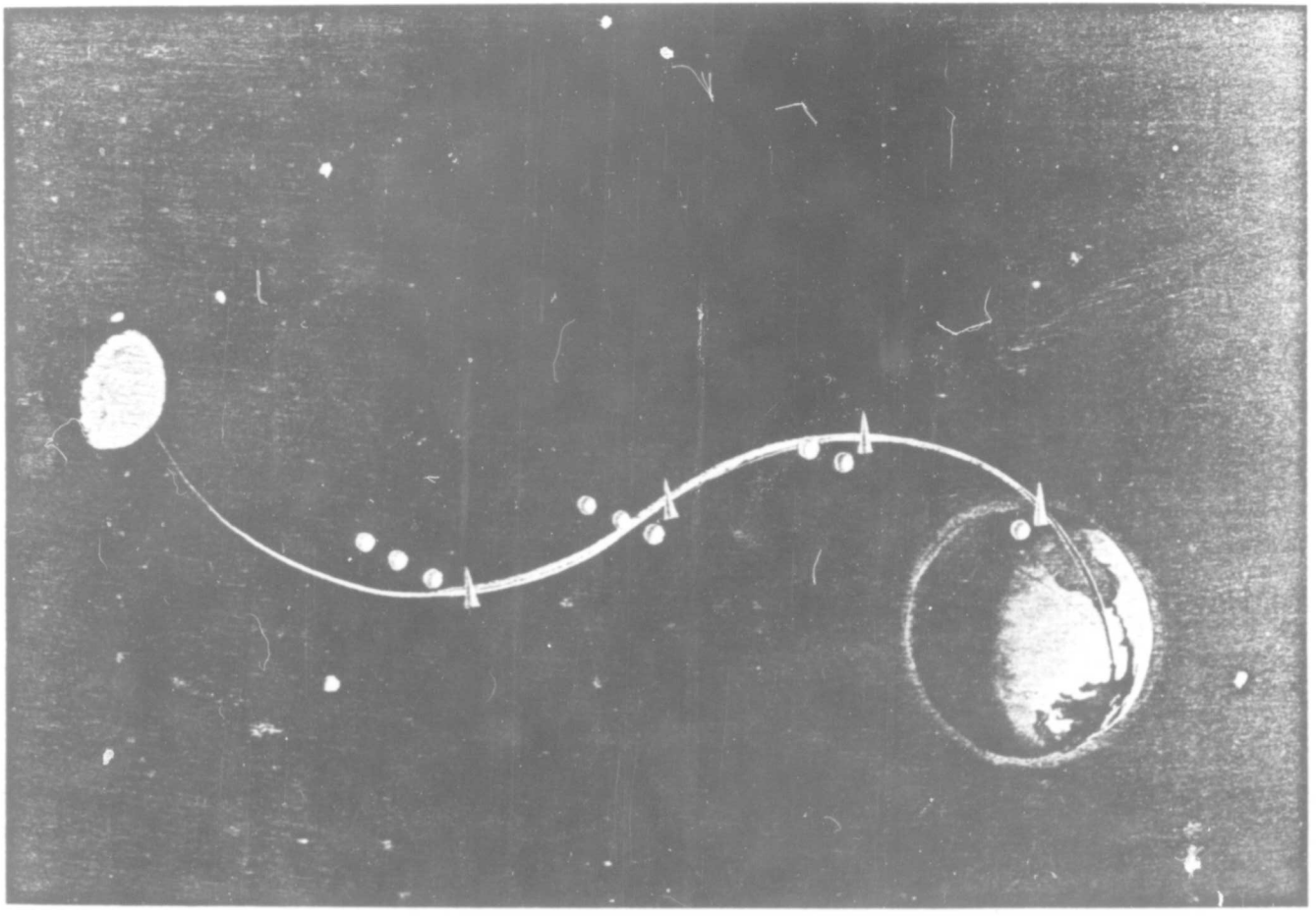

FIGURE 2-1 ARTIST'S CONCEPTION TRACKING BALLOONS

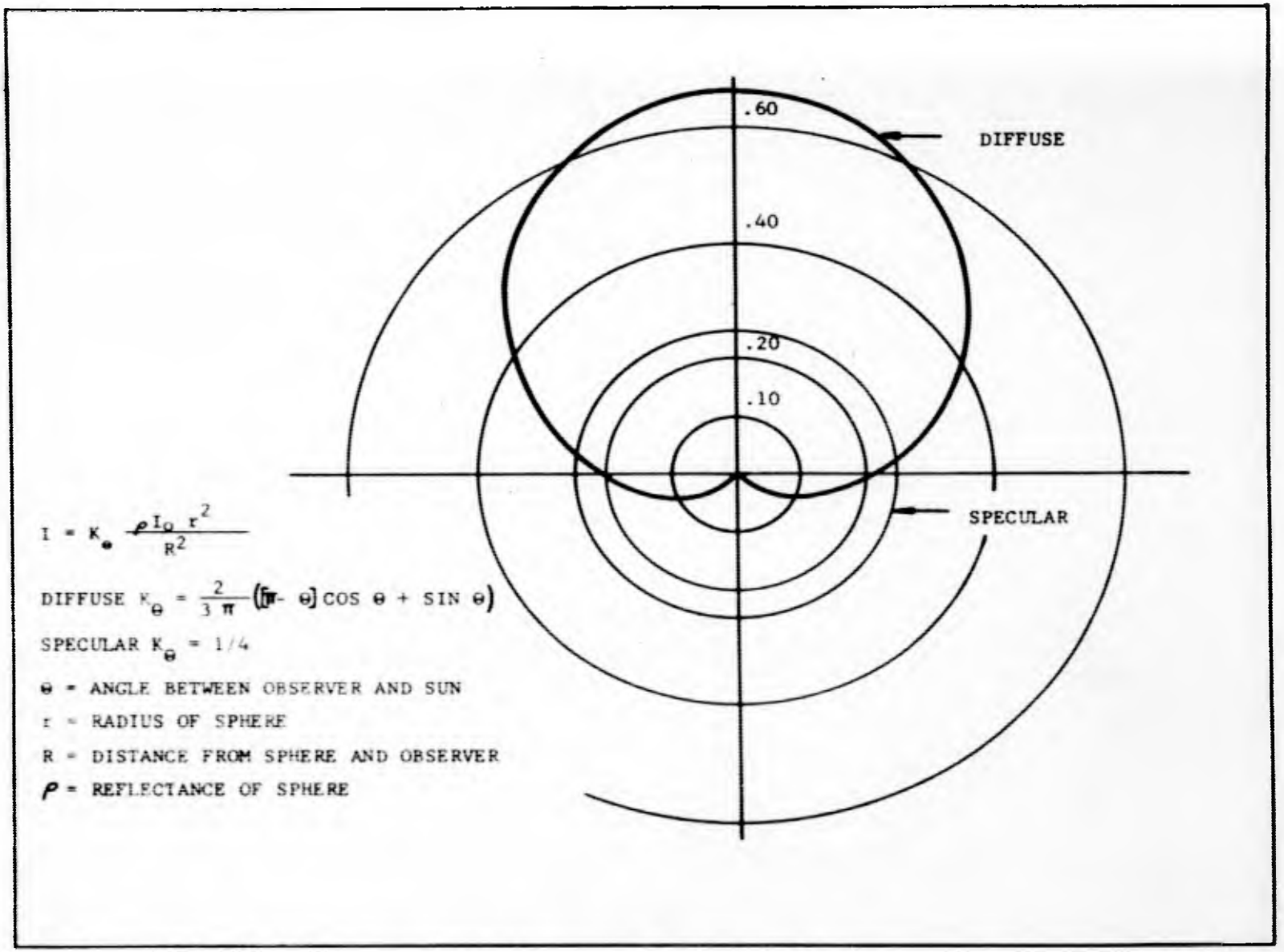

FIGURE 2-2 COMPARISON OF DIFFUSE AND SPECULAR REFLECTING SPHERES

specular and diffuse spherical surfaces as a function of phase. The light intensity at a distance capital R from the reflector is given by the relation

$$I_R = K_\theta \frac{\rho I_o r^2}{R^2}$$

where

θ is the elevation angle of the sun,

small r is the radius of the reflecting sphere,

I_o is the intensity of parallel light incident on the sphere,

and ρ is the reflectance of the sphere.

As seen K_θ is constant (1/4) with respect to θ for the specular reflector but has the value

$$K_\theta = \frac{2}{3\pi} \left([\pi - \theta] \cos \theta + \sin \theta \right)$$

for a diffuse reflector. The light received from a specular reflector, then, does not depend on the phase angle of the sun, but for a diffuse reflector the reflected light intensity will vary from zero to better than two and one-half times the intensity for a specular reflector of the same size at full phase. At quadrature the values are almost equal (the specular is better by about 17%) and for convenience in the following discussion are considered equal. The calculation of diffuse and specular spherical reflectors is treated in detail in Appendix C.

The problem of reflector visibility is most acute at the full lunar distance. In Figure 2-3, the stellar magnitude of diffuse reflectors at this distance is plotted as a function of their diameter in feet. The other curve shows the required telescope diameter to view them from the earth. For this calculation the reflectors are assumed to be viewed in quadrature and the value of K_θ above reduces to $\frac{2}{3\pi}$. The energy reaching the earth from a reflector of this type

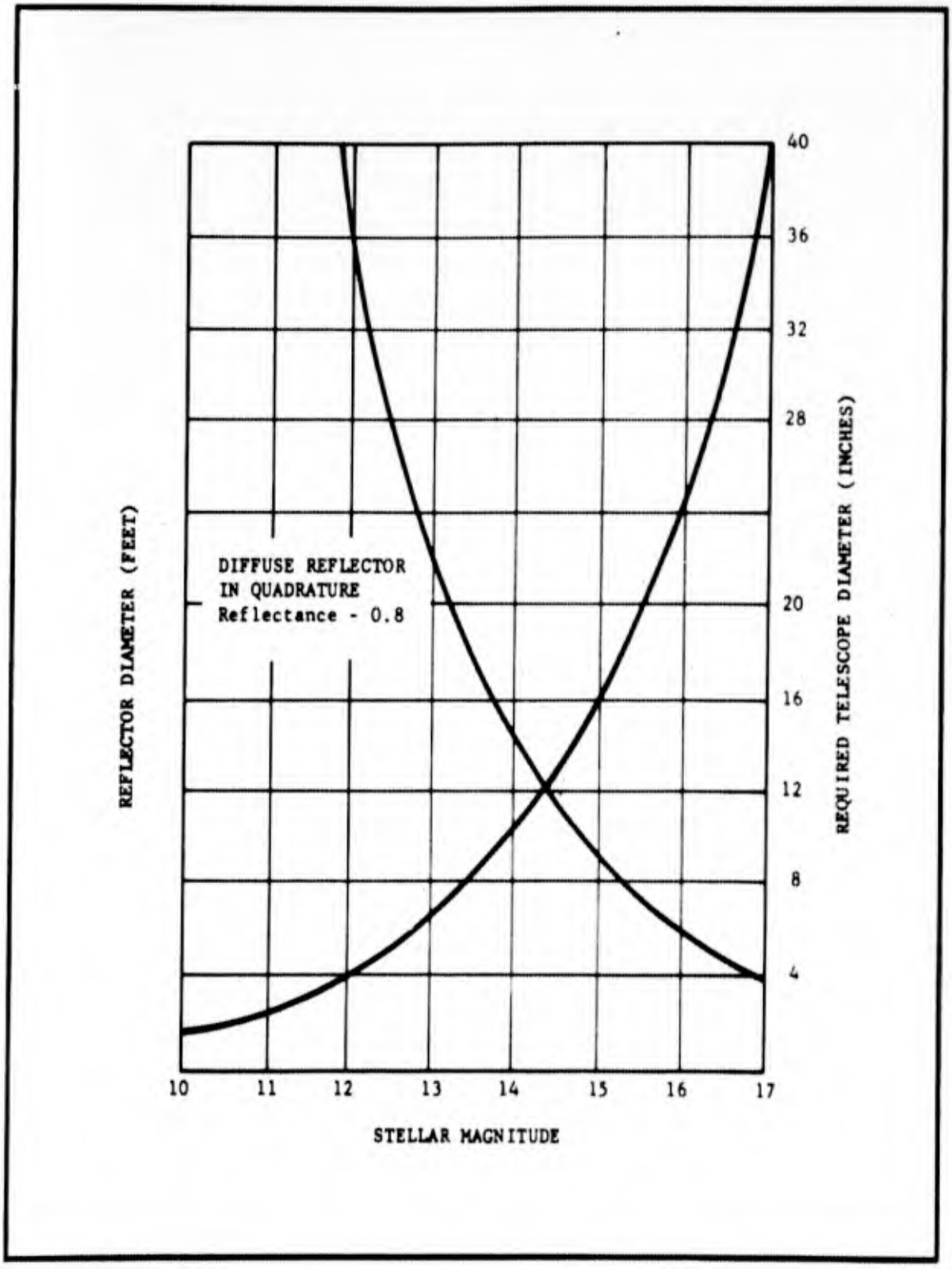

FIGURE 2-3 STELLAR MAGNITUDE AND REQUIRED TELESCOPE DIAMETER FOR DIFFUSE SPHERICAL REFLECTORS IN QUADRATURE AT LUNAR DISTANCE.

will be given by

$$I = \frac{2 \times 0.8 \times 0.134 \times r^2}{3\pi (2.4 \times 10^5 \times 5.28 \times 10^3)^2} \text{ watts - cm}^{-2}$$

where r is the radius of the balloon in feet. In this relation the solar light flux is taken to be 0.134 watts - cm^{-2} at one astronomical unit. For a 10 foot balloon the light energy received at the earth will then be about 3.5×10^{-19} watts - cm^{-2}. A 17th magnitude star which has 5.33×10^{-20} effective watts - cm^{-2} can be recorded by a 40 inch telescope. On the basis of the above calculation this telescope would record a balloon of about 4 foot diameter. Allowing for uneven illumination it is assumed that the 10 foot reflector will be equivalent to the 17th magnitude star. From the curves of Figure 2-3, a 100 ft. diameter reflector would have an apparent magnitude of slightly less than 12 which can be seen with a 4 inch telescope. Since the mass of the balloon and launching complexity increases with balloon diameter, a compromise of 30 ft. or 10 meter diameter appears acceptable. This selection leads to a requirement for 12-16 inch telescopes. Telescopes of this size should be available for use in observatories around the world. Figure 2-4 shows the stellar magnitude of the 30 ft. reflector as a function of their distance from the earth. At about .06 lunar distance, (15,000 miles) the magnitude would be about 8, or somewhat weaker than is visible to the naked eye.

2.3 LIGHT PRESSURE ACCELERATION

Since the mass to surface ratio of the balloons will be very small, pressure due to sunlight will accelerate them away from the parent missile. Consider, initially, a plane reflecting surface with incident electromagnetic radiation. In this case, the radiation gives rise to a normal pressure, P_N, and a tangential stress P_T,

$$P_N = u (1 + \rho) \cos^2\theta \tag{1}$$

$$P_T = u (1 - \rho) \cos\theta \sin\theta \tag{2}$$

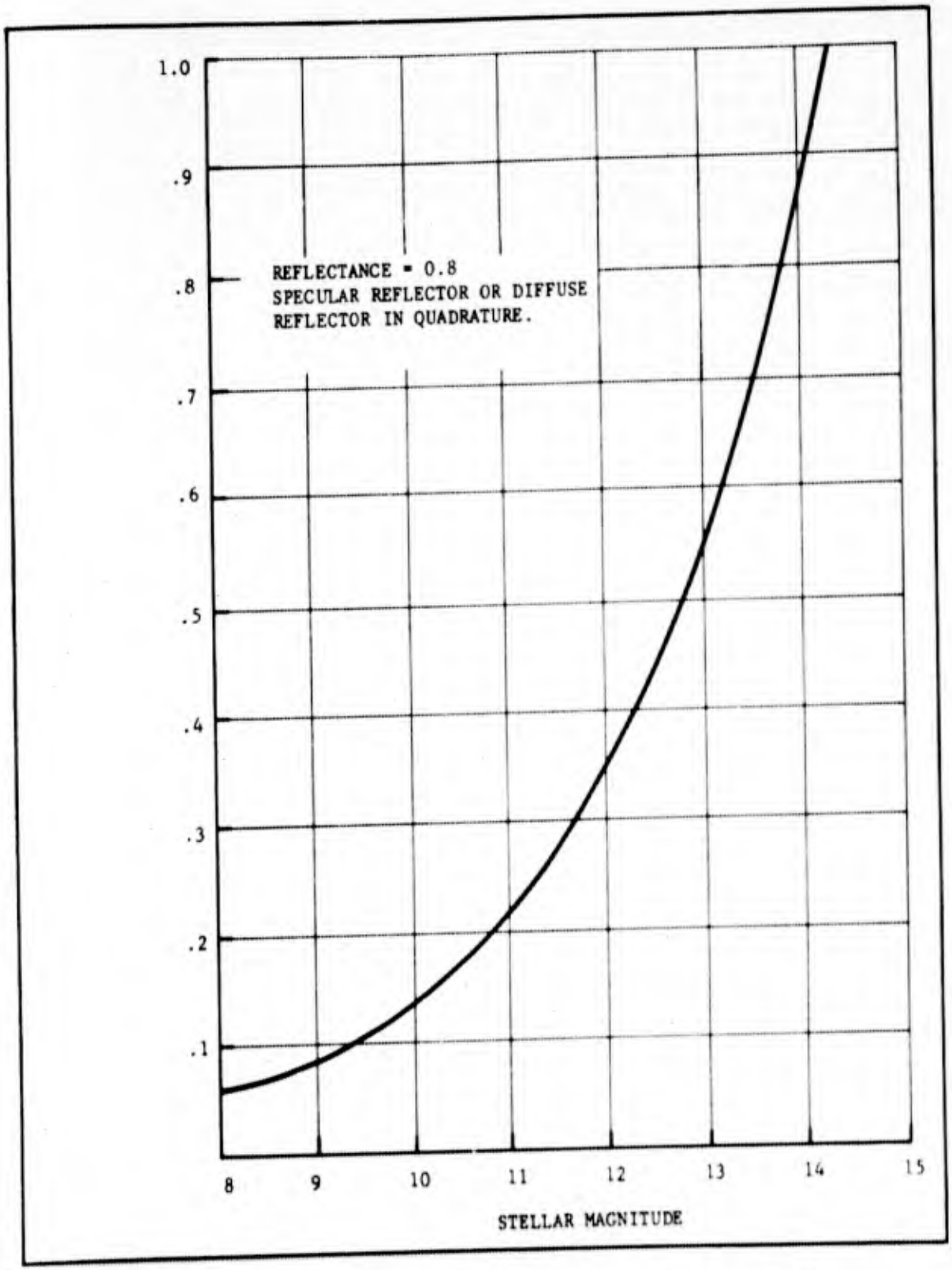

FIGURE 2.4 STELLAR MAGNITUDE VS FRACTION OF LUNAR DISTANCE FOR TEN METER REFLECTORS

u is the energy density of the incident radiation, θ is the angle between the surface normal and the propagation direction for the incident radiation, and ρ is the surface reflecting power.

For a spherical reflecting surface, the net force due to radiation pressure is obtained by integrating expressions (1) and (2) over the appropriate hemisphere; thus

$$F = \pi R^2 u \qquad (3)$$

R is the radius of the sphere while F is the net force due to radiation pressure. For sunlight, F will be along the solar vector and directed away from the sun. Expression (3) has been obtained by assuming ρ to be independent of θ and wavelength.

For a balloon 30 feet in diameter at one astronomical unit from the sun,

$$F = \pi \times (4.57 \times 10^2)^2 \text{ cm}^2 \times 4.5 \times 10^{-5} \text{ ergs/cm}^3$$

$$= 29.6 \text{ dynes}$$

The mass of 1/4 mil Mylar balloons reflectorized with 2000 Angstroms of aluminum is plotted as a function of diameter in figure 2-5. A 30 foot reflector of this type will have a mass of about 5 1/2 lbs. or 2500 grams. Thus the acceleration of the balloon due to light pressure will be about 1.2×10^{-2} cm - sec^{-2}. Separation from the parent body due to light pressure will be about 77 kilometers at 10 hours, and almost 1770 kilometers after 48 hours. As a result, the balloons will stretch out in a line from the missile. Separation of the balloons from the vehicle due to light pressure is given as a function of time after ejection in Figure 2-6.

2.4 BALLOON SURVIVAL

The balloon reflectors must survive in the cis-lunar environment for a period of about 3 days if they are to serve their purpose. Damage to the balloon can result from solar winds, equilibrium temperature, and meteoritic damage. Solar winds are

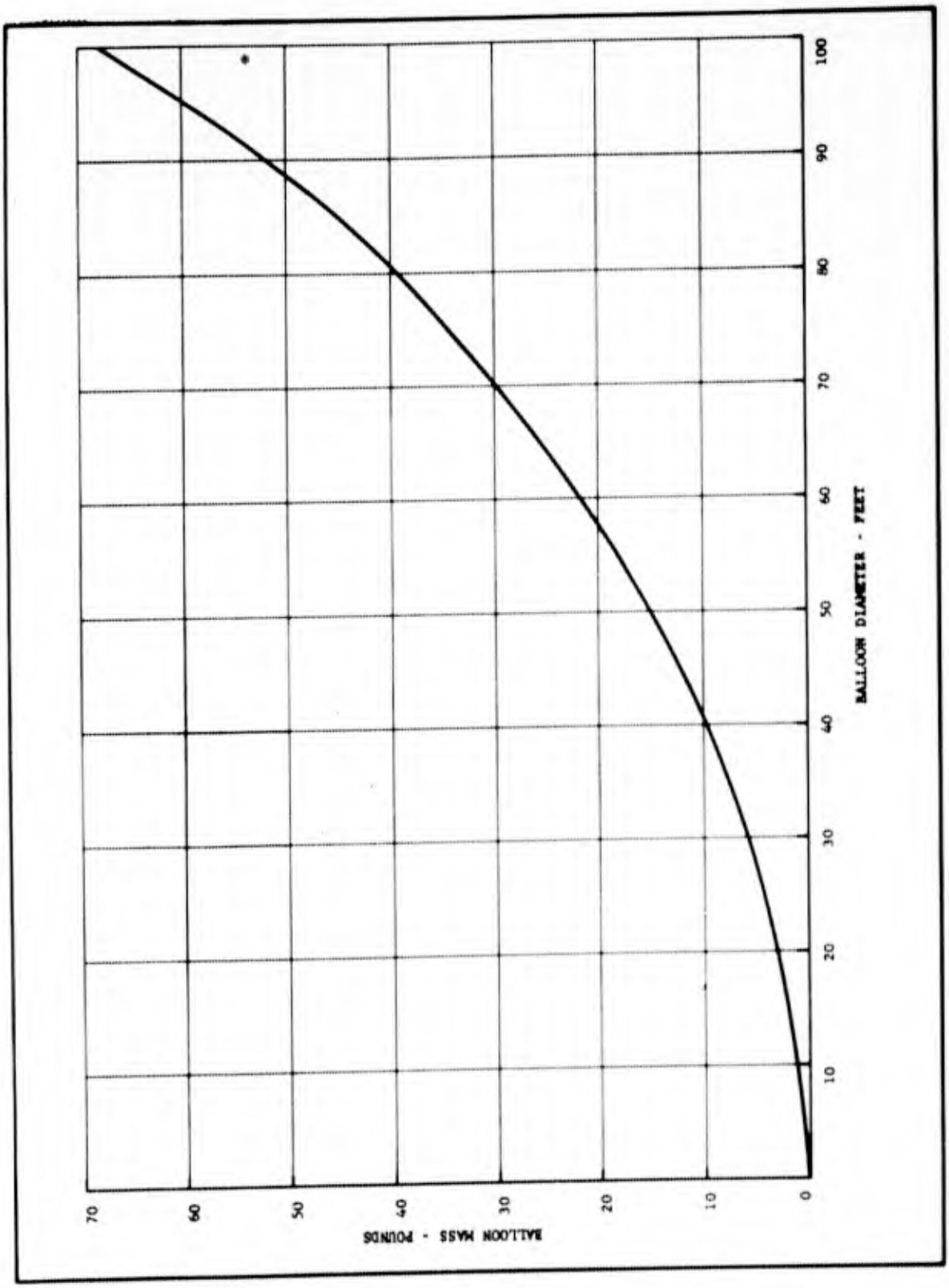

FIGURE 2.5 MASS OF MYLAR (1/4 MIL) BALLOON VS DIAMETER

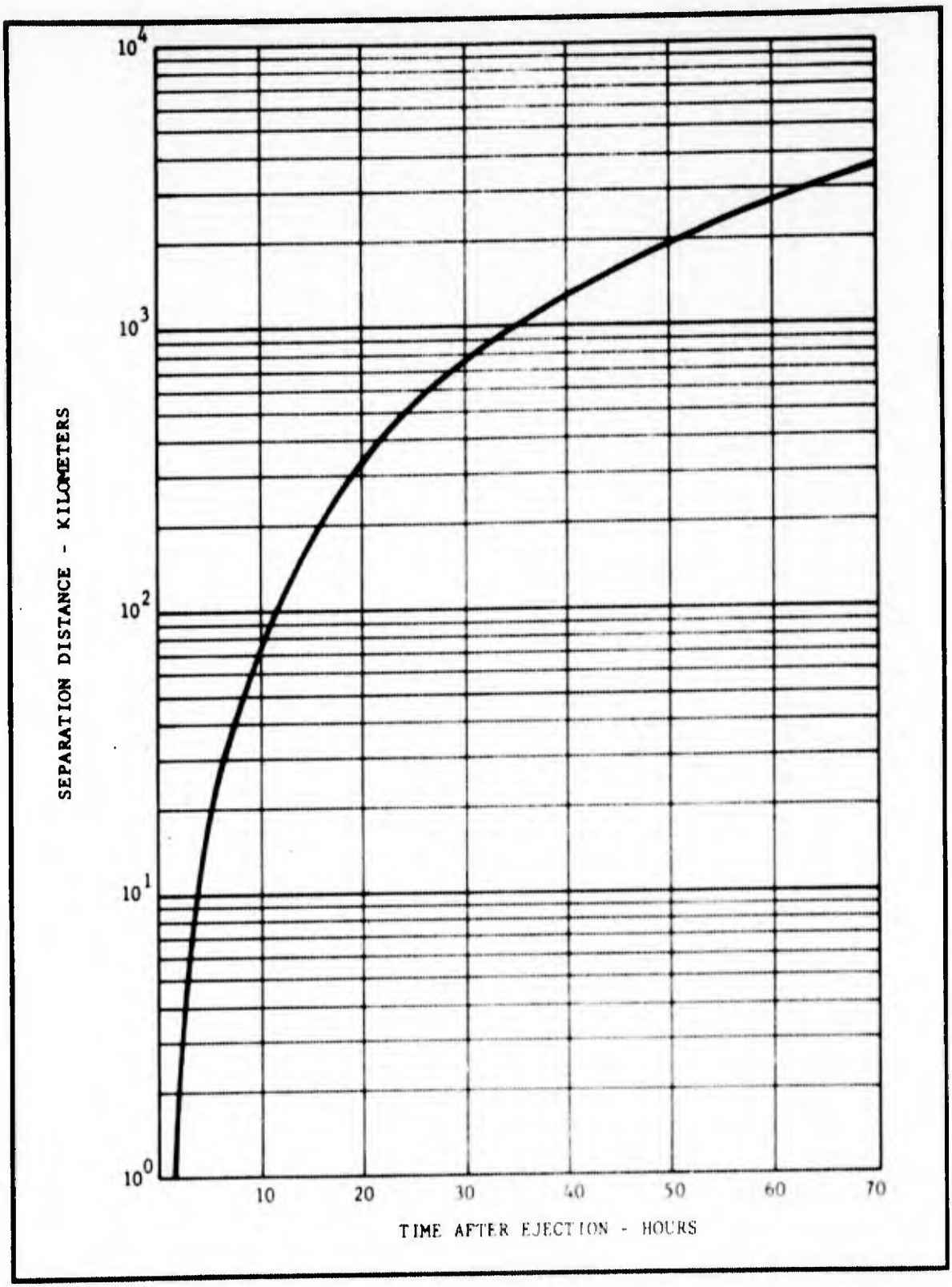

FIGURE 2-6 SEPARATION OF 30 FT. BALLOON DUE TO LIGHT PRESSURE

considered in some detail in Section 7 and therefore will not be discussed here.

2.4.1 Balloon Temperature

The general problem of equilibrium temperature of a balloon above the earth can be considered as follows. A balloon ejected at an altitude of x miles above the surface of the earth will reach temperature equilibrium within a few seconds with the radiation from the sun and the earth. The temperatures on aluminum coated Mylar balloons can be calculated for noon and for night. For this calculation it will be assumed that aluminum absorbs 7% of the solar radiation, but is only 3% black to thermal radiation (mostly in the region 5 - 15 microns). Calculations will be made with Mylar assumed to be transparent to solar radiation but 7% black, 27% black and 48% black to thermal radiation.

The radiation absorbed on the top of the balloon will be $0.14\ f \cos \theta$ watts/ cm^2 while the radiation absorbed on the bottom (from the Earth) will be $0.035\ F_o K \cos \phi$ watts/cm^2. In addition there will be heat transfer in the interior of the balloon. f is the blackness of the balloon to solar radiation, θ the angle from the zenith, F_o the blackness of the outside surface to thermal radiation, K is proportional to the solid angle subtended by the earth, and ϕ is the angle away from a line pointing toward the earth.

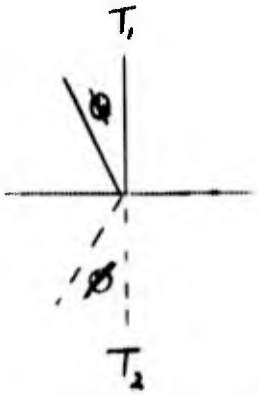

The interior of the balloon is a hohlraum and will have a constant radiation density determined by the average value of T^4 over the surface. The temperature at any point on the surface can be determined by setting the heat absorbed equal to the heat radiated,

or for the top

$$0.14\ f \cos \theta + F_i \sigma T^4 = (F_i + F_o)\sigma T_1^4$$

and for the bottom

$$0.035\ K\ F_o \cos \beta + F_i \sigma T^4 = (F_i + F_o)\sigma T_2^4$$

where the average radiation from the Earth is 0.035 watts/cm^2, and F_i is the blackness of the interior surface. For the balloons at a large distance from the earth the radiation received is zero.

The balloon will be made of 1/4 mil Mylar coated with aluminum. f for aluminum is 0.07 and F is 0.03. F for Mylar will be assumed to be 0.30. The average value of σT^4 can be calculated by setting the received radiation equal to the emitted radiation over the whole surface, or

$$0.14\ f \pi R^2 + 0.035\ F_o K \pi R^2 = 4\pi R^2 \sigma T^4 F_o$$

or

$$0.14\ f + 0.035\ F_o K = 4\ F_o \sigma T^4$$

At 800 miles K = 0.6. With aluminum on the outside

$$0.14 \times 0.07 + 0.035 \times 0.6 \times 0.03 = 0.12 \sigma T^4$$

$$T^4 = 0.0865 \text{ watts/cm}^2$$

and $T = 351^\circ K$

the temperature of a ball in the center of the balloon. If the

aluminum is on the inside, then $F_o = 0.30$ and $F_i = 0.03$, and

$$T^4 = 0.0133 \text{ watts/cm}^2$$

and $$T = 220^{\circ}K$$

The best estimate for 1/4 mil Mylar is that it is 30% black although it may be as high as 50% or as low as 7% (10% with aluminum). The temperature distribution around a balloon of this type away from the earth has been calculated and is given in Table 2-1. The calculation has been made for the aluminum coating on the inside and the outside, and for three values of Mylar absorptivity from 10% to 50%. The temperature is fairly uniform about the reflector for the aluminum outside and is well within the limits for Mylar. The lower temperatures reached for the aluminum on the inside are below the safe range for Mylar, but this may not be a problem once the balloon is inflated. Available characteristics of Mylar are given in Table 2-2.

2.4.2 Meteoritic Damage

The balloon reflectors will be subjected to meteoritic bombardment resulting in a number of small holes permitting escape of the inflation gas. This effect will depend upon the fraction of the surface area which is perforated. Since the Mylar thickness is 1/4 mil or about 6 microns, meteorites of this diameter or larger will cause holes of approximately their own size on penetration. Smaller meteorites may cause holes larger than the meteor diameter. Pessimistically, one micron diameter meteors can be assumed to penetrate and cause holes as large as 5 times their radius. The analysis by Watson(2) of the number of meteors striking the earth per day per unit of magnitude has generally been adopted. The frequency distribution is represented by the relation

$$N_m = 4.5 \times 10^5 \times 10^{\frac{2m}{5}}$$

Thus there are 4.5×10^5 meteors in the unit magnitude range around zero striking the earth per day. Although there is no experimental

TABLE 2-1

EQUILIBRIUM TEMPERATURE (DEGREES KELVIN)

FOR ALUMINUM COATED MYLAR SPHERICAL REFLECTORS

ANGLE FROM DIRECTION TO SUN	ALUMINUM COATING ON OUTSIDE MYLAR ABSORPTIVITY			ALUMINUM COATING ON INSIDE MYLAR ABSORPTIVITY		
	10%	30%	50%	10%	30%	50%
0	394	367	360	349	270	239
30°	387	362	357	329	261	232
60°	366	353	350	288	228	203
90° - 180°	329	337	341	135	106	95
Interior Temperature	347	347	347	195	195	195

TABLE 2-2

CHARACTERISTICS OF MYLAR

ρ	1.29 gm cm^{-3}
Tensile Strength	25,000 p.s.i. at 20° C
Zero Strength Temp.	250°C
Tear Resistance	27 gms/mil
Cold Brittle Temp.	- 65°C
Infrared Absorption	(2 - 7μ) 3 times that of polyethylene. Both absorb well above 7μ.
U. V. Absorption	Opaque below 3150 Å
Metalizing	Very good
Seal Strength	16 - 20 lbs/inch

verification of this frequency distribution for meteors fainter than the 10th magnitude it has often been extrapolated as far as the 33rd magnitude. There are several arguments leading to a belief that the number of incident meteors in the larger magnitudes (smaller sizes) must be greater than that given by an extrapolation of the Watson relation. Bauer[3] has revised the figures for meteor incidence as function of magnitude on the assumptions:

1) The total amount of meteoric material reaching the earth is 1000 tons/day.

2) The excess incidence above that given by the Watson distribution arise from an excess number of micrometeors in the magnitude range 20 to 30 (1.2×10^{-8} gm to 1.2×10^{-12} gm).

3) The number of micrometeors in a unit magnitude range is still proportional to the factor $10^{\frac{2m}{5}}$. He calculates the revised impact rates in the region of interest as given in Table 2-3.

On this basis a fairly pessimistic estimate of meteor damage can be obtained if a flux of 10^{-4} cm^{-2} sec^{-1} is assumed for meteorites which can create holes of about 5 microns average diameter. The mass of gas escaping through a small hole of area A into a vacuum can be closely approximated as

$$L = \frac{1}{4} \rho \bar{V} A \quad (4)$$

where ρ is the density of the gas in the volume and $\bar{V}$ is its mean thermal velocity. From this, the fraction of the total gas content of the balloon which escapes per second through the hole will be

$$F_e = \frac{\frac{1}{4} \bar{V} A}{\frac{4}{3} \pi r^3}$$

TABLE 2-3

METEOR IMPACT RATES (AFTER TAUER)

Magnitude	Mass Grams	Diameter cm	Number/Dry Incident on Earth	Number cm^{-2} sec^{-1}	Kinetic Energy Ergs
26	5.0×10^{-11}	4.6×10^{-4}	2.0×10^{18}	2.2×10^{-6}	34
27	2.0×10^{-11}	3.4×10^{-4}	5.0×10^{18}	5.5×10^{-6}	14
28	7.9×10^{-12}	2.5×10^{-4}	1.3×10^{19}	1.4×10^{-5}	5.4
29	3.1×10^{-12}	1.8×10^{-4}	3.2×10^{19}	3.5×10^{-5}	2.2
30	1.2×10^{-12}	1.3×10^{-4}	8.0×10^{19}	8.8×10^{-5}	0.86

Expressing the hole size, or total damaged area of the balloon as

$$A_D = f\ 4\pi r^2$$

where f is now the fraction of the surface area which has been perforated, the fractional escape rate becomes

$$F_e = \frac{3}{4}\ \bar{V}\ f/r$$

Using the 10^{-4} cm^{-2} sec^{-1} flux rate given above the fractional area perforated per second will be approximately 2×10^{-11} sec^{-1}. If the mean thermal velocity, $\bar{V}$, is taken as 3×10^4 cm sec^{-1} and r = 450 cm, then the pressure change rate will be

$$\frac{dp}{dt} = -\frac{3 \times 10^4 \times 2 \times 10^{-11} \times \frac{3}{4}}{450}\ tp_t$$

$$= -\ 10^{-9}\ tp_t$$

and integrating

$$p_t = p_o\ e^{-ct^2}$$

The fractional pressure change as a function of time of ejection is plotted in Figure 2-7.

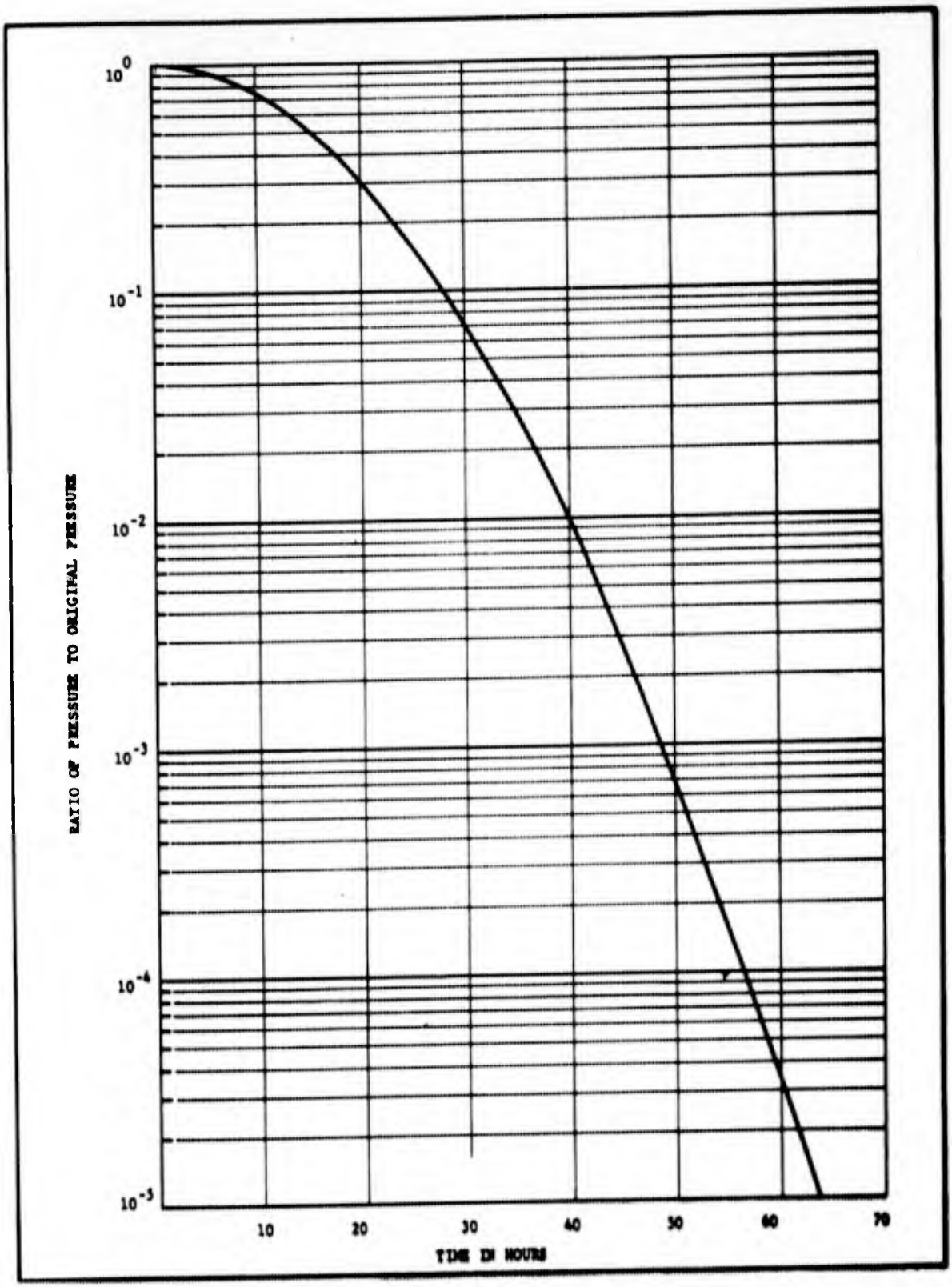

FIGURE 2-7 PRESSURE CHANGE DUE TO METEORITIC DAMAGE
10 METER DIAMETER SPHERICAL BALLOON

REFERENCES

1. Page, Intro. to Theor. Phys. , page 509.

2. F. G. Watson, Between the Planets, Blakeston Co., 1941.

3. C. A. Bauer, Meteoroids in the Upper Atmosphere, Lockheed Aircraft Corp., MSC-3134 (1956).

4. Jeans, The Dynamical Theory of Gases, Dover, p. 121.

SECTION 3

MAGNETIC FIELD MEASUREMENTS

3.1 INTRODUCTION

A lunar probe can provide the carrier for two magnetic field measurements of considerable interest. The first of these is the magnetic field in cis-lunar space, and the second the lunar magnetic field itself.

A measurement of the magnetic fields in space will certainly contribute to our knowledge of cosmic rays since the number and character of charged particles which reach the earth are strongly affected by the magnetic fields which they must traverse. Further than this, whatever field exists in the space near the earth-moon system is probably a composite resulting from the superposition of the magnetic fields of the earth, the sun, the moon, and possible galactic fields all of which may be modified by solar winds or streams of ionized particles from the sun. Of these, only the field of the earth is reasonably well known, and measurement of the ambient field by a lunar probe can help to shed light on this complex situation.

The lunar field itself is, of course, of great interest Knowledge of this field may provide information as to lunar and terrestrial origins. Also a knowledge of the field will permit a calculation of the probable effect of cosmic rays and solar wind particles on the surface of the moon.

Unfortunately, present knowledge concerning solar and other magnetic fields is quite speculative - but from available information and theories some estimate of the field strengths to be expected must be derived in order that the sensitivity and range of the measuring devices can be selected. Obviously, these estimates will be subject to considerably uncertainty. The background information relating to the magnetic fields of the earth, sun and moon is discussed in some detail in Appendix D.

3.2 GEOMAGNETIC FIELD

Fig. 3.1 shows the calculated variation of the earth's dipole field out to about 6 earth radii, assuming a value of 0.5 gauss at the surface. Near the earth the field will vary due to local anomalies, and in the 100 - 200 km region due to ionospheric current systems. In the figure the field variations are shown as the maximum value estimated by Chapman[1] for passage through an auroral arc. Following this, the field will decrease with the dipolar value out to a distance of several earth radii. In the region of 5 - 8 earth radii, the field may be perturbed by the current ring postulated by the Chapman-Ferraro[2] theory of magnetic storms. The maximum allowable current density in the ring is that giving rise to a field which is equal and opposite to the geomagnetic field. There is a possibility of near zero field strength in this region. At some distance from the earth the energy of the geomagnetic field may become comparable to the kinetic energy of the solar gas, and this region will more or less represent the limit of the earth's dipole field.

In the region near the earth, the dipole field will govern. The vector field intensity H, due to a dipole parallel with the z axis is given in polar coordinates by

$$H = \frac{M}{R^3}\sqrt{1 + 3\sin^2 \phi}$$

where R is the radial distance, ϕ the angle with the normal to the dipole and M the magnetic moment. It may be seen that the total field will have a possible maximum variation of a factor of two due to position with respect to the dipole. Therefore, not only will the intensity fall off inversely with the cube of the distance but under certain conditions of vehicle launching, determination of the angle with respect to the earth's

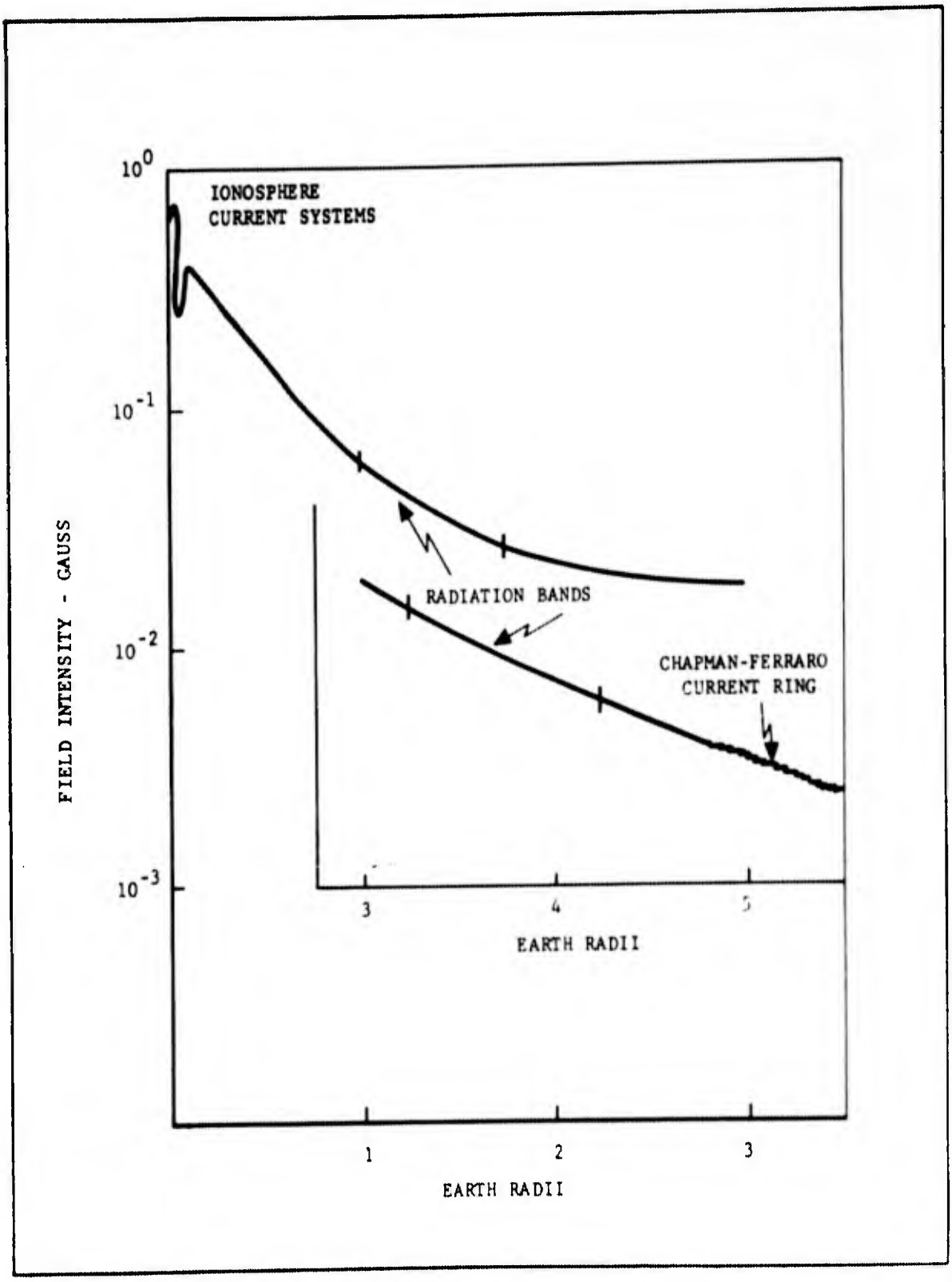

FIG. 3.1 DIPOLE FIELD NEAR EARTH

dipole may be necessary. For an angular deviation of 30° which is not unlikely in a minimal energy trajectory, the field will be approximately 30% greater than in the plane of the geomagnetic equator. The rate change of the field with respect to angle is slightly less than 1% per degree except along the magnetic poles and equator where it is zero. This means that a tracking error of one minute of angle, will result in an error in field intensity of the order of one part in 10^4.

At constant angle the rate of change of field intensity will be inversely proportional to the radial distance. At 1000 km for example the gradient will be about 20 γ per kilometer. The magnitude of the expected perturbations of the field in this region is close to this value and therefore accurate measurement will require that radial distance be known to the order of 0.1 km or better. Since the vehicle may have a velocity of perhaps 10 km sec^{-1} at this distance, the field intensity will be decreasing at the rate of about 200 γ sec^{-1}. This in turn places a lower limit on the response time and requires a high sampling rate. Additional discussion of instrumentation is given in Appendix D.

3.3 LUNAR MAGNETIC FIELD

Various alternatives or possibilities for a lunar field can be considered The estimated values based on these alternatives are given in Table 3.1. The first value would certainly be a maximum and is that which would result if we assumed the magnetic moment of an astronomical body to be proportional to its mass Considerably more modest values have been estimated by Vestine[3] from other considerations. Temperature inequalities in a solidifying moon could give rise to currents which would result in appreciable magnetization of the condensing lunar rocks This would result in a thermoelectric field of possibly 100 gamma as shown As another possibility, if the moon were once part of the earth its cooling through the Curie point in the field of the earth would cause it to have a remanent magnetization. This thermoremanent field would be of the order of 40 gamma if the susceptibility of the moon were similar to that of the earth's crust. Finally, as Blackett[4] has suggested, if rotating bodies have magnetic fields proportional to their angular momenta, a very small fundamental field would result

TABLE 3.1

POSSIBLE LUNAR MAGNETIC FIELDS

BASED UPON	FIELD AT SURFACE GAUSS x 10^{-5}
Mass	30,000
Thermoelectric	100
Thermoremanent	40
Fundamental	7

3.4 CIS-LUNAR MAGNETIC FIELD

In Fig. 3.2 we have attempted to estimate the magnetic fields which might be expected in cis-lunar space. Near the earth there will be perturbations of the dipole field due to ionospheric current systems and other local anomalies. At some distance from the earth the charged particles from the sun may have sufficient energy to cause an appreciable variation in the local magnetic field This may give rise to a region shown here as shaded in which the field may be variable in magnitude and possibly in direction. The projected earth's dipole field has been chosen as an upper bound. The maximum solar dipole field in this region for a field of 10 gauss at the sun's surface is used as the lower bound.

The rather generous value of a possible lunar field due to mass only is drawn as the greatest value one could expect to encounter. Although a composite curve of this nature cannot be taken too seriously, it does provide an indication of the range and sensitivity required of the measuring instruments.

3.5 GALACTIC AND INTERPLANETARY FIELDS

If the field of the moon itself is small, a lunar probe after reaching distances beyond a few earth radii, may measure a relatively constant interplanetary field.(5) Evidence seems to be accumulating for the existence of some sort of wave structure for the field in the

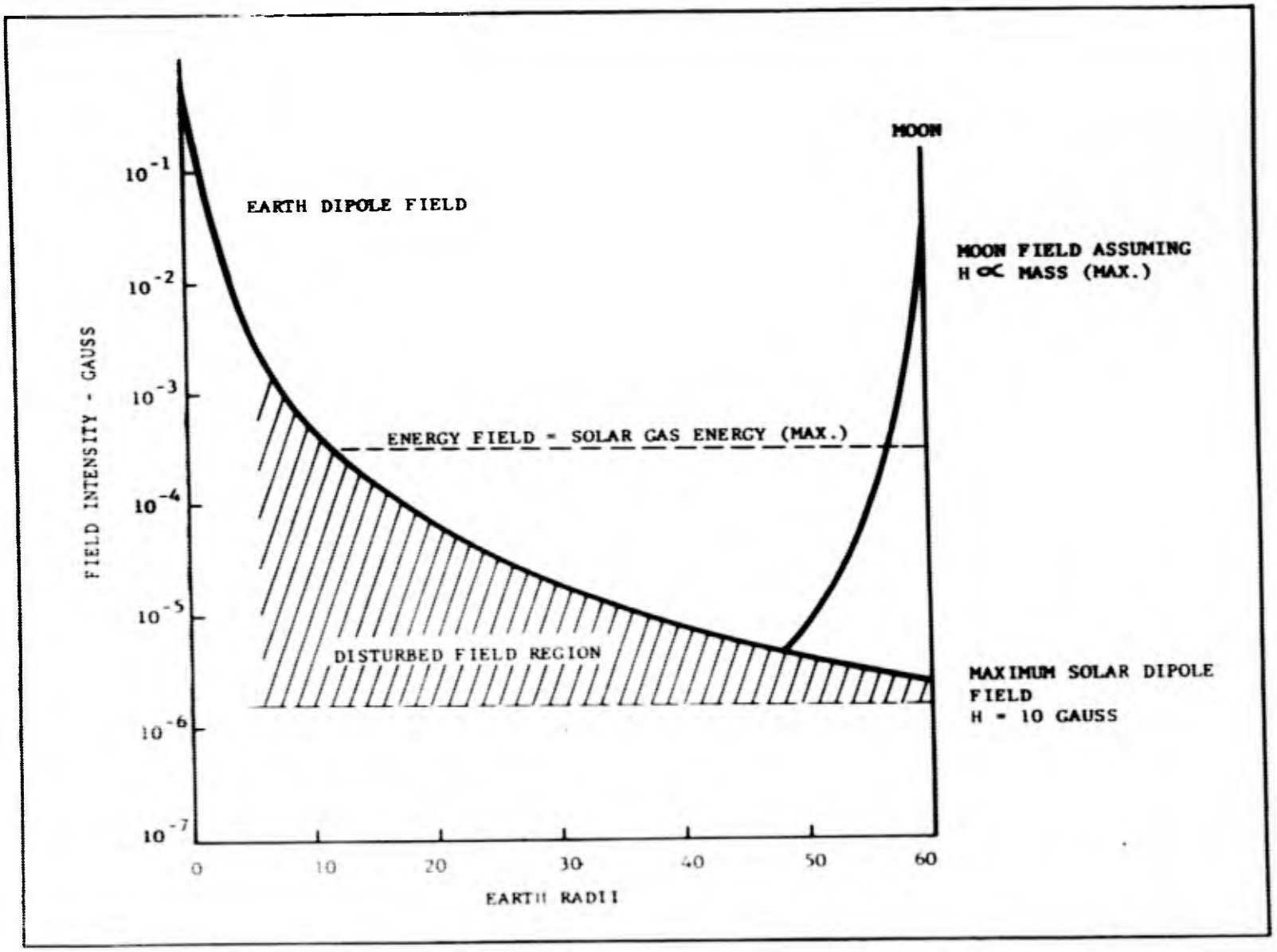

FIG. 3.2 CIS-LUNAR MAGNETIC FIELDS

inner solar system[6]. Magnetic fields are known to exist on the sun. While from study of the Zeeman effect the field distribution over the solar disk is quite irregular, the general field at the surface has been estimated to be from 1 to 10 gauss. A solar field of 10 gauss would result in a field of about 10^{-6} gauss at the orbit of the earth or about equal to the earth's field at the moon. It has been suggested that the sun's field will decrease more slowly than that of a dipole due to trapping of the magnetic lines in expanding interplanetary gas. In this case the maximum field intensity at the moon would be about 30 γ.

Chapman[2] shows that a relatively thin (compared with the stream dimensions) current sheet can completely shield the earth's field from the oncoming particles. If the ring current is at a distance of 6 earth radii (where the earth's field is of the order of 200 γ), it may be possible to obtain some idea of the field change by the use of a crude approximation. The field at the center of a current ring is given by

$$H = \frac{2\pi i}{10a}$$

where a is the radius.

If H = 100 γ, a value comparable to that of the disturbed field changes at the earth, the current would be about 10^7 amperes. The field at the lunar vehicle may be estimated by considering it to be due to current of the above magnitude in an infinitely thin sheet. In this case the field will be opposite on either side and equal to $0.2\pi I$ with I in amperes km^{-1}, or for the above current approximately $\pm$ 20 γ. The magnetic measurements made with the Pioneer I vehicle[7] indicate that this current system may be as far out as 10 radii (flight was made on a magnetically quiet day). Fields of the order of 10^{-4} to 10^{-5} gauss were observed with a strong suggestion of wave structure.

The existence of any glactic field in the region of the earth-moon system is doubtful, although the arguments concerning these fields are at least quite speculative. Fermi[8] has interpreted measurements of the polarization of star light as evidence for the existence of a magnetic field extending along the spiral arm of the galaxy. He concludes that the field intensity is of the order of 10^{-5} gauss. The minimum field which is compatible with isotropism of the cosmic radiation is about 10^{-12} gauss, and has a probable value greater than 10^{-9} gauss[9].

Davis[10] has suggested that the energy in the solar gas streams will be sufficient to force galactic fields of this magnitude from the inner solar system. He uses a value of 200 astronomical units as the probable radius of the region surrounding the sun which at ordinary times is swept free of the galactic field. If at the distance of the earth's orbit (1 A.U.) there are assumed to be 10^3 protons cm^{-3} at a velocity of 10^7 cm sec^{-1}, then this would be equivalent to equating the energy in the solar wind at 200 A.U. to a magnetic field energy of 10^{-5} gauss. Figure 3.3 illustrates this situation as postulated by Meyer, Parker and Simpson[11] based on cosmic ray flare data but for a much smaller wind-swept region. Since the energy density of the solar wind during solar flares is generally taken to be much greater than that given above, the radius of 1.4 A.U. for the central region is by no means in agreement with the energy balance quoted. For example, this field-free cavity is formed by emission from the sun of ionized gas which tends to establish equilibrium between its momentum flux ρV^2 and the magnetic pressure $H^2/8\pi$, of the galactic field. The radial distance to which the solar gas can disturb the geomagnetic field is

$$R_1 = r(H_o^2/4\pi\rho V^2)^{1/6}$$

where r is the radius of the earth
and H_o the field intensity at the surface.

According to Parker[12], for a quiet sun there are 10^2 ions cm^{-3} and $V = 5 \times 10^7$ cm sec^{-1}, $R_1 = 5.6$ r. For a disturbed sun he gives 10^5 ions cm^{-3} with $V = 1.5 \times 10^8$ cm sec^{-1}, $R_1 = 1.2$ r. However, even here the galactic fields are kept beyond the earth-moon region, and the solar field in this region will probably be strongly modified by the proton streams and be far from a dipole field.

3.6 INSTRUMENTATION

From Fig. 3.2 the range of field intensity is from about $10^5\gamma$ to perhaps $10^{-1}\gamma$. The accuracy required for measurement of the magnetic field near the earth is high because of the weakness of the perturbations. Here a precision of the order of 1γ would be useful. However, the field near the earth can probably be measured more easily and accurately with shorter range rockets and with artificial earth satellites than with a lunar probe transiting this

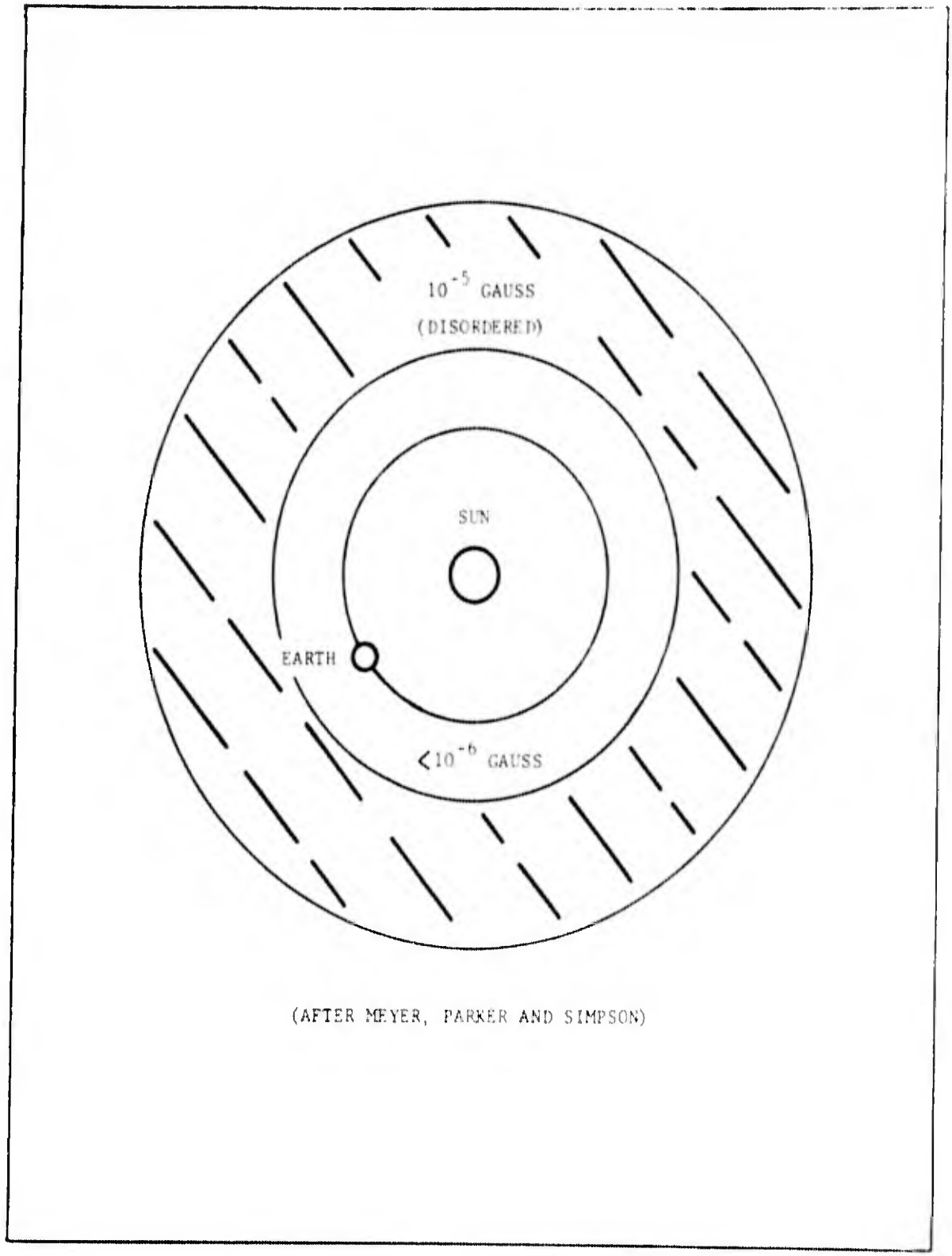

(AFTER MEYER, PARKER AND SIMPSON)

FIG. 3.3 GALACTIC MAGNETIC FIELD NEAR SUN

region at high speed. However, field measurements carried out along the trajectory of a lunar research flight can give valuable information about the existence of current systems at great distances from the earth and possibly about the sun's role in their formation.

Obviously it is desirable to have the instrumentation as small and light in weight as possible. Magnetometers of suitable physical characteristics have been designed for rocket experimentation and valuable data obtained with them. Magnetic measurements of the kind being considered here do not in general require large and bulky apparatus and laboratory instruments of extremely high sensitivity and great precision have been constructed. The wartime problem of detecting submarines led to the development of the flux-gate magnetometer and within the last few years instruments based on entirely different principles have appeared; namely, the proton precession and alkali vapor magnetometers. The availability of rockets and satellites also has led to the design of equipment suitable for these vehicles which has been constructed principally for the purpose of measuring the external geomagnetic field near the earth.

The flux-gate, proton precession and alkali vapor magnetometers are approximately equivalent in size and weight. The total weight in each case probably will be somewhat less than 10 pounds including batteries. The latter two instruments have the advantage of measuring the vector field. The rotating coil magnetometer while providing only one magnetic coordinate is simpler and probably will weigh less than one-half as much as the above instruments.

3.7 SUMMARY

The field between the earth and the moon will be the vector sum of the dipole fields of the earth and sun, the disturbing field due to high velocity ionized solar gas impinging upon the earth's magnetic field, the magnetic field due to currents in interplanetary gas, and the field of the moon.

The principle requirement for a magnetometer suitable for a lunar research vehicle is high sensitivity (0.1γ if possible) in addition to obvious weight and size limitations. At the present time the rotating coil device probably more nearly satisfies the requirements than the other instruments that are available although the orientation independence of the alkali vapor magnetometer would be of great value if the device can be constructed in suitable form and with the required sensitivity.

Perhaps it would be well to discard the idea of measuring the small perturbations of the field near the earth. The accuracy requirements are extremely high and there is the additional disadvantage of attempting to measure these small changes at high velocities. Therefore probably the measurements should extend from 1000 miles to lunar distances and beyond if possible.

The magnetic field intensities at distances of a few radii should give information of great importance for cosmic ray studies. It should be possible to obtain some idea as to the existence of Störmer-type ring currents. The extent of the solar disturbances both on quiet and disturbed days will be of great importance also. Measurement of the lunar field intensity will be of the utmost scientific interest since it will allow conclusions to be drawn as to the formation of the earth-moon system. It will also provide experimental evidence which is fundamental to the theories of terrestrial magnetism.

REFERENCES

(1) S. Chapman "Rocket Exploration of the Upper Atmosphere" Ed. R.L.F. Boyd and M. J. Seaton Pergamon London (1954)

(2) S. Chapman and Bartels "Geomagnetism" Vol. I and II Oxford (1940)

(3) E. H. Vestine RAND Res. Memo RM-1933, ASTIA, AD133008, 9 July (1957)

(4) P. M. S. Blackett Nature 159 658 (1947)

(5) A. Beiser J. Geophys. Res. 60, 155 (1955)

(6) L. Davis Phys. Rev. 100, 1440 (1955)

(7) C. Sonnet Lunar and Planetary Exp. Coll. 1, No. 4 42 (1959)

(8) E. Fermi, A. J. 119, 1 (1954)

(9) L. Spitzer Jr. Phys. Rev. 70 777 (1946)

(10) L. Davis Phys. Rev. 100, 1440 (1955)

(11) Meyer, Parker and Simpson Phys. Rev. 104 768 (1956)

(12) E. N. Parker, Phys. Rev. 110, 1445 (1958)

SECTION 4

INFRA-RED MEASUREMENTS

4.1 INTRODUCTION

By means of infra-red measurements of the daytime and nighttime lunar surface information can be obtained as to the nature of the surface. The classic measurement of the lunar surface temperature was made by Pettit and Nicholson[1] with the Mt. Wilson 100 inch reflecting telescope. Their measurements indicate a variation of surface temperature from over 400°K at the sub-solar point at full phase to less than 120°K with varying phases of the moon. The daytime measurements require a rather difficult and uncertain correction for the fraction of radiation absorbed in the earth's atmosphere. The nighttime temperatures are uncertain by a very large factor since the radiation received at the earth's surface at this lunar temperature is very small. Their best experiments provide a resolution of an area of about 50 miles square on the moon's surface. The temperature at any spot will depend upon the solar power received, the time, the roughness of the surface, the conductivity and the heat capacity. The surface is more than 90% black in most areas at all wave lengths from 0.4 microns to 100 microns. A measurement of the infra-red radiation from the surface can therefore be used to determine roughly the structure of the surface. Night time temperatures can be determined with a moon satellite and because of the shorter distance a higher resolution (one mile or less) is possible during the day time. With the higher resolution local outcroppings of bare rock and deep canyons can be discovered

Fig. 4-1 shows the basic reason for the difficulty of measuring lunar temperatures from the surface of the Earth. This is the infra-red transmission of the atmosphere in the region between 1 and 15 microns as measured by Shaw(2) in 1954. The per cent of total energy transmitted is rather low except for the "window" between 8 and 14 microns. Even so, the transmission in this region is still varied somewhat by water content of the atmosphere.

4.2 LUNAR RADIATION

At the sub-solar point, the Moon receives about 0.14 watts - cm^{-2} from the Sun. About 7% of this energy is reflected on the average and the remaining 93% is absorbed and reradiated as infra-red. In Fig. 4-2 the fraction of the infra-red energy radiated in the 8 - 14 micron band for different black-body temperatures is plotted. At 400° K about 40% of re-radiated energy lies in this band and assuming 100% transmission of this energy through the atmosphere the heat radiation received at the Earth telescope will be about 6 times the reflected sunlight. The reflected radiation can be determined with filters, since most of it is at wavelengths shorter than 3 microns and the temperature of the Moon can be established. At this temperature the total energy received at the Earth from the Moon is about 10^{-6} watts - cm^{-2}. As the lunar surface temperature decreases in going away from the sub-solar point, the fraction of the infra-red energy which is radiated in the 8 - 14 micron window decreases, as shown, making the temperature measurements more difficult. For example, at 100° K the total radiation is less than 1/250 th of that from a body at 400° K. The fraction of this energy which lies between 8 - 14 microns is down by an additional factor of 40 so that the overall reduction is a factor of 10^4. Since there will also be fluctuations in radiation from the Earth's atmosphere, measurement of temperatures as low as 100° K from the Earth is impractical. The minimum detectable energy for a thermistor with a 10 cps bandwidth system is about 10^{-8} watts. With a slower system (seconds) and a thermopile a sensitivity of 4×10^{-10} watts is possible. With a 100 inch telescope radiation as low as 10^{-14} watts/cm^2 can be detected. The maximum resolution through the Earth's atmosphere, assuming perfect seeing conditions, is shown in Table 4-1. (Of course the slow response of the 4×10^{-10} watt detector will require a long time for a survey of the Moon.) The resolution given assumes no interference from the Earth's atmosphere. The Earth's atmosphere has a radiation temperature of about 200° K. Radiation from the Moon of less than 6% of this (~ 100° K) will be difficult to measure.

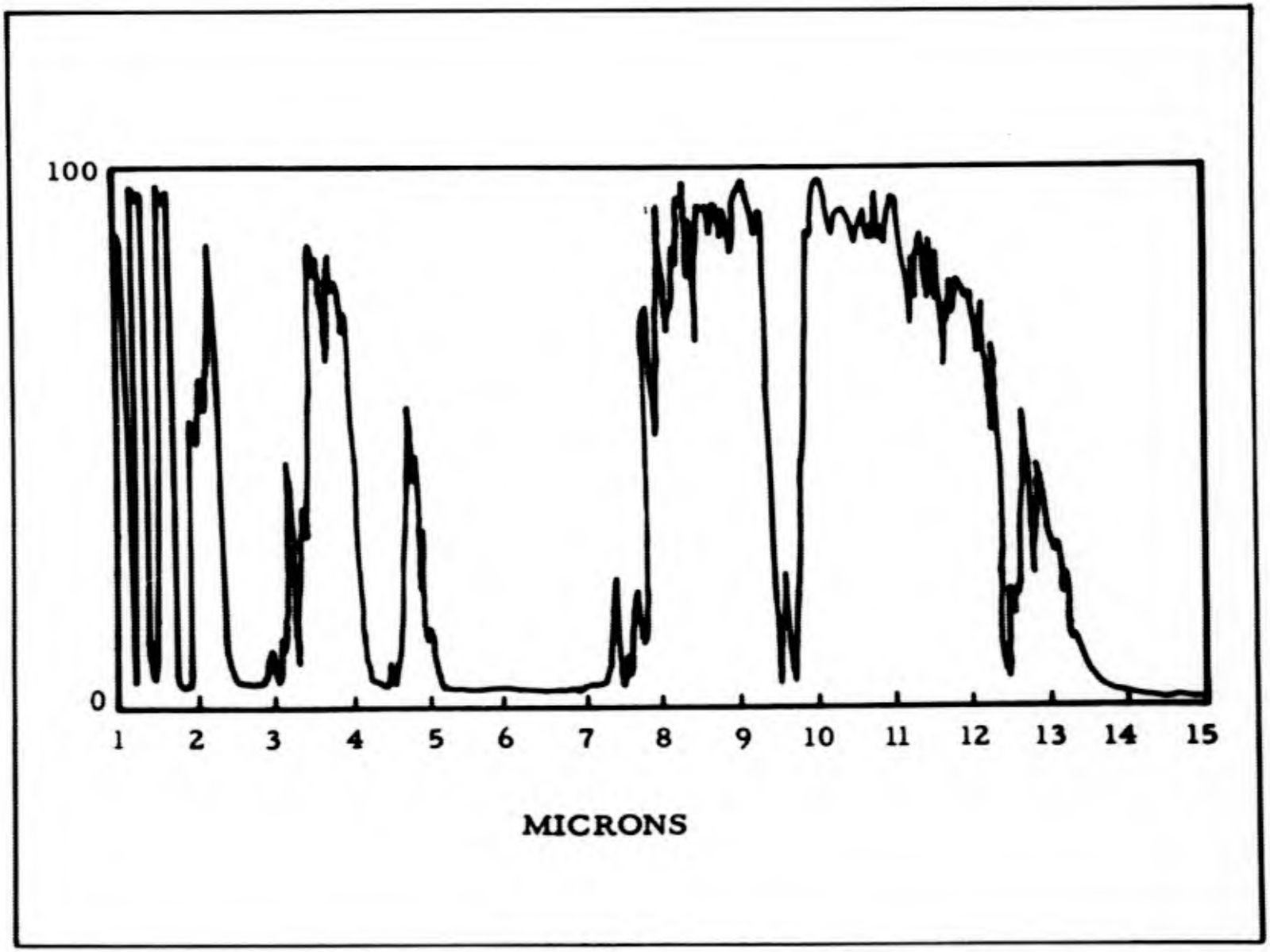

FIGURE 4-1 INFRA-RED TRANSMISSION OF ATMOSPHERE BETWEEN 1 AND 15 MICRONS (SHAW, OHIO STATE, 1954)

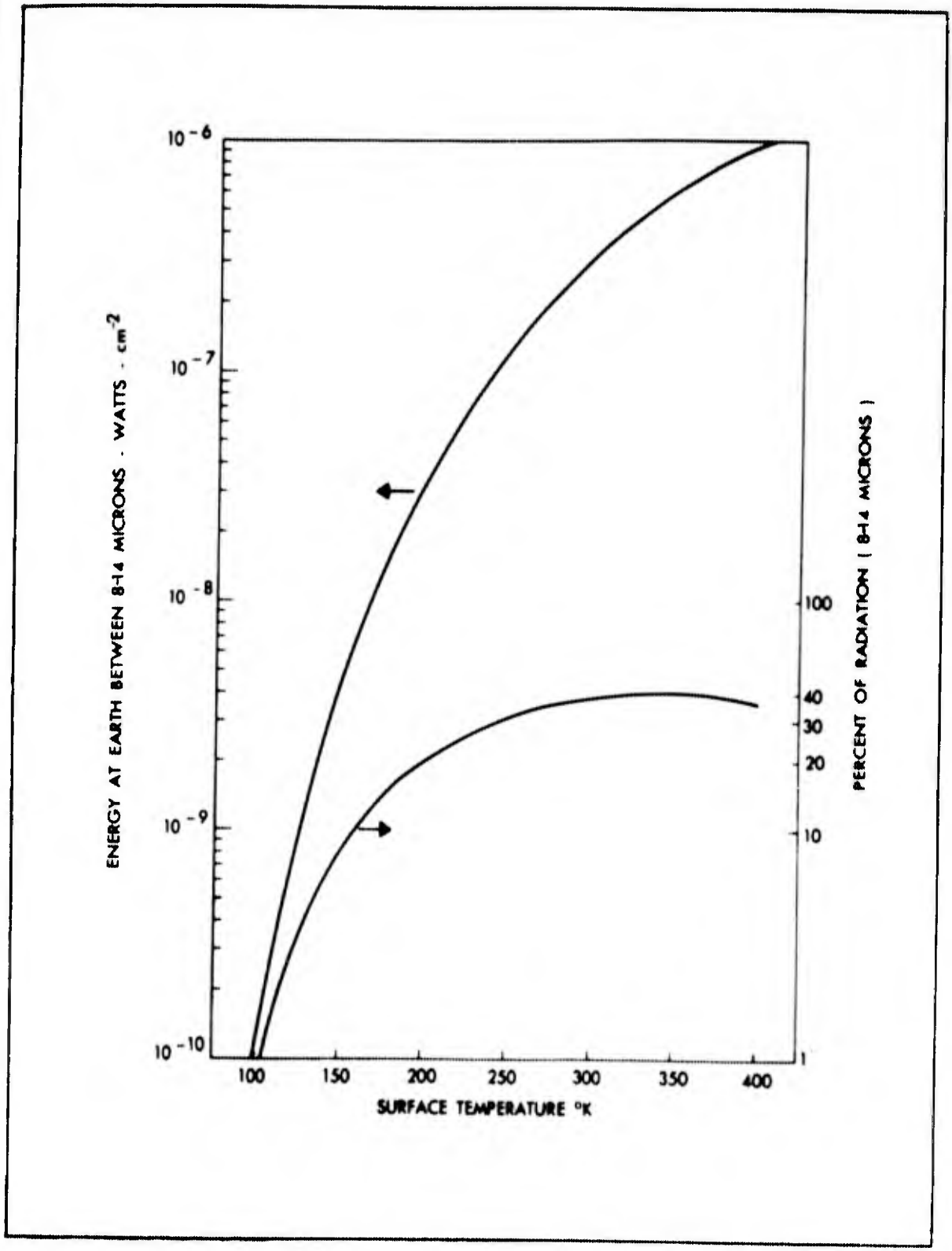

FIGURE 4-2 LUNAR RADIATION RECEIVED AT EARTH'S SURFACE

TABLE 4-1

TEMPERATURE OF MOON	RADIATION ABOVE EARTH'S ATMOSPHERE FROM FULL MOON	PERCENT 8-14 MICRONS	RESOLUTION IN MILES WITH 100 INCH MIRROR AND ONE PERCENT ACCURACY	
			WITH 4.10^{-10} WATT DETECTOR	WITH 10^{-8} WATT DETECTOR
DEGREES K	WATTS/CM^2			
400	2.5×10^{-6}	38	2	10
350	1.5×10^{-6}	40	2.6	13
300	8.0×10^{-7}	38	3.6	19
250	3.8×10^{-7}	32	5.7	28
200	1.6×10^{-7}	21	11	55
150	5.0×10^{-8}	8	31	150
100	1.0×10^{-8}	1	200	1000

Actually this curve represents a very idealistic condition of the most excellent seeing which is quite rarely available. The optimism is indicated by a calculated resolution of 2 miles at 400° K as opposed to Pettit and Nicholson's best obtainable resolution of 50 miles.

4.3 SATELLITE BORNE INFRA-RED MEASUREMENTS

With infra-red equipment carried in a lunar satellite, resolutions of one mile or less may be obtained with respect to lunar daytime surface temperature measurements. With such improved resolutions out-croppings of bare rock or variations in the dust layer thickness may be determined. Nighttime temperature can be measured and the existence of deep canyons if they exist may be established with adequate resolutions. To illustrate these measurements, calculations have been made for existing infra-red scanning equip-

ment. Table 4-2 gives characteristics of two possible lunar satellite infra-red scanners based on Barnes Engineering Co. thermistor radiometers. Although both scanners employ 8 inch mirrors, the field of view and sensitivities have been adjusted by using thermistors of different area. The system time constant of each is 0.016 sec. corresponding to a 10 cps bandwidth which is about reasonable for a lunar satellite transmitter. The noise equivalent power of each system is calculated as shown at the bottom of the table. Also shown are the noise equivalent power and energy of the detectors. Compared to a theoretical limit for such detectors as given by Havens[3], these detectors are within a factor of 40 of the limit given, which is quite good. For these systems, using space as the reference temperature, the noise temperature errors at 300°K and 100°K using the energy from 5-200 microns will be as shown. If a window with a 34 micron cut off were used the 100°K error would be increased by somewhat more than 2. These temperature error values are plotted in Fig. 4-3. The temperatures are measured by comparing a known source with the unknown body. For a satellite system the reference could be space at 0°K. (The mirror itself will radiate and if its temperature is 300°K the space temperature may appear to be about 120°K. For night time temperature measurement the mirror will have to be cooled to less than 150°K).

For these scanners the resolution (or field of view) of the systems are shown in Fig. 4-4 as a function of the altitude of the satellite above the lunar surface. For example, at 1000 miles altitude, the resolution of the 1/16° scanner will be about one square mile, and for the 1/2° scanner the value will be about 8 miles square. As the satellite proceeds along its trajectory over the surface the scanner can view a path whose width will be determined by the satellite velocity (fixed), the time constant of the system and the field of view. The scan width possible with the reference systems is shown in Fig. 4-5. Thus for a satellite altitude of 1000 miles the 1/16° scanner will provide a measurement of the temperature over a path 24 miles wide with a resolution of about 1 mile. The 1/2° system will essentially scan the entire lunar surface on each pass with a resolution of about 8-10 miles.

4.4 SUB-SURFACE TEMPERATURE

A simple calculation can be made of the sub-surface temperature as a function of the average night surface temperature. This is based on an average daytime surface temperature of 320°K, maximum of

TABLE 4-2

INFRA-RED SCANNER CHARACTERISTIC *

	FIELD OF VIEW	$1/2^{\circ} \times 1/2^{\circ}$	$1/16^{\circ} \times 1/16^{\circ}$
	THERMISTOR AREA	2.5 x 2.5 MM.	0.3 x 0.3 MM.
	MIRROR DIAMETER	8 INCHES	8 INCHES
	SYSTEM TIME CONSTANT	0.016 SEC	0.016 SEC
	BANDWIDTH	10 CPS	10 CPS
	NEP (WATTS - CM^{-2})	1.7×10^{-10}	2.1×10^{-11}
	NEE (DETECTOR) WATTS	1.8×10^{-8}	2.2×10^{-9}
	NEE (DETECTOR) JOULES	2.9×10^{-10}	3.6×10^{-11}
	NEE (LIMIT) JOULES	7.5×10^{-12}	9×10^{-13}
	RATIO	39	39
**	T (300° K) 5-200μ	016° C	0.1° C
	T (100° K) 5-200μ	0.42° C	3.3° C
	T (100° K) 8-34μ	1.1° C	8.8° C

** $\frac{\sigma T^3 \Delta T \phi^2}{57^2}$ = NOISE EQUIVALENT POWER (WATTS-CM^{-2})

REFERENCE TEMPERATURE - TAKEN AS SPACE

* BASED ON BARNES ENGINEERING CO. RADIOMETERS

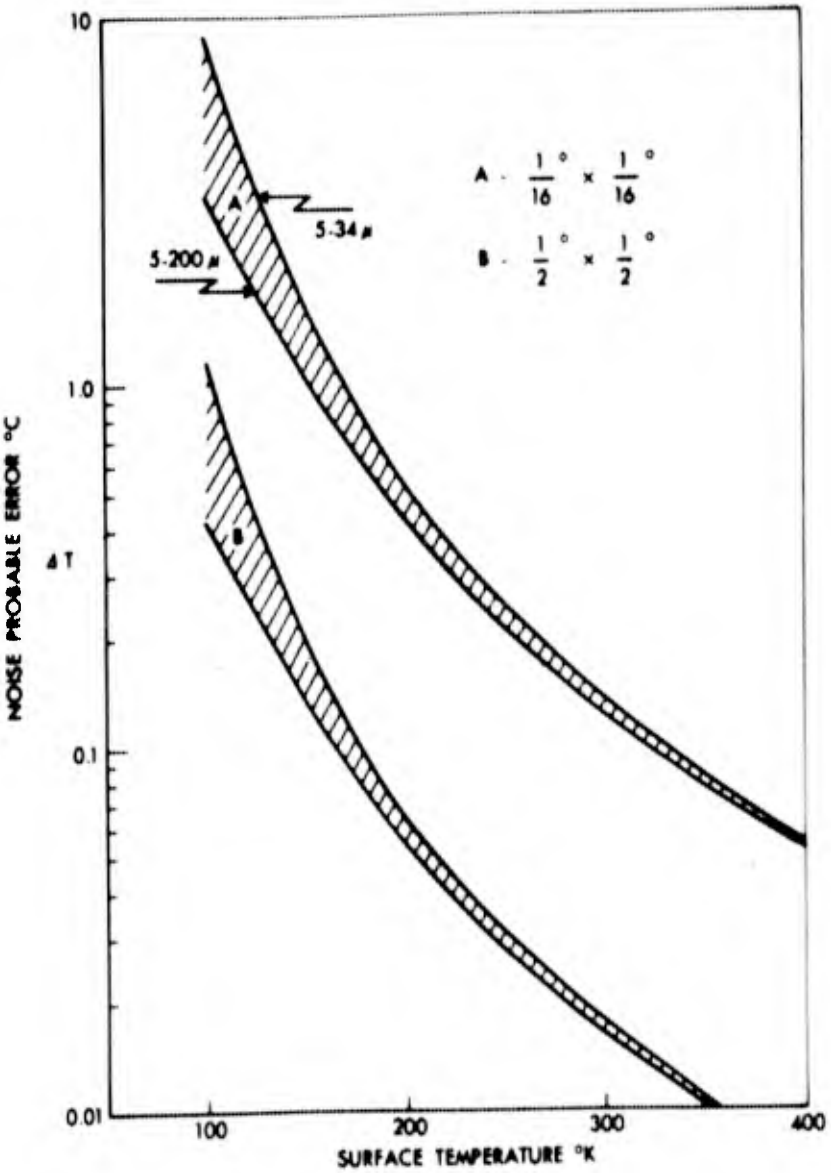

FIGURE 4-3 SYSTEM TEMPERATURE ERROR AS A FUNCTION OF SURFACE TEMPERATURE

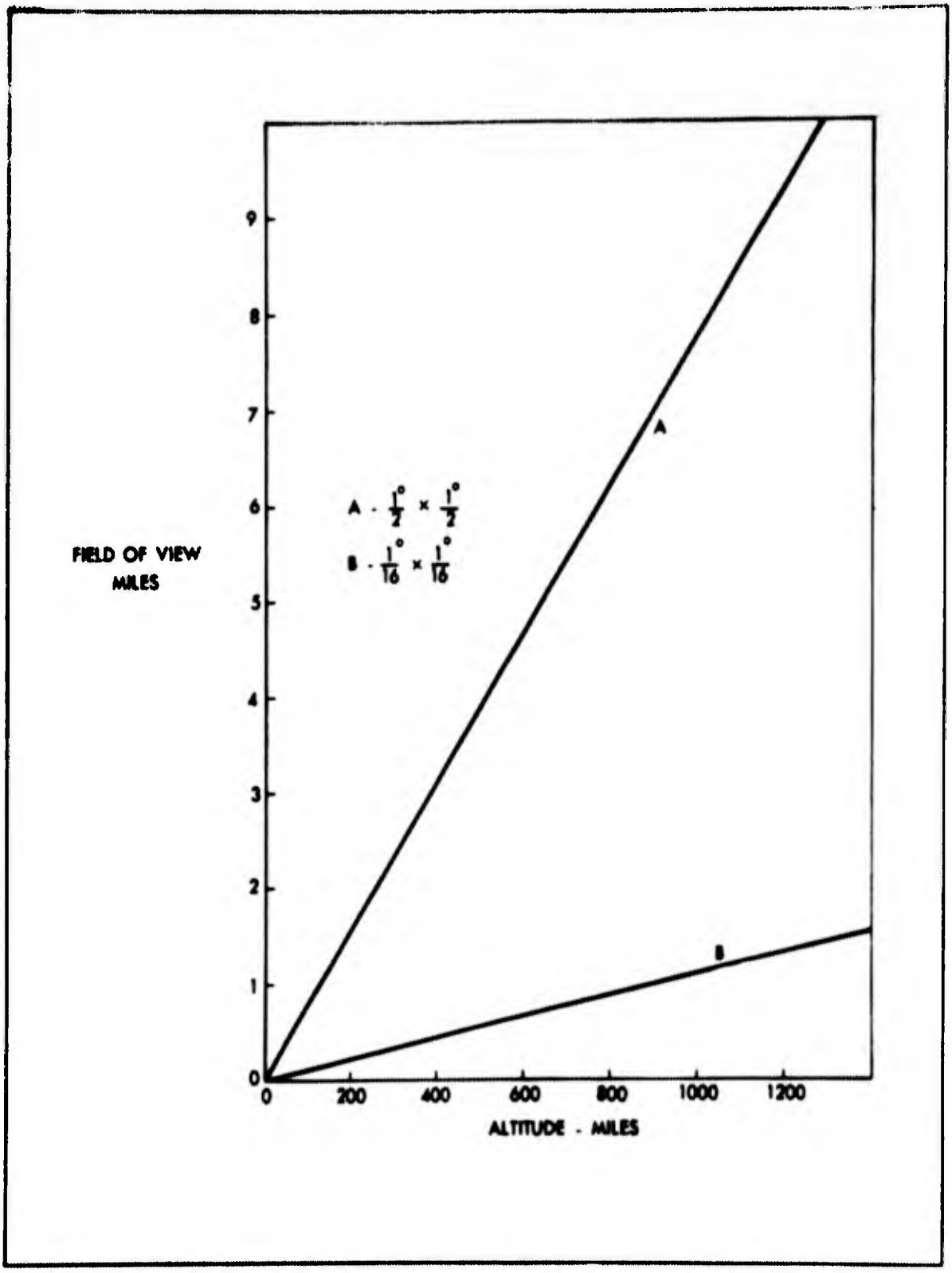

FIGURE 4-4 LUNAR SATELLITE INFRA-RED SCANNERS FIELD OF VIEW VS ALTITUDE

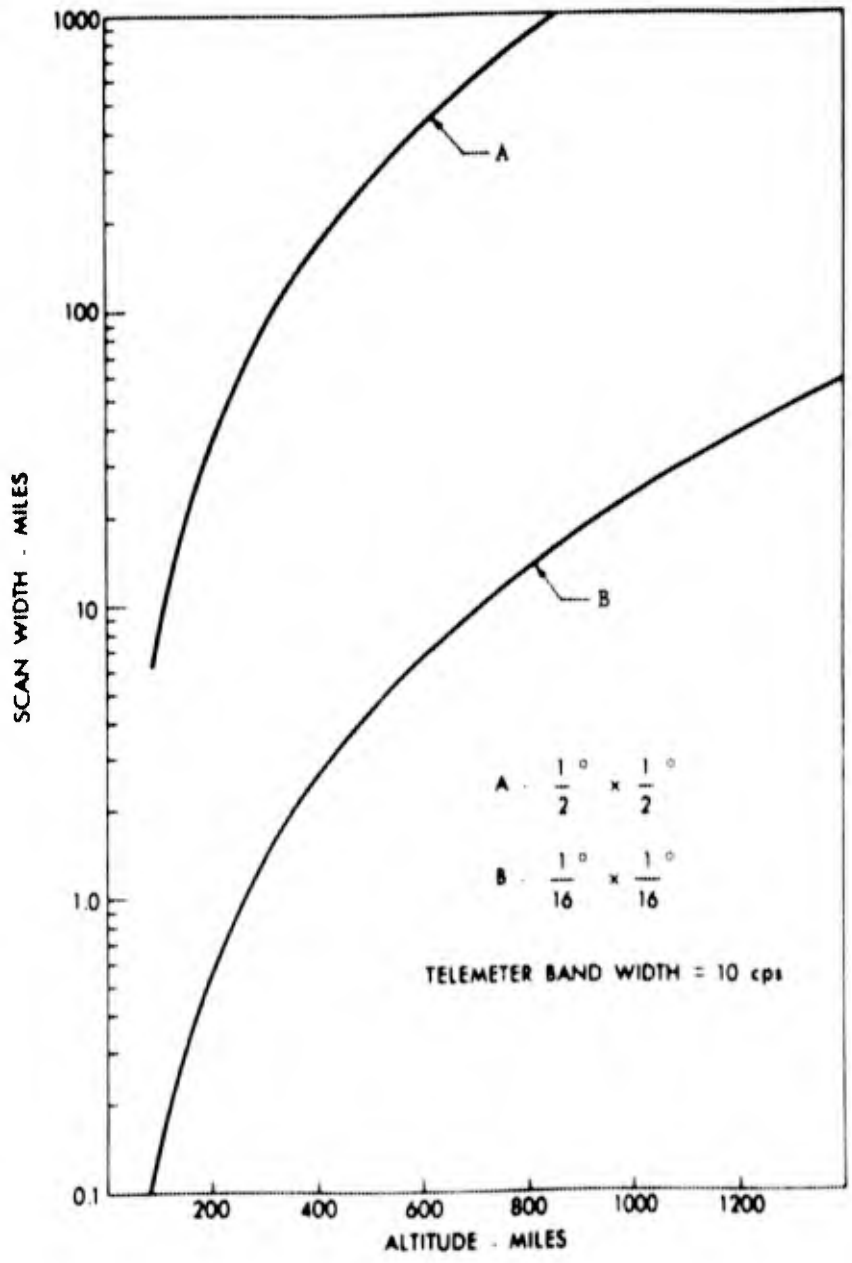

FIGURE 4-5 SCAN WIDTH VS ALTITUDE

400°K, and the equating of the heat conducted inward during the day to the heat conducted outward at night. This can be expressed as:

$$\frac{\alpha}{X}\left(T_d - T_o\right) = \frac{\alpha}{X}\left(T_o - T_N\right)$$

where α = conductivity

X = dust layer thickness

T_d = daytime surface temperature

T_n = nighttime surface temperature

T_o = sub-surface temperature in constant region

This leads to

$$T_n = 2T_o - 320$$

The value of the sub-surface temperature as a function of nighttime surface temperature is plotted in Fig. 4-6. Piddington and Minett[4] have found by means of measurement of the lunar radiation at 2400 megacycles that the sub-surface temperature is about 240°K. This would lead to a nighttime surface temperature of 160°K which is known to be too high. A more likely nighttime surface temperature of 125°K would lead to a sub-surface temperature of about 225°K.

The heat radiated from the nighttime surface must also be equal to the heat conducted to the surface from which:

$$\frac{\alpha}{X}\left(T_o - T_n\right) = \sigma T_n^4$$

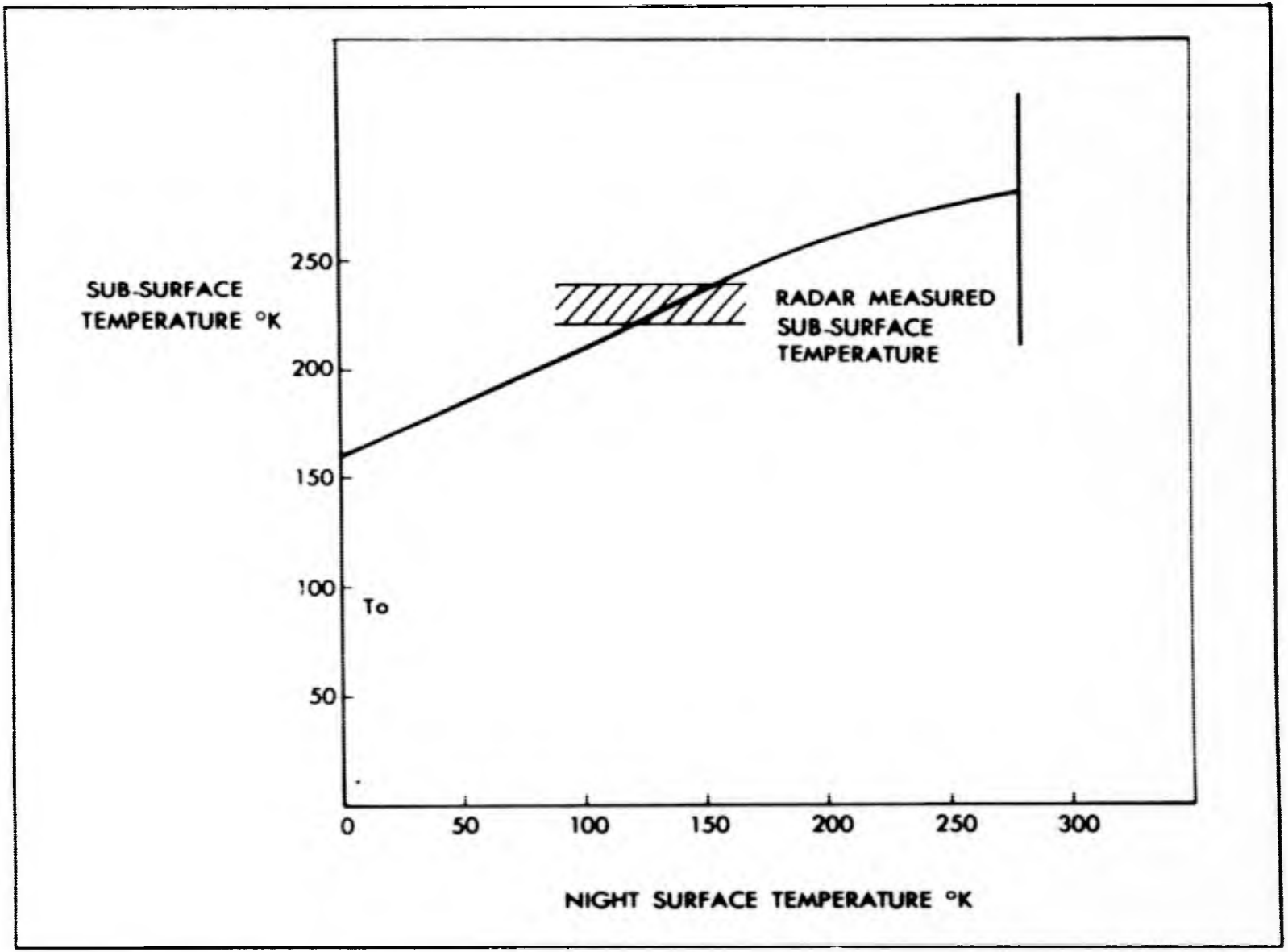

FIGURE 4-6 LUNAR SUBSURFACE TEMPERATURE VS AVERAGE NIGHT SURFACE TEMPERATURE

so $$\frac{\alpha}{X}\left(160 - \frac{T_n}{2}\right) = \sigma T_n^4$$

or $$\frac{\alpha}{X} = \frac{2\sigma T_n^4}{320 - T_n}$$

Values of the dust layer thickness, X, as a function of T_n are shown in Fig. 4-7, assuming $\alpha = 10^{-3}$ watts/cm ^{o}C, 10^{-4} watts/cm ^{o}C and 10^{-5} watts/cm deg.

Because of the heat capacity of the dust (assume one joule/deg cm^3) there will be a lower limit to the temperature (T_n). It is known that the temperature drops to below 150 ^{o}K, so that α must be 3×10^{-4} watts/cm deg or less.

There may be local mountains or canyons where the dust layer is thin. In this case the average day temperature would be less than 320^{o}K and the night temperature would be greater than 125^{o}K. A dust thickness of 6 millimeters over solid granite ($\alpha = 10^{-1}$) or iron ($\alpha = 0.6$) would result in an average night temperature of 200^{o}K if α (dust) = 10^{-4}. It is probable that the sides of mountains and canyons could not hold more than 6 mm of dust.

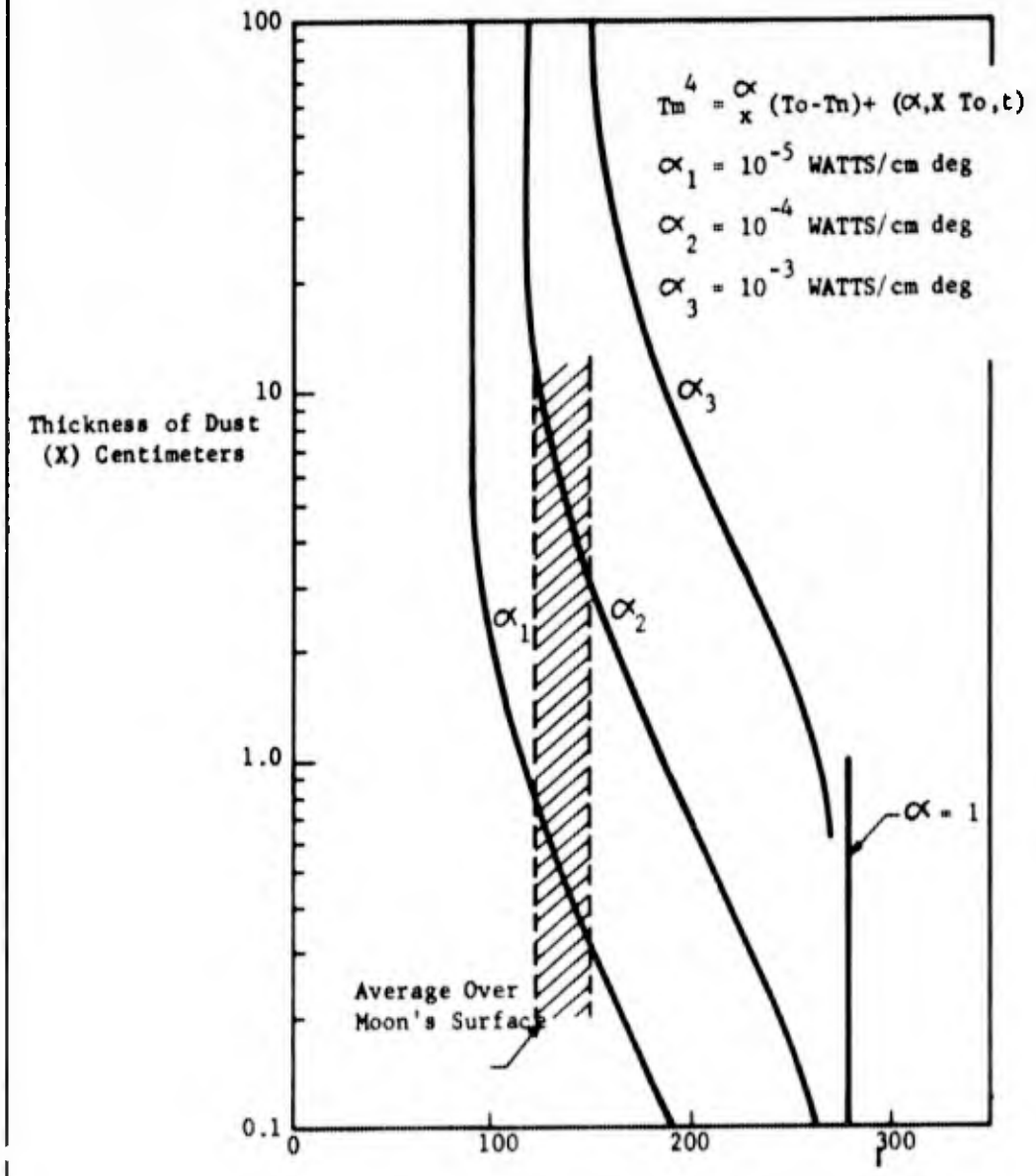

FIGURE 4-7 AVERAGE NIGHT SURFACE TEMPERATURE

REFERENCES

1. E. Pettit and S. B. Nicholson, Astrophys. J., 71, 102 (1930)
E. Pettit, Astrophys. J , 81, 17 (1935)
E. Pettit, Astrophys. J., 91 408, (1940)

2. Shaw, Ohio State Report, 1954

3. R. J. Havens, IRIS Report, June 1957, Vol. 2, No. 1, Page 5.

4. J. H. Piddington and H. C. Minett, Aust J. Sci. Res., A2, 63 (1949).

SECTION 5

LUNAR RADIOACTIVITY

5.1 INTRODUCTION

One source of information as to the lunar composition which is completely unavailable except in a research vehicle is the radioactivity of the moon. There appears to be a reasonable possibility that measurements can be made without actually landing. Neutron capture radiation and other radioactivity due to cosmic rays may be observed also. Of course all estimates of lunar radioactivity must be based on known facts about terrestrial and meteoritic materials as well as whatever can be inferred from observational techniques.

Information about the concentration of radioactive elements in the lunar surface will be important in determining the origin and geological history of the moon. It should be possible to determine whether the moon was ever molten and whether differentiation into a mantle and crust has occurred as in the case of the earth. It may be possible to resolve the question of the heat balance which is strongly dependent on radioactive composition. In addition measurement of lunar radioactivity can provide an indication of proximity.

5.2 RADIOACTIVITY OF THE EARTH

The naturally radioactive nuclides which are found on the earth are widely distributed in low concentrations in practically all rocks and soil. From considerations of the rate of heat generated by the radioactive processes, it seems certain that the bulk of this material must be contained in the outer few kilometers of the crust. Table 5.1 gives some of the measured concentrations (corrected for isotopic abundance) of the known radioactive elements in igneous rock and in meteorites. The figures in the table are for the individual isotopes. Other nuclides produced by spontaneous fission of the heavy elements have been found but are not listed because of the minute quantities involved. It may be seen that uranium, thorium and potassium account for most of the terrestrial and meteoritic radioactivity. Uranium and thorium have complicated chains of decay products which usually can be considered to be in secular equilibrium with the parent substance. Most of the uranium and thorium radiation is associated with the daughter products. Potassium is weakly radioactive but because of its abundance contributes significantly to the total radiation. Rubidium 87 is a beta emitter only, and samarium 147 is an alpha emitter. Therefore measurement of these radiations will be difficult because of absorption. The other elements, lutetium and rhenium, plus some isotopes from spontaneous fission of heavy elements make only a small contribution to the total radioactivity. The disintegration rates shown in the last column are the total disintegration rates for the various elements. To obtain the activity per gram of rock or meteorite this disintegration rate must be multiplied by the concentration as given in the other columns. For stone meteorites a range of values is shown. While the higher values have been measured, the lower values are those estimated by Urey[1] based on his theory of lunar formation and composition.

The lower value for thorium in iron meteorite is quoted from recent work at Argonne[2] using neutron activation techniques. The figures assume only one gamma ray per disintegration for uranium and thorium.

5.3 RADIOACTIVITY OF THE MOON

The lunar composition has been discussed at some length, principally by Urey[3][4]. The average density of the moon is about 3.34 which has led to the conclusion that it contains relatively little iron and nickel. Furthermore it appears to be essentially a rigid body

TABLE 5.1

CONCENTRATION OF NATURALLY RADIOACTIVE SUBSTANCES IN THE EARTH

ELEMENT	CONCENTRATION - GM/GM x 10^{+6}			DISINTEGRATIONS SEC^{-1} GM^{-1}
	IRON METEORITES	STONE METEORITES	IGNEOUS ROCKS	
URANIUM	0.007	0.106 - 0.4	4.0	2.5×10^{4}
THORIUM	0.04	0.03 - 4.4	11.5	4.1×10^{3}
POTASSIUM-40	----	0.10 - 0.2	3.1	31
RUBIDIUM-87	----	1.2	85	110
SAMARIUM-147	----	0.18	---	110
LUTETIUM-176	----	0.0016	(0.002) Shale	66
RHENIUM-187	0.0052	0.0005-0.0014	0.0006	90

without a liquid core. Certain light elements probably are not present since they would have been lost as a result of the low gravitational attraction.

There is some question as to whether the moon was originally molten or not. If it were built up by accretion of smaller bodies such as meteorites it is possible that it never was fluid. Consideration of the heating effects however requires that the concentration of radioactivity in the moon be less than in stone meteorites. The high concentration of uranium and thorium in the crust of the earth may be explained by the tendency of these elements to become enriched in granitic and pegmatitic melts. Therefore the moon may have a vastly different composition depending upon whether there has been sufficient melting to cause magmatic differentiation.

Table 5.2 gives values for the gamma radiation from the three most important elements assuming various lunar compositions. No value for potassium in iron meteorites is available but the ratio of potassium to thorium and uranium should be about the same as for stone meteorites. The lower value for thorium is from a recent measurement at Argonne using neutron activation techniques. A lunar surface resulting from meteorite accretion should include an admixture of iron and stone.

The moon has no atmosphere[6], or at least it is not significant with respect to the absorption of gamma radiation. Therefore the measured counting rate as a function of distance from the moon depends only on the solid angle subtended by the moon at the counter, the gamma ray energy and the mean free path in the lunar surface material.

Figure 5.1 shows the geometrical relationships upon which the calculation is based. The counting rate I, at point P from a volume element dV will be

$$I = \frac{N_o}{4\pi r^2} \, dV$$

where N_o is the surface disintegration rate.

TABLE 5.2

LUNAR GAMMA RADIATION

COMPOSITION	URANIUM	THORIUM	POTASSIUM
	DISINTEGRATIONS (10^{-3} SEC^{-1} GM^{-1})		
IGNEOUS ROCK	100	47	96
STONE METEORITE	2.7 - 10	1.2 - 18	3.1 - 6.2
IRON METEORITE	0.2	10^{-8} - 0.16	------

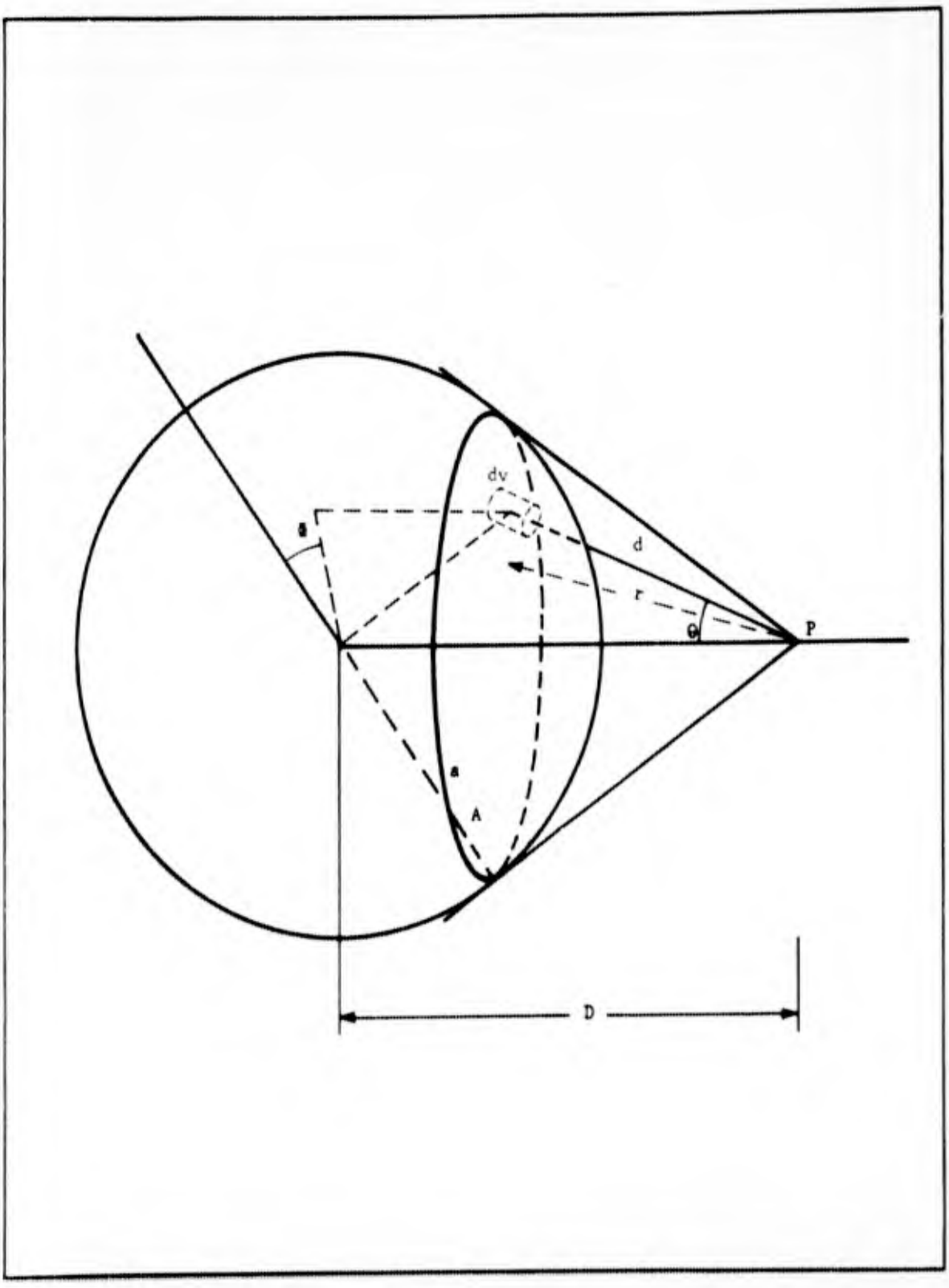

FIG. 5.1 GAMMA-RAY COUNTING RATE AS FUNCTION OF DISTANCE FROM MOON

Since

$$dV = r^2 \sin\theta \, d\theta \, d\phi \, dr$$

the total counting rate at P will be given by

$$I_T = \frac{N_o}{4\pi} \int_0^{\infty} \int_0^{2\pi} \int_0^{\cos^{-1}\frac{(D^2-A^2)^{1/2}}{D}} e^{-\frac{(r-d)}{\lambda}} \, dr \, d\phi \sin\theta \, d\theta$$

where λ is the absorption mean free path for the gamma radiation under consideration and θ is integrated from zero to the horizon given by $(D^2 - A^2)^{1/2}/D$. Performing the indicated integration

$$I_T = \frac{N_o}{2} \left[1 - \frac{(D^2 - A^2)^{1/2}}{D} \right]$$

The result of this calculation which is plotted in Figure 5.2 for distances out to 3.8 moon radii merely represents the solid angle subtended by the moon at these distances. Because of the relatively small radius of curvature, the counting rate will continue to increase almost until contact.

Making use of the above, the gamma ray flux for three possible lunar surface compositions is shown in Figure 5.3. The gamma radiation from uranium and thorium has been taken as two gamma rays per disintegration and the mean energy as 1 MeV. The lunar surface is assumed to have a density of three. Actually there should be a somewhat greater number of gammas and multiple scattering will tend to degrade the already fairly complicated spectrum of radiation. Both the upper and lower limits for stone meteorites are shown.

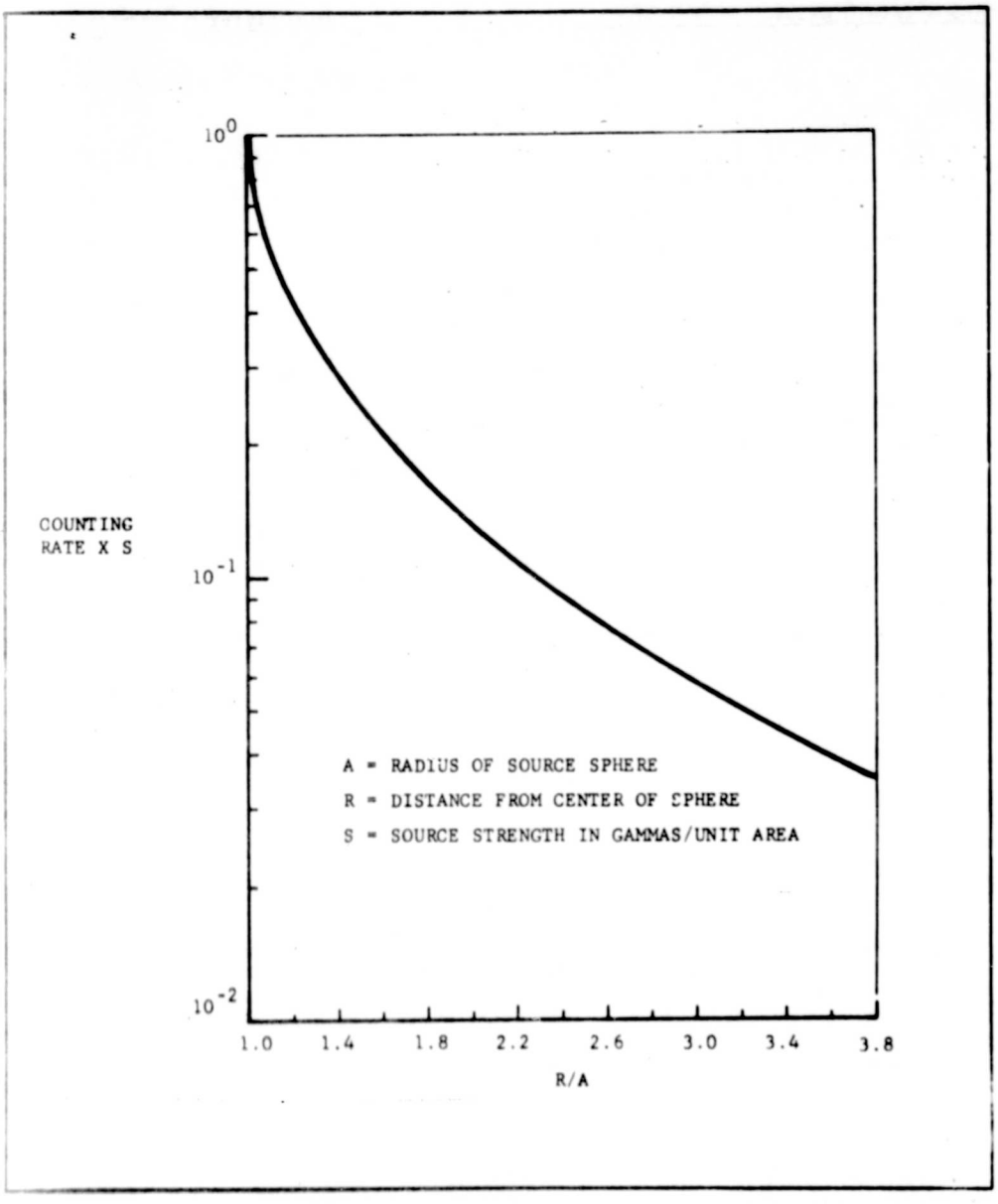

FIG. 5.2 GAMMA-RAY FLUX VS DISTANCE FROM SPHERICAL SURFACE SOURCE

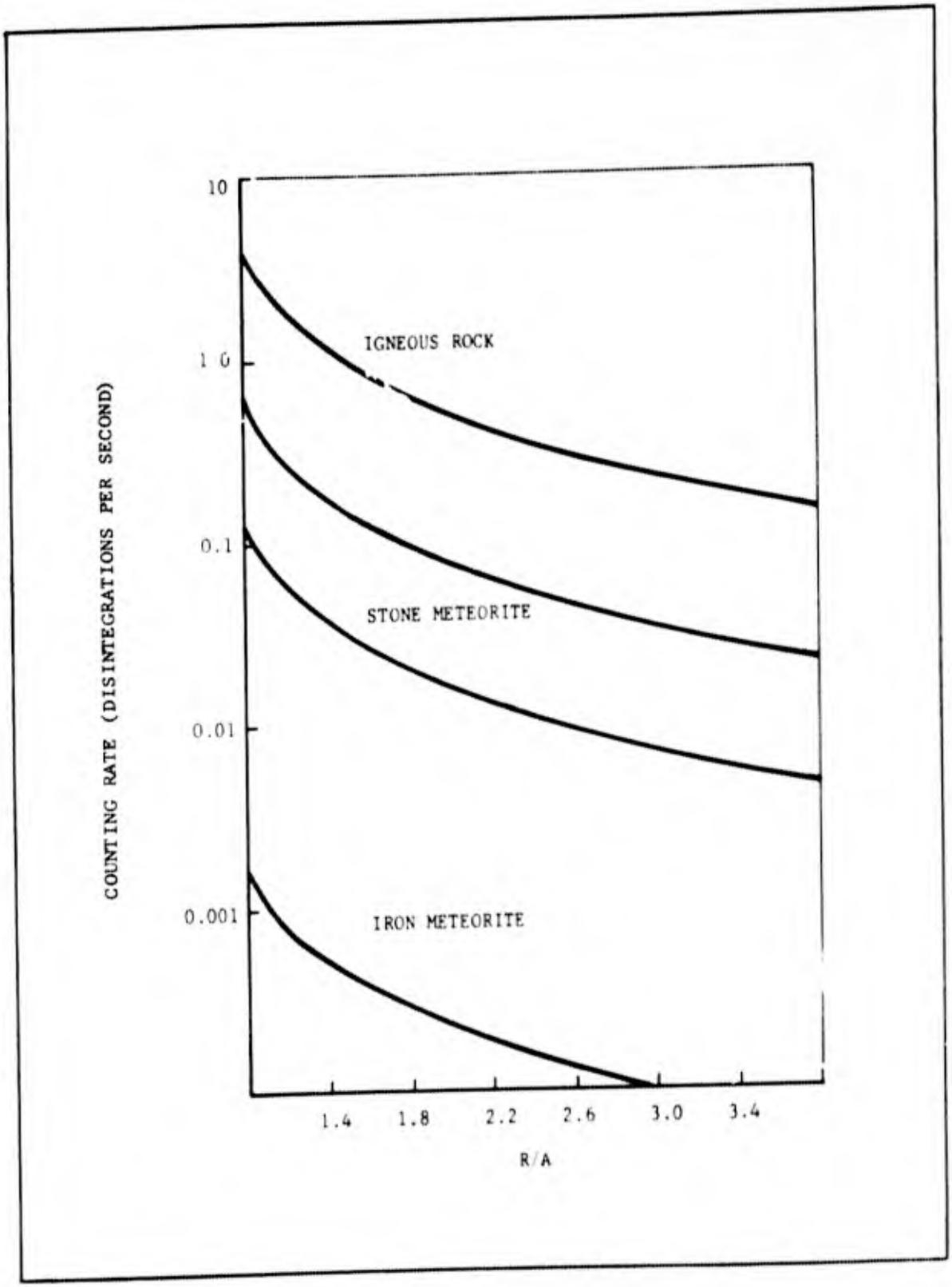

FIG. 5.3 GAMMA RADIATION FROM MOON

Because of the lack of an atmosphere cosmic ray primary radiation will interact with the surface material to form secondaries and finally gamma rays. As shown in Figure 5.4 the primary cosmic radiation will decrease as the lunar surface is approached and because of solid angle considerations will approach a limiting value of one half at the surface. In the assumed lunar surface these primaries have a mean free path of about one meter. The absorption lengths for the secondaries have been arbitrarily set at 167 gm - cm^{-2} for the hard component and 5 gm - cm^{-2} for the soft.

Another problem that may be considered is the contribution to the counting rate by the radioactive gas, radon. Since radon condenses at the temperature of the dark side of the moon it is possible that it would flow to the cold lunar surface nearly as fast as it is formed, producing a surface layer of radioactivity.

A further refinement of the measurement of lunar radioactivity would be the determination of the energy of the gamma rays. This will allow the relative amounts of potassium, uranium and thorium contained in the surface to be ascertained. In addition the spectrum of the neutron capture gamma rays produced by cosmic radiation may be measured and provide estimates of the concentration of such elements as iron, manganese and silicon. Induced radioactivity as well as annihilation radiation (0.51 MeV) may also be detectible. The most prominent gamma rays from the naturally radioactive elements are shown in Table 5.3. Arnold[5] has measured experimental spectra with large samples of "simulated chondrite" and it appears from this preliminary information that sufficient discrimination can be obtained for identification of the naturally occurring isotopes.

5.4 INSTRUMENTATION

From Figure 5.4 it is apparent that if the lunar surface has a composition similar to that of stone meteorite, both the primary and induced cosmic radiation intensity may be of about the same magnitude. It will be advisable therefore to employ anticoincidence counters to eliminate or at least reduce the cosmic ray background.

The circuitry could be arranged so that both the gamma rays from the surface and the ambient cosmic radiation can be measured simultaneously. The counting rate will probably be low so that real-time telemetry can be employed at a bandwidth of about 1 cycle. The

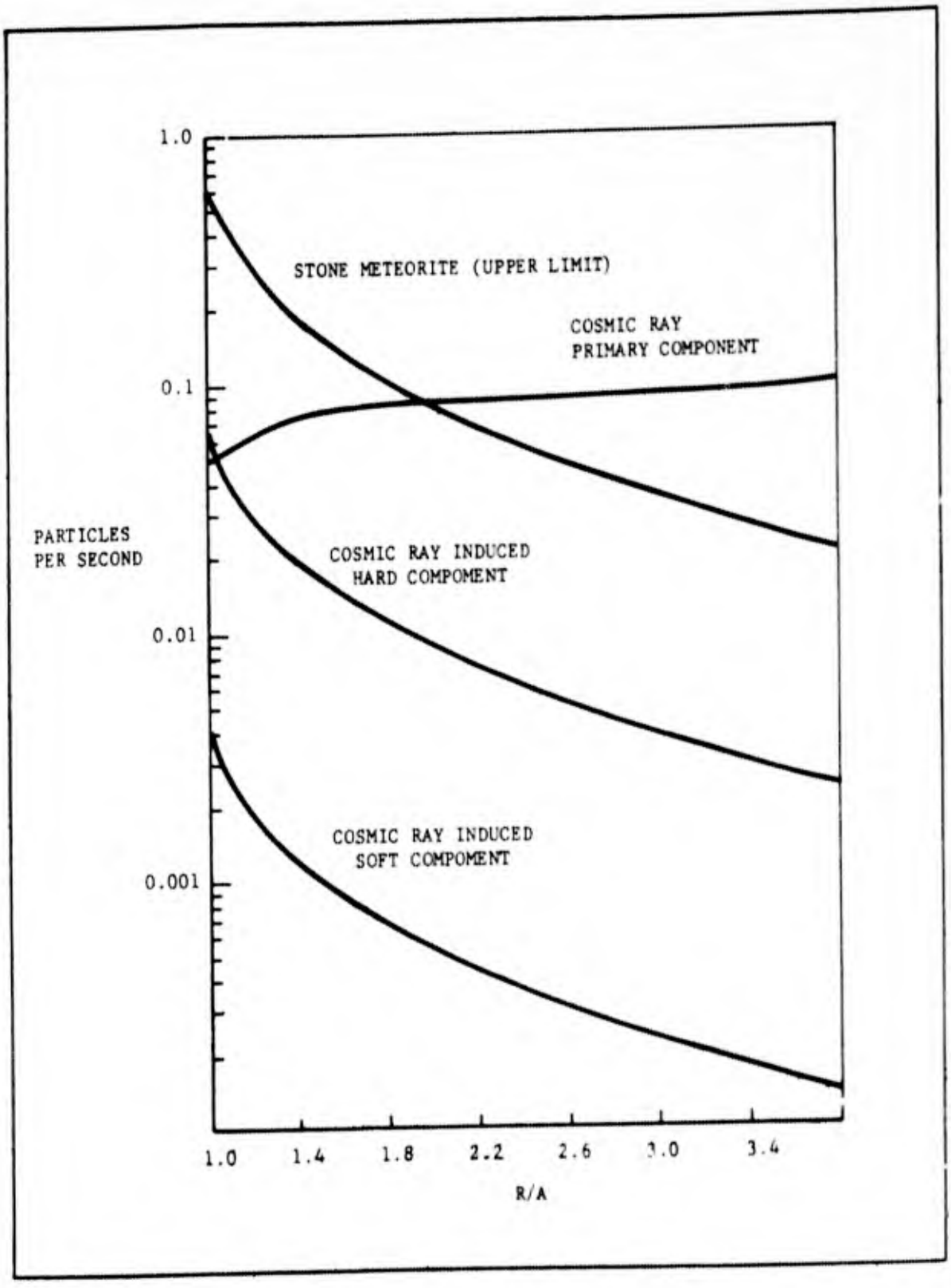

FIG. 5.4 INDUCED COSMIC RADIATION FROM MOON

TABLE 5.3

ENERGY OF NATURALLY RADIOACTIVE SUBSTANCES

Parent	Isotope	MeV	γ's Per Disintegration
U^{238}	RaB(Pb^{214})	0.24	0.12
		0.29	0.26
		0.35	0.45
	RaC(Bi^{214})	0.61	0.66
		1.12	0.21
		1.76	0.26
Th^{232}	Ac^{228}	0.34	0.09
	ThB(Pb^{212})	0.94	0.45
		0.24	0.80
	ThC'' (Tl^{208})	0.58	0.27
		0.62	0.34
K^{40}	K^{40}	1.46	0.1

above instrumentation would be more or less equivalent to that used for studies of the Van Allen radiation[6][7] and should be well within the vehicle payload capability.

A gamma ray spectrometer is of course somewhat more complicated. The detecting element in this case will be a large scintillation crystal and suitable photomultiplier. The electronic elements will include a high voltage supply, linear amplifier and multi-channel analyzer. Because of the low counting rate per channel it will be desirable to make measurements for as long a time as possible. This would require that counts be accumulated during the approach and perhaps once again after passing, assuming of course a non-impact trajectory. Arnold, et al[5] recommended 64 channels and a 2000 bit magnetic memory unit and state that the above instrumentation can be constructed to weigh about 20 lbs.

REFERENCES

1. Urey, H. C., Geochim, et Cosmoshim. Acta, 1, 209 (1951).

2. Bate, G. L. et al, Geochim et Cosmochim Acta, 14, 118 (1958).

3. Urey, H. C., The Planets, Yale Univ. Press, (1952).

4. Kuiper, G. P., Proc. Nat. Acad. Sci. 40, 1096 (1954).

5. Arnold, J. A. et al, Proposal to NASA, Mar. 17, 1959.

6. Van Allen, J. A. et al, Jour. Geophys. Res., 64, 271 (1959).

7. Sonnet, C., Lunar and Planetary Exp. Coll. 1, 42, (1959).

SECTION 6

LUNAR FLUORESCENCE

6.1 INTRODUCTION

The property which some minerals have of emitting light of characteristic color upon irradiation in the ultraviolet is useful in the identification of mineralogical specimens. If such radiation can be detected from the moon, it is possible that it would provide evidence as to its surface composition. It is obvious from even casual observation that the moon does not show marked color. This of course is not surprising in view of its low albedo. The average albedo is about 7% or comparable to that of moist earth. Although colors have been reported for various lunar objects many observers deny that any marked color differences are apparent. Further systematic and objective research in this area is needed.

6.2 SOLAR ENERGY INPUT

Because of the absence of a lunar atmosphere the short wavelength solar radiation can strike the surface. If the moon has no magnetic field or if the field is small, as seems to be quite likely, solar protons and the cosmic radiation will also penetrate down to the surface. The limiting field intensity which allows penetration to the lunar surface (neglecting effect of the atmosphere) will be

$$H_o = \sqrt{4\pi\rho v^2}$$

Even for a quiet sun solar protons may strike the surface unless the lunar field is at least 200γ at the surface.

The solar energy contained in various wavelength regions is given in Table 6.1.

TABLE 6.1

SOLAR ENERGY INPUT AT VARIOUS WAVELENGTHS

	Erg/cm^2/sec
Particulate	10^4 - 10^5
1000 Å	0.4
1000 - 1760 Å	10^2
1760 - 3000 Å	10^4
3000 - 10,000 Å	10^6

It is evident that the total energy received below say 3000 Å is sufficient to produce only a relatively small effect. Therefore rather sensitive instrumental techniques will be required to detect any possible fluorescence. Unfortunately absolute measurements of the lunar brightness as a function of lunar geography are not available, and spectrographic results are likewise unavailable.

6.3 FLUORESENCE

Fluorescence, or the emission of light upon irradiation, has been studied extensively.[7] Many organic phosphors such as fluorescein are known, but can hardly be important on the moon. On the other hand, it is not unreasonable to assume the presence of fluorescent minerals similar to those found on the earth.

According to Pringsheim [5] luminescent minerals fall into three classes:

1. Luminescence as an essential property, as in the case of uranium (uranyl) containing minerals
2. Luminescence due to minute traces of impurities
3. Luminescence resulting from exposure to ionizing radiation

For impurity fluorescence the spectral distribution of the emitted light is in general complex and does not exhibit a simple line

structure from which it is possible to identify a given substance. The same mineral will often fluoresce in different wavelength regions depending on the impurity which is present. Willemite ($Zn_2 SiO_4$ + impurity) which was reported by Dubois[9] on the basis of his spectrographic measurements, falls in this group.

While the formation of the moon has been the subject of some controversy, the possibility that fluorescent minerals exist on the lunar surface cannot be excluded, whether meteoritic accretion or a terrestrial origin is assumed. Table 6.2 gives the mineralogical composition of stone meteorites. The most abundant minerals are those common to the crust of the earth. For example, feldspar (anorthite) minerals are often fluorescent due to minute amounts of impurities. Table 6.3 is taken from DuBois and shows fluorescent terrestrial minerals which are known to occur extensively in open deposits.

TABLE 6.2

MINERALOGICAL COMPOSITION OF STONY* METEORITES

	Chondrites		Achondrites	
Mineral	Metal	Metal Free	Metal	Metal-Free
Free Metal	10.6	--	1.6	--
Olivine	42.3	47.3	12.8	13.0
Pyroxenes	28.9	32.4	62.3	63.2
Anorthite	3.3	3.7	13.2	13.4
Albite	7.4	8.2	5.8	5.9
Orthoclase	1.1	1.2	1.7	1.7
Troilite	5.0	5.6	1.5	1.6
Schreibersite	--	--	0.40	0.41
Chromite	0.70	0.78	0.68	0.69
Cohenite	--	--	--	--
Apatite	0.67	0.73	--	--

*Stony meteorites make up over 80% of all meteorites

TABLE 6.3

LIST OF MINERALS LUMINESCENT UNDER IRRADIATION BY NEAR ULTRAVIOLET, WHICH OCCUR EXTENSIVELY IN OPEN DEPOSITS

Name	Chemical	Location of Important Deposit	Principal Emitted Wavelength
Anglesite	$PbSO_4$	Arizona	4000 Å
Autunite	$Ca(UO_2)_2(PO_4)_2$	Bohemia	5500 Å
Calcite	$Ca\ CO_3$	common	6000 Å
Fluorites	CaF_3	Alston, Moor (Eng.) Ohio, Ariz., Calif.	5000 - 4000 Å
Hackmanite	Salt of Ca	Dungannon Township	5500 - 6000 Å
Kunzite	$Al_2O_3nSiO_2$	Maine	6000 Å
Opal	SiO_2	common	4500 Å
Scheele	$CaWO_4$	common in Europe, Spain France, America	4800 Å
Willemite	Zn_2SiO_4	large deposit in New Jersey	5500 Å

6.4 FLUORESCENCE OF THE LUNAR SURFACE

Dubois[1,2] has reported measurement of fluorescent radiation from the moon and Link[3] cites excess brightness observed during the penumbral phase of an eclipse as evidence for this phenomenon. Dubois has made extensive measurements of lunar fluorescence using a line deepening technique. He compares the relative intensity of the Fraunhofer lines in light from the moon with the intensity of the same solar lines diffused through neutral magnesia. The additional light indicated by decreased line depths in microphotometer traces of the lunar spectrum is attributed to fluorescence of the lunar rocks. In fact Dubois reports the identification of Willemite as a surface constituent. Kopal[4] analyzed spectrographic measurements of Kozyrev[9] as support for the non-existence of a lunar magnetic field.

TABLE 6.4

LUNAR FLUORESCENCE

Lunar Region	Red 6560	Yellow 5893	Green 5200	Blue 4861	Violet 4300
	Relative Intensity of Luminescence				
Limb		0.14	0.20	0.40	
Region between Maria Serenitatis and Imbrium		0.05			0.06
Sinus Medii	0.12			0.10	
Mare Tranquillitatis	?	0.14			
Mare Fecunditatis	0.08	0.10			
Regiomontanus	0.25	0.13		0.05	
Mare Crisium		0.15	0.20	0.08	
Mare Frigoris (W)		0.06	0.07	?	0.04
Lat 12° S, long. 60° W.	0.07	0.10			0.03
Mare Nubium	0.12	0.07		0.14	
Oceanus Procellarum	0.20				0.10

6.5 SUMMARY

In view of the lack of knowledge of the lunar surface and the conflicting theories as to origin, it is probably not profitable to assume

any given mineralogical composition. Rather it may be useful to consider the available solar energy incident on the moon and to try to obtain an estimate of the intensity of the fluorescent radiation. Another factor which limits speculation as to the surface mineralogy is that by far the most common type of fluorescence is due to extremely small concentrations of elements which are present only as impurities in the lattice structure.

It may be noted also that fast particles such as occur in the solar wind can cause luminescence. For solar bursts of 10^5 protons cm^{-3} and 1.5×10^8 cm sec^{-1}, the energy flux at the lunar surface assuming no magnetic field would be about 3×10^5 erg cm^{-2} sec^{-1}. For a quiet sun condition it would be 1.1×10^2 erg cm^{-2} sec^{-1}.

It is only for the most intense solar bursts that the incident energy density would be comparable to that of the solar radiation in the region of the visible spectrum. For quiet sun conditions the incident energy would be reduced by a factor of more than 10^3. However, it may be that a search for this phenomenon at the time of solar disturbances would be valuable, although of course the probability of observing an effect is low.

It is observed that the lunar rays and certain craters brighten markedly with increasing solar angle.[6] It appears that maximum brightness occurs appreciably before full moon while after full moon the rays disappear rapidly. It is tempting to speculate that this brightening of the rays may be due to fluorescence.

Many substances (fluorites for example) are thermoluminescent.[7] It is possible in many cases to irradiate substances at low temperatures and to release the stored energy as luminescence by raising the temperature. Since the night time surface of the moon is at approximately -140°C and increases to about 100°C at the sub-solar point, it is conceivable that a thermoluminescent effect could occur. The decrease in light intensity with increasing temperature which is often observed for terrestrial materials may also have a counterpart on the moon.

A search for a sudden flash using spectrographic techniques as the terminator crosses a given lunar object may be worthwhile. The relatively low efficiency for producing fluorescence at low temperatures, may account for the absence of this effect on the dark surface of the moon. Kopal has suggested on the other hand that the lack of visible fluorescence during the lunar night indicates the absence of a magnetic field. He suggests that the curvature of the field if present would direct solar particles across the terminator.

From Table 6.4 the average effect for all spectral regions appears to be about 15 percent. Since luminescence in general is an efficient process (values near 100 percent have been reported), on the basis of the solar energy distribution it must be conceded that fluorescence could occur. Measurements at the present time are confined to rather difficult spectrographic techniques. These measurements are not likely to be feasible from a lunar research vehicle, at least based upon present knowledge. However if more information can be obtained and if perhaps certain wavelengths could be associated with specific lunar objects,[8] photoelectric detectors would be sufficiently sensitive to delineate the areas of interest. Therefore there exists not only the possibility of identifying the surface composition but also of devising a guidance system based on this principle.

REFERENCES

1. M. J. Dubois, Jour. de Phys et le Radium, 18, 138-158 (1957).

2. M. J. Dubois, Bull. l'Astron. Soc. Astron. France, 70, 224-34 (1956).

3. Link, Bull. l'Astron., 8, p. 77, (1933).

4. Z. Kopal, New Scientist 1052. (1958).

5. P. Pringsheim, Fluorescence and Phosphorescence, Interscience, 1949.

6. D. Alter, Pub. Astron. Soc. Pac. 67 237 (1955).

7. G. F. J. Garlick, Luminescent Materials, Oxford, 1949.

8. R. W. Wood, A. J., 36, p. 75 (1912)

9. Kozyrev, Izvestia of the Crimean Astro. Obs. 16, 148 (1956).

SECTION 7

LUNAR ATMOSPHERE

7.1 INTRODUCTION

While it is evident from optical measurements that the moon does not possess a dense atmosphere similar to that of the earth, there is both experimental and theoretical evidence for the existence of some sort of extremely tenuous atmosphere. For example, from measurements of the refraction of radio waves from the Crab Nebula during a lunar occultation, Elsmore[1] has obtained a value of the density which is about 2×10^{-13} of that of the earth's atmosphere.

In Section 7.2 planetary atmospheres in general are considered and plausibility arguments are given for the existence of a tenuous Argon atmosphere whose density may be as high as 10^{16} atoms cm^{-3}.

Section 7.3 discusses the effect of the "solar wind" on the lunar atmosphere. Estimates of the equilibrium density are made under rather broad assumptions and much lower densities of the order of 10^{9} atoms cm^{-3} are indicated.

Finally, in Section 7.4 the distribution of the lunar atmosphere is considered. Two different mechanisms, viscous flow and diffusion, are considered.

7.2 ORIGIN OF THE ATMOSPHERE AND ESCAPE OF THE SECONDARY ATMOSPHERE

Estimates of the nature of the lunar atmosphere can be made from the general theory of planetary atmospheres described by Kuiper [2] (Chapter XII). It is now generally believed that atmospheric evolution occurred in two stages. After a planet was first formed and was hot it was surrounded by a thick atmosphere called the proto-atmosphere. This atmosphere almost completely escaped before the planet cooled.

After the cooling, a secondary atmosphere was formed by volcanic action and seepage of gases up through the crust. This secondary atmosphere was formed by chemical reactions which liberated such gases as H_2O, NH_3 and CH_4. Further reactions among these gases, stimulated photochemically in some cases, produced H_2, O_2, N_2 and CO_2.

Gases which cannot be produced chemically, such as neon, are seriously depleted on the earth with respect to their cosmic abundance, supporting the idea that they escaped with the proto-atmosphere. If we assume a similar thermal history for the moon we may postulate that several billion years ago the moon had a secondary atmosphere of H_2, H_2O, O_2, N_2 and CO_2 with some traces of He, Ne, A, Xe, Kr.

The theory of escape of an isothermal planetary atmosphere was first derived by Jeans. For a planet of radius R and gravitational constant g, the time for the atmosphere to decay to 1/e of its initial density is given by

$$t = \frac{(\bar{v}^2)^{3/2}\, e^{\frac{3gR}{\bar{v}^2}}}{2g^2R} \qquad (7.2\text{-}1)$$

where $\sqrt{\frac{3k_2T}{M}} = \sqrt{\bar{v}^2}$ is the root mean square molecular velocity.

This formula actually underestimates the escape rate of a heavy atmosphere, since a heavy atmosphere is not really isothermal, but is cooler and therefore denser near the surface of a planet. Kuiper (Chapter VII) discusses this more fully and obtains correction factors on the order of 10^5. This applies to an atmosphere which has a density comparable to that of the earth now; as the density of an atmosphere decreases, so does the correction factor.

As shown in Table 7.2-1, the decay time changes quite rapidly with the average molecular velocity.

TABLE 7.2-1

THE ATMOSPHERE DECAY TIME ON THE MOON

t (years)	v (cm/sec)
10^3	6.1×10^4
10^6	5.4×10^4
10^9	4.8×10^4

Using a value of 100°C for the daytime temperature of the lunar surface,

$$\sqrt{\overline{v^2}} = \frac{1}{\sqrt{A}} \times 3 \times 10^5 \text{ cm sec}^{-1} \qquad (7.2\text{-}2)$$

where A is the atomic or molecular weight of the particle. It is clear from Tables 7.1-1 and 7.1-2 that the decay time for elements with molecular weights greater than 40 will be much larger than geological times. Possible atmospheric constituents would then be argon, krypton, xenon, carbon dioxide and sulfur dioxide.

TABLE 7.2-2

THE ROOT MEAN SQUARE MOLECULAR VELOCITY OF GASES AT 100°C

Element	A	$\sqrt{\overline{v^2}}$ (10^4 cm/sec)
H	1	30
He	4	15.4
N	14	8.3
O	16	7.7
N_2	28	5.7
O_2	32	5.4
A	40	4.9
CO_2	44	4.6
O_3	48	4.5
SO_2	64	3.8
Kr	84	3.4
Xe	131	2.7

Argon

The table giving the composition of the earth's atmosphere, taken from Kuiper (Chapter I), shows an anomalous amount of argon.

TABLE 7.2-3

COMPOSITION OF DRY ATMOSPHERE

Gas	10^6 x Fraction (Volume)	Amount (cm S.P.T.)
N_2	780,900	624,600
O_2	209,500	167,600
A	9,300	7,440
CO_2	300	220
Ne	18	14
He	5.2	4.2
CH_4	1.5	1.2
Kr	1	0.8
N_2O	0.5	0.4
H_2	0.5	0.4
O_3	0.4	0.3
Xe	0.08	0.06
H_2O	10^3 - 10^4	10^3 - 10^4

Argon is the only gas present in any appreciable amount in the earth's atmosphere which could not have been obtained from any chemical reaction.

The mean molecular velocity corresponding to a 1/e atmospheric decay time of 10^9 years (for the earth) is 213×10^5 cm/sec. This number is high enough so that neon would be retained even at a temperature of 2000 degrees. The cosmic abundance ratio of neon to argon is 5,900/800 (XII), emphasizing the anomalous amount of argon in the earth's atmosphere.

There is a simple explanation for this in that potassium 40 beta-decays to argon 40 with a half life of 1.9×10^9 years. Thus there is a continuous source of argon. Vestine[6] has estimated that in 3×10^9 years 4.0×10^{22} atoms of argon per cm^2 of lunar surface would have been produced. For a uniform atmosphere extending to 20 km this gives 2×10^{16} atoms per cm^3.

Some of this argon would have escaped and not all of it could have filtered out of the interior of the planet, so the above figure is high; still, outside of depletion by the solar wind (to be described later), there is a good probability that the moon possesses a tenuous argon atmosphere.

7.3 EFFECT OF SOLAR WIND ON THE LUNAR ATMOSPHERE

Basic Considerations

The lunar atmosphere problem is considerably changed by the "solar wind" concept. The "solar wind" (Section 8) which is the outermost region of the sun's corona is believed to have a proton density in the vicinity of the earth of about 10^3 cm^{-3} and the particles have a velocity of approximately 10^7 cm sec^{-1} during quiet sun conditions.

The "solar wind" will affect the lunar atmosphere in several ways. Since it is presumed that all of the proton flux that reaches the surface is reemitted it will contributed a hydrogen component to the lunar atmosphere. If a proton strikes a particle in the lunar atmosphere it will probably give enough energy to the particle to remove it from the lunar gravitational field. Another effect is the possibility that the solar protons if they reach the lunar surface will sputter particles into the atmosphere.

With the assumption of a strong "solar wind", any remnants of the secondary atmosphere discussed in Section 7.1 would soon be blown from the moon. The moon's atmosphere would then consist of

hydrogen from the "solar wind", sputtered atoms and gas which is still being evolved from the lunar surface.

A rough idea of the equilibrium atmosphere attained when these processes balance can be derived as follows. It will be assumed (1) that there is an incoming flux of particles Φ, (2) that there is a cross-section σ for one of these particles to strike an atmospheric particle and give it enough energy for escape, (3) that if one of these particles reaches the surface it knocks out an average of $\bar{n}$ particles which do not have enough energy to escape, (4) some other mechanism exists for the depletion of the atmosphere such that each particles has a probability P per second of being removed, and (5) that the number of particles emitted by the lunar surface per cm^2 sec is given by J.

For the moment the addition of hydrogen to the atmosphere will be neglected and only the possible equilibrium between the other four mechanisms will be discussed.

If N(t) is the number of particles per unit area of the lunar surface at time t then

$$N(t+\Delta t) = N(t) + \bar{n}\,(\Phi - N\sigma\Phi)\,\Delta t + J\Delta t$$

$$- N\Phi\sigma\,\Delta t - PN\Delta t$$

and

$$\frac{dN}{dt} = (\bar{n}\Phi + J) - N\left[\Phi\sigma(1+\bar{n}) + P\right] \qquad (7.3\text{-}1)$$

The solution of this equation if P is constant is

$$N = \alpha \exp -\left[\Phi\sigma(1+\bar{n}) + P\right]t + \frac{(\bar{n}\Phi + J)}{\left[\Phi\sigma(1+\bar{n}) + P\right]} \qquad (7.3\text{-}2)$$

where

$$\alpha = N_o - \frac{\bar{n}\Phi + J}{\left[\Phi\sigma(1+\bar{n}) + P\right]} \qquad (7.3\text{-}3)$$

The equilibrium value of N is

$$N_{eq} = \frac{(\bar{n}\Phi + J)}{[\Phi\sigma(1 + \bar{n}) + P]} \qquad (7.3\text{-}5)$$

If P is assumed small in comparison to $\Phi\sigma$ (i.e., the isothermal decay time is long compared to the time to be swept out by the solar wind) then the above equation reduces to

$$N_{eq} = \frac{\bar{n}\Phi + J}{[\Phi\sigma(1 + n)]} .$$

Numerical values

Experimental values of $\bar{n}$ for 50 volt protons ($v = 10^7$ cm sec^{-1}) are not known. In fact there are discrepancies of orders of magnitude in the values quoted in the literature for sputtering coefficients for low energy protons(3)(4)(5). In spite of this uncertainty it seems that a reasonable upper limit for $\bar{n}$ is 10^{-3} and possible less. So for the present calculation this value will be used.

Massey and Smith have calculated the differential cross-section for scattering of 72 volt protons from argon using the self-consistent field method. Given the incident proton energy of 72 volts, the scattering angle when a given amount of energy is given to the Argon atom can be found from momentum consideration. The scattering angle in C.M. coordinates when the Argon atom is given the escape energy of 1.2 volts (2.4 Km/sec) is 50°. It should be pointed out that even if the atom is scattered with the escape energy in most cases it will strike the lunar surface. It will be assumed for this calculation that all atoms which have received 1.2 volts of energy escape even though they collide with the surface.

Using the values given by Massey and Smith for the differential cross-section, the total cross-section for imparting escape valoeity can be found by numerical integration. The result is

$$\sigma_{esc} = (3)\ 10^{-17}\ cm^2.$$

Of course, an atmosphere obtained from solar-wind processes will not consist of argon; but other cross-sections should not be radically different.

Estimates of the rates of emission of gases from the lunar surface based on terrestrial data have been made by Vestine[6]. He indicates $J \cong 5 \times 10^5/cm^2$ for argon and $J \approx 10^{10}/cm^2$ sec for volcanic gases. For the purpose of this calculation it will be assumed that $J = 10^{10}/cm^2$ sec.

The time constant for this process is

$$\tau = \left[\Phi\sigma(1 + \bar{n})\right]^{-1} \qquad (7.3\text{-}6)$$

Neglecting $\bar{n}$ compared to 1

$$\tau = \left[10^3 \times 10^7 \times (3)\ 10^{-17}\right]^{-1}$$

$$= (3.3)\ 10^6 \text{ sec.}$$

$$\approx 39 \text{ days.}$$

The number of particles in the equilibrium atmosphere is

$$N_{eq} = \frac{\bar{n}\Phi + J}{[\Phi\sigma]}$$

if $\bar{n}$ is neglected in comparison to 1.

$$N_{eq} = \frac{(10^{-3})\ 10^{10} + 10^{10}}{10^{10}\ (10^{-16})\ (.3)}$$

$$\cong (3)\ 10^{16} \text{ particles cm}^{-2}.$$

For a scale height of 20 Km this gives

$$\rho_{eq} \approx (1.5)\ 10^{10} \text{ particles cm}^{-3}$$

The equilibrium value for an isothermal hydrogen atmosphere at 100°C if all the solar protons are thermalized when they strike the lunar surface is

$$\rho_{eq} \approx (3) \times 10^{7} \text{ atoms cm}^{-3}.$$

This is negligible compared to the possible atmosphere from volcanic gases but is about equal to that expected from sputtering and does represent a lower limit based on the values assumed for the number density of the solar protons.

The accuracy of all of the numbers which have been used in the above calculations is uncertain. Hence not much significance should be attached to the actual numerical results which have been obtained. What is if significance is the demonstration of the importance of the "solar wind" to the equilibrium density of the lunar atmosphere(7).

7.4 THE DISTRIBUTION OF THE LUNAR ATMOSPHERE

In Sections 7.2 and 7.3 we discussed the possible sources of the moon's atmosphere and made estimates of the atmospheric density. The particle densities obtained are average densities, while the actual distribution of particles is certainly not uniform. The altitude variations are not important, and so we assumed a uniform layer 20 km thick. There is, however, a horizontal variation in density caused by the tremendous temperature differences between the bright and dark sides of the moon. This horizontal variation is clearly important since a nuclear explosion in a region of low density would lead to the mistaken conclusion of "no atmosphere". In this section we examine this horizontal variation in density; first with the assumption that the density is large enough to justify the treatment of the flow from the hot side to the cold side as the flow of a viscous fluid, and then the other extreme of low densities is treated as a diffusion problem. These two processes are illustrated schematically in Figure 7.4-1.

Viscous Flow in the Lunar Atmosphere

The temperature of the lunar surface, and therefore of the atmosphere above it, should vary with lunar longitude, being greatest at the sub-solar point and least at the limbs. This will

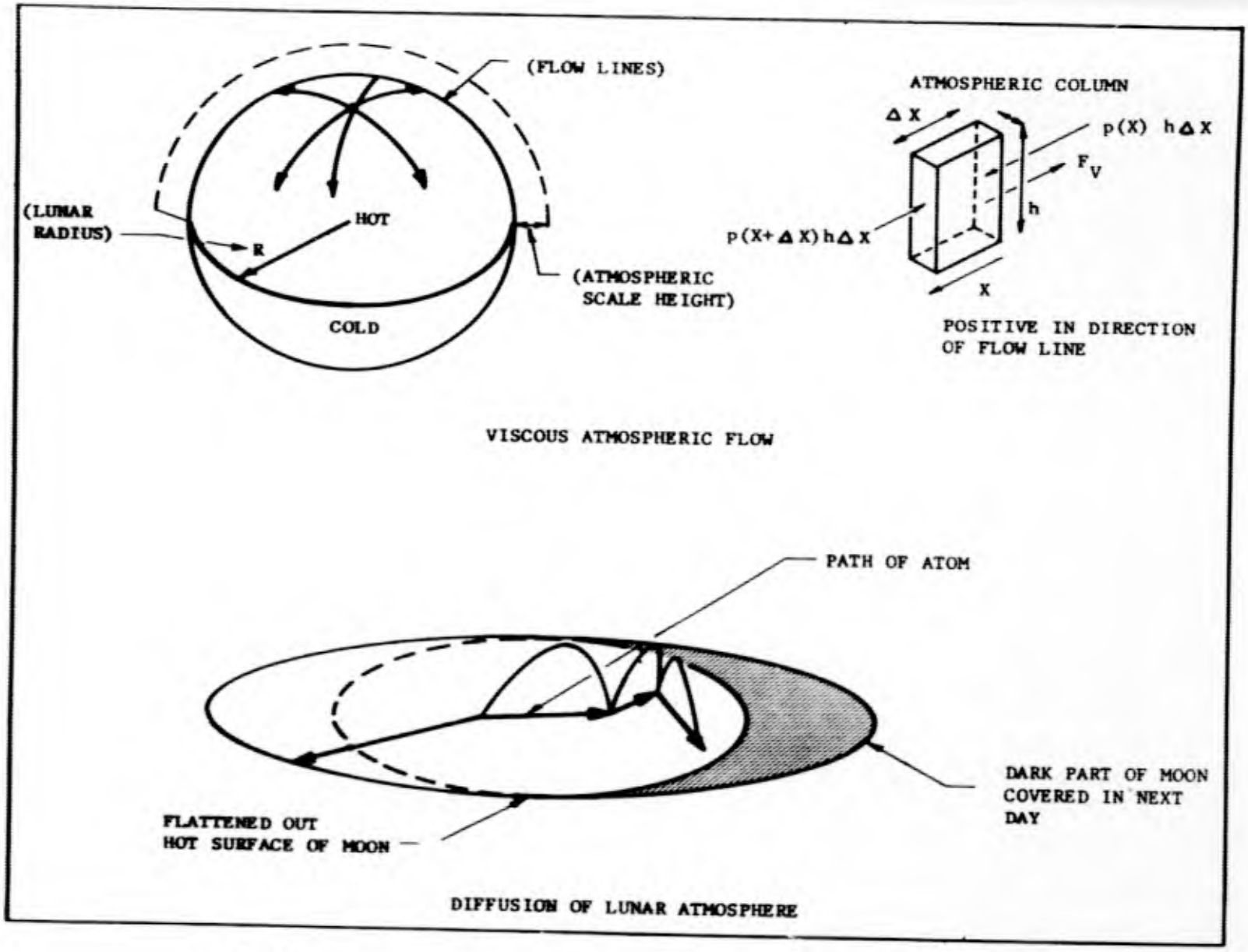

FIG. 7.4-1 MECHANISMS FOR DISTRIBUTING THE LUNAR ATMOSPHERE

cause a pressure difference resulting in a flow of gas toward the coldest region.

For particle densities great enough so that the mean free path is less than the scale height of the atmosphere, the pressure differential will cause coherent viscous flow. The kinetic cross-section of argon is approximately 4×10^{-15} cm^2. A scale height of 20 km gives the result that the particle density for a viscous flow must be about 10^8 cm^{-3} or greater.

The equilibrium flow rate for this process will be the rate for which viscous force balances the force due to the pressure difference. This can be estimated by a simple one dimensional calculation. For the purpose of this calculation assume that the sub-solar point is at $x = 0$ and the limb at $\pi R/2$.

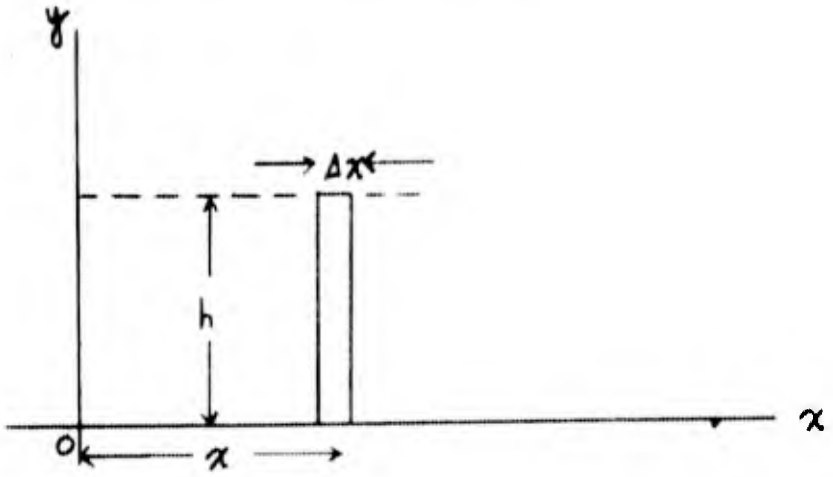

Assume that the lunar atmosphere has a particle density (which may be a function of x), and a scale height h. Assume further that the pressure p is P_o at $x = o$, P at $x = \pi R/2$ and varies linearly with x, so that

$$p(x) = P_o + \frac{2\,(P - P_o)}{\pi R}\,x. \qquad (7.4\text{-}1)$$

The force per unit length on a strip of width Δx and height h centered at x is then

$$F = \left\{ p\left(x - \frac{\Delta x}{2}\right) - p\left(x + \frac{\Delta x}{2}\right) \right\} h$$

$$= - \frac{2\, h \Delta x}{\pi R} \left(P - P_o\right) \qquad (7.4\text{-}2)$$

In general, the viscous force per unit area caused by a velocity gradient in a gas is given by

$$F_v = \eta \frac{\partial v}{\partial y} \qquad (7.4\text{-}3)$$

where $\frac{\partial v}{\partial y}$ is the velocity gradient normal to the force and η is the coefficient of viscosity. Kinetic theory gives

$$\eta = \frac{1}{3} m \frac{\bar{v}}{\sigma} ,$$

where σ is the collision cross-section of the molecules, m their mass and

$$\bar{v} = \sqrt{\frac{8kT}{\pi m}} \quad \text{the mean velocity.}$$

In this problem, if the velocity is zero at the surface and v at y = h, the velocity gradient can be taken to be v/h. This gives a viscous force per unit length of

$$F_v = \eta \frac{v}{h} \Delta x \qquad (7.4\text{-}4)$$

Equating the two force expressions gives

$$- \frac{(\Delta x)\ 2}{\pi R} \; h \left(P - P_o\right) = \eta \frac{v}{h} \Delta x$$

or, substituting for η and solving for v,

$$v = - \frac{2h^2 (P - P_o)}{1/3 \frac{m\bar{v}}{\sigma} \pi R} \qquad (7.4\text{-}5)$$

The pressure P is equal to $m \rho gh$. Substituting this gives

$$v = - \frac{6 \sigma h^3 g (\rho - \rho_o)}{\pi \bar{v} R} \qquad (7.4\text{-}6)$$

For argon at $0^\circ C$, $\bar{v} = 3.9 \times 10^4$ cm/sec. The kinetic cross-section for argon is about 4×10^{-15} cm^2. For the moon R = 5,900 km = 5.9×10^8 cm and g = 160 cm/sec^2. Using 2×10^6 cm for the scale height gives

$$v = - \frac{(6) (4 \times 10^{-15}) (2 \times 10^6)^3 (160) (\rho - \rho_o)}{(5.9 \times 10^8) (3.9 \times 10^4) \pi} \qquad (7.4\text{-}7)$$

A case of interest would be the case where the gas was freezing at the coldest point making ρ_o close to zero. In this case

$$v = 3.4 \times 10^{-7} \rho \text{ cm sec}^{-1} \qquad (7.4\text{-}8)$$

This is the velocity at y = h. The average velocity will be half this or $1.7 \times 10^{-7} \rho$ cm/sec.

This problem as set up represents a fairly crude approximation to the real picture; however, the time for gas to flow a distance of one quarter the moon's diameter using the velocity given should give a reasonable idea of the 1/e decay time for an atmosphere that is freezing out. For an atmosphere that is not freezing this time should be the time constant for the approach to the equilibrium atmospheric distribution which will be considerably denser on the colder side. Thus, for this process to be significant, this time should be shorter than the lunar day (30×10^5 sec).

The value of ρ for which the time constant is just equal to the length of the lunar day is found by solving

$$\frac{\pi R}{2v} = 30 \times 10^5 \text{ sec}$$

or

$$\rho = \frac{5.9\times10^{8}}{30\times10^{5}} \cdot \frac{1}{2(3.4\times10^{-7})} \qquad 7.4\text{-}9)$$

$$\simeq 5\times10^{8} \text{ particles cm}^{-3}$$

Thus for atmospheres of 10^{9}/cc or greater there could be appreciable condensation or flow toward the cold side. This will tend to inhibit the escape of the atmosphere since it tends to concentrate atoms where their escape rate is slower. Another possibility is the permanent freezing out of large quantities of gas in a cave which never sees sunlight.

Diffusion of the Lunar Atmosphere

When the atmosphere is too rare for coherent viscous flow, movement of particles from regions of high density to regions of low density can still take place by means of a type of a diffusion process. A particle that leaves the surface will describe a parabolic path under the action of the moon's gravitational field.

Suppose that when the particle strikes the surface again and rebounds, it does so with sufficient randomness that the velocity distribution at any point on the surface may be assumed to be Maxwellian. With these assumptions, it is possible to compute an effective mean free path, ℓ, for the progress of the molecule along the surface and also a mean velocity, $\bar{v}$. In any diffusion process, the current is given by

$$\vec{j} = -\frac{\ell\bar{v}}{3}\nabla\rho = -D\nabla\rho \qquad (7.4\text{-}10)$$

where ρ is the density, and D is the diffusion constant. This, coupled with the continuity equation

$$\frac{\partial\rho}{\partial t} = -\nabla\cdot\vec{j} \qquad (7.4\text{-}11)$$

gives the usual diffusion equation

$$\frac{\partial\rho}{\partial t} = D\nabla^{2}\rho \,. \qquad (7.4\text{-}12)$$

Suppose a molecule starts out from the surface with velocity components v_x parallel to the surface and v_z perpendicular to it. It will then move as illustrated.

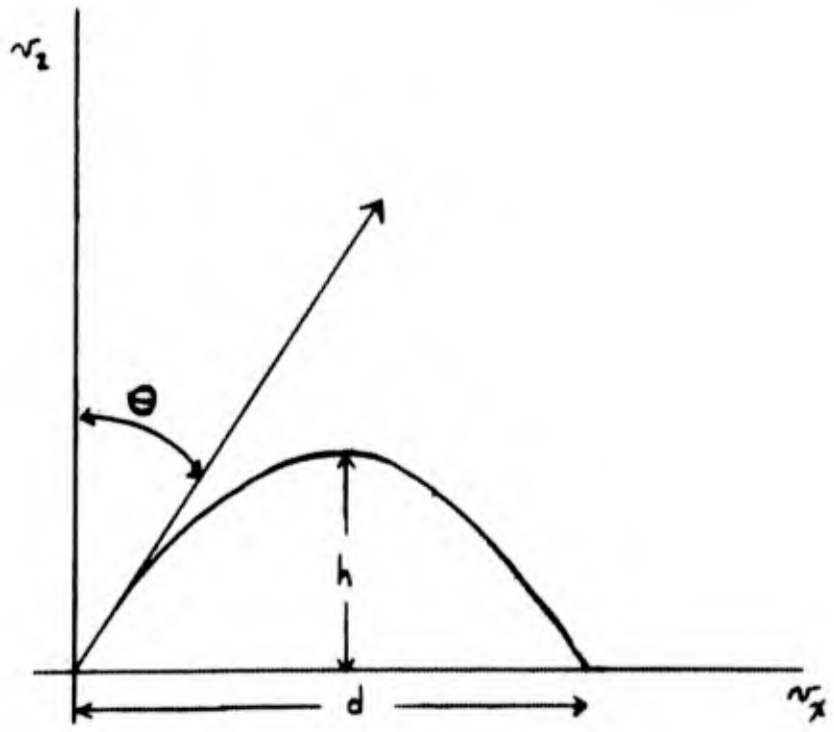

This is a standard problem and the answer is well known. Since

$$v_z = v \cos \theta$$

and

$$v_x = v \sin \theta,$$

$$h = \frac{v^2 \cos^2 \theta}{2g}$$

and

$$d = 2 \frac{v^2 \sin \theta \cos \theta}{g} \qquad (7.4\text{-}13)$$

where $g = 160$ cm sec^{-2} is the moon's gravitational constant. Also, the time of flight is

$$t = \frac{2v \cos \theta}{g}$$

The θ distribution is completely random, so that average values are appropriate.

$$\langle \cos \theta \sin \theta \rangle = \frac{\int_0^{\pi/2} \sin \theta \cos \theta \sin \theta \, d\theta}{\int_0^{\pi/2} \sin \theta \, d\theta} \qquad (7.4\text{-}14)$$

and

$$\langle \sin \theta \rangle = \frac{\int_0^{\pi/2} \sin^2 \theta \, d\theta}{\int_0^{\pi/2} \sin \theta \, d\theta} = \frac{\pi}{4} \qquad (7.4\text{-}15)$$

From kinetic theory

$$\langle v \rangle = \bar{v} = \sqrt{\frac{8\,k\,T}{\pi\,m}} \tag{7.4-16}$$

and

$$\langle v^2 \rangle = \overline{v^2} = \frac{3\,k\,T}{M} \tag{7.4-17}$$

This gives for the mean free path

$$\ell = \langle d \rangle = \frac{2}{g} \langle v^2 \rangle \langle \sin\theta \cos\theta \rangle$$

$$= \frac{2\,k\,T}{mg}, \tag{7.4-18}$$

and for the mean velocity

$$\bar{v} = \langle v_x \rangle = \langle v \rangle \langle \sin\theta \rangle$$

$$= \frac{\pi}{4} \sqrt{\frac{8\,k\,T}{\pi\,m}} \tag{7.4-19}$$

When these expressions for ℓ and $\bar{v}$ are substituted in the expressions for the diffusion constant, we get

$$D = \frac{\ell \bar{v}}{3}$$

$$= \frac{1}{3} \frac{\pi}{4} \sqrt{\frac{8\,k\,T}{\pi\,m} \cdot \frac{2\,k\,T}{m\,g}}$$

$$= \frac{\sqrt{\pi}}{6\,g} \left(\frac{2\,k\,T}{m}\right)^{3/2} \tag{7.4-20}$$

It is possible to solve the diffusion equation exactly for the case of two dimensional diffusion on a spherical surface; however, for the order of magnitude calculations used here, the solution for the one dimensional process will be adequate. In this case, the diffusion equation (7.4-12) becomes

$$\frac{\partial \rho}{\partial t} = D \frac{\partial^2 \rho}{\partial x^2} \qquad (7.4\text{-}21)$$

Substituting $\rho(x,t) = f(x)\, e^{-\lambda t}$

gives $f'' = -\frac{\lambda}{D} f(x)$

The solution for this is

$$f(x) = A \sin\sqrt{\frac{\lambda}{D}}\, x + B \cos\sqrt{\frac{\lambda}{D}}\, x \,.$$

This one dimensional solution should be thought of as a mirror image solution as in the viscous flow problem so that the proper boundary condition is

$$\frac{\partial f}{\partial x} = 0$$

at the boundaries which will be taken to be $x = 0$ and $x = \pi R$. Applying this boundary condition gives $A = 0$ and

$$\sqrt{\frac{\lambda}{D}} = n/R$$

where n is an integer. The longest time constant is the most important one for getting an idea of the times involved and is

$$\tau_{max} = \frac{1}{\lambda_{min}} = \frac{R^2}{D}$$

For a temperature of 100°C, and m = 40 a.m.u., $D = 1 \times 10^{12}$ cm^2/sec. This gives

$$\tau_{max} = \frac{(1.85 \times 10^{8})^{2}}{10^{12}} = 3.4 \times 10^{4} \text{ sec.}$$

This is about 1/100 of a lunar day.

Thus if the cold side of the moon is regarded as a sink, an appreciable part of a tenuous atmosphere could flow to it during the course of a lunar day. The flow rate on colder portions of the moon will be less because of the $T^{-2/3}$ time dependence of the time constant.

An interesting application of this problem may be the flow of the radioactive gas, radon. Although the abundance of uranium and thorium in the lunar crust is unknown, it seems reasonable to postulate at least some radon evolution. Since radon condenses at a temperature of -71°C and has a half life of 3.8 days which is appreciably shorter than the longest time constant for diffusion, it should be possible for it to reach the cold sink before decaying. This effect may well concentrate the radon and its decay products at the terminator.

REFERENCES

1. B. Elsmore, Phil Mag., 8, Ser. 2, 1040 (1957).

2. G. Kuiper ed. The Atmospheres of the Earth and Planets.

3. W. J. Moore, et al, Ann. N.Y. Acad. Sci. 67, 600 (1957).

4. C. D. O'Briain, et al., J. Chem. Phys. 29, 7 (1958).

5. A. Weiss, et al., J. Chem. Phys. 29, 7 (1958).

6. E. H. Vestine, RAND, RM-2106, ASTIA No. AD 150683.

7. J. R. Herring, and A. L. Licht, Science 130, 266 (1959).

SECTION 8

SOLAR WIND PHENOMENA

8.1 INTRODUCTION

In recent years a large body of experimental information has been accumulating for the existence of a tenuous, highly ionized gas of solar origin in interplanetary space. Although the composition of this gas is not known with any certainty, the observations lead to the belief that it consists mainly of electrons, protons, helium ions and a small proportion of heavy elements. This gas may be considered to be an extension of the solar corona, and is prevented from reaching the earth's surface by the geomagnetic field. These "solar winds" seem to vary in intensity with visible solar activity and interact with the magnetic field of the earth to produce auroral displays, as well as perturbations of the steady field.

While the existence of neutral beams of solar particles is well established, the velocity and density of these particles in space is much less well-known. For this reason, measurements of the proton and electron densities may well be one of the most important measurements to be made in the cis-lunar space although, of course, it will be possible to infer something about the above properties from magnetic field measurements[1]. Radiation counters similar to the Geiger counters, scintillation counters and crystal counters used on Explorer IV[2] should be suitable for measurements from a lunar probe vehicle. Photographic detection methods[3] could provide the most positive determination of the composition and velocity of the particles, but an experiment of this type probably would require recovery and for a lunar research vehicle may not be feasible.

The presence near the earth of charged particles of solar origin was first proposed as an explanation of magnetic storms and aurorae. The velocity of the beam of solar particles is inferred from the time lag between the visual observation of a flare on the sun and the commencement of magnetic storm disturbances. This time is of the order of 1 day and therefore indicates velocities of 1000 km sec^{-1}. Weak storms show a 27 day periodicity which points to more or less continuous emission. Due to certain fundamental considerations the beams of particles must be electrically neutral.

The number density and velocity under burst conditions most often quoted is that determined by Unsöld and Chapman[4] from optical and radiofrequency absorption. They obtained a number density of about 10^5 cm^{-3}. Biermann[5] has deduced a value for the number density of the order of 10^3 - 10^4 cm^{-3} from cometary tail motions. Alfven[6] on the other hand, from a magnetohydrodynamic wave theory believes that the tail motions can be accounted for by ion densities of the order of 0.1 cm^{-3} and velocities of 10^8 cm sec^{-1}. Block[7] has calculated the particle density in the solar beams from auroral and magnetic storm phenomena and derives a maximum particle density of about 10 cm^{-3} with a lower limit during storm conditions of 0.1 cm^{-3}. Recently Kozyrev[8] has detected weak luminescence of the lunar surface which he ascribes to solar beams with a density of $5x10^3$ cm^{-3}. The polarization of the zodiacal light[9] has been used as a measure of electrons and particulate matter in space. At the present time these measurements seem to be inconclusive.

It is clear from the above discussion that precise information concerning the solar wind is not available and in fact the estimates of number density and velocity vary by orders of magnitude. The following values which are often quoted are listed in Table 8-1 along with the kinetic energy corresponding to the stream velocity

TABLE 8-1

SOLAR WIND PARAMETERS

	Solar Condition	
	Average	Disturbed
Velocity	10^7	$1.5x10^8$
No. Cm^{-3}	10^3	10^5
Energy (eV)	50	$11.3x10^3$

However, if the solar winds are present in the solar system in the magnitudes which have been postulated, it appears that erosion effects on particulate matter such as meteorites and the particles responsible for the zodiacal light will be rather severe. Certain materials such as thin, metal-coated plastic films used for balloons, solar sails or satellite surfaces may be destroyed rapidly by these radiations.

8.2 SPUTTERING BY SOLAR PROTONS

Reiffel[10] has presented arguments for the destructive effects of the solar plasma on thin plastic and metallic films. These materials are important not only for the construction of balloons, solar sails, etc., but may have use as temperature regulators and in the scientific instrumentation for windows and filters. He gives the time t for removal of a layer by sputtering as

$$t = \frac{NLd}{M\delta\,(nv)}$$

where N = Avogadros No.

L = coating thickness

δ = sputtering yield

M = coating atomic wt. and d the density

nv = solar flux

At a flux of 6×10^{10} cm^{-2} a 300 Å Al. coating would be destroyed in 10^4 sec., if the sputtering yield is assumed to be one. The same author points out that the presence of He and heavy elements in the solar plasma will lead to effects of comparable magnitude.

It is further shown that radiation damage to plastic materials can also be important. For example, the dosage delivered by a proton flux of 600 cm^{-3} at 10^8 cm sec^{-1} would be about 5×10^5 Rads sec^{-1} over the range of the protons in the material ($\sim 10^{-5}$ gm cm^{-2}). Since damage may occur with about 10^{10} Rads, carbonization would require 2×10^4 sec.

It should be mentioned however, that as shown in the following sections a sputtering coefficient of one is probably too high by a factor of at least 50. Reiffel's figures for the time of removal therefore would be increased. A similar computation using the lower sputtering yield gives a time of 10^6 seconds to remove a 1000 Å coating or in a burst lasting 10^4 seconds about 1% would be removed.

The difficulty with interpreting such calculations in practical terms arises principally from two uncertainties: (1) lack of information concerning the solar flux, particularly the particle velocities, and its variation with solar conditions and (2) lack of experimental information as to sputtering rates for the presumed proton energies involved. Rather than draw conclusions as to these matters the following sections will discuss some of the available evidence and point out additional seemingly paradoxical effects to which high values of the solar flux will lead.

8.2.1 Sputtering Yield Values

The amount of sputtering damage due to solar wind particles depends directly upon the sputtering coefficient (i.e., no. of sputtered particles/incident particle) and of course upon the values assumed for the solar wind. The sputtering yield therefore is especially sensitive to the velocity which is taken for the solar wind.

A great deal of the information on sputtering is due to the work of Wehner[11]. Some of the results, both of his measurements and calculations, are given in Table 8.2. In the last column of the table the values are extended to protons. The energy dependence of the threshold has been assumed to be proportional to the ratio of the masses of the striking to the struck atoms.

As mentioned by Wehner[11], materials such as aluminum which form strongly-bound oxide layers on their surfaces have much lower sputtering rates. They may be bombarded at high rates for long times without noticeable effect. Although we have no quantitative information, this may account for the long lifetimes for meteorites and should also be favorable to the stability of the aluminum coated balloons. It should be noted that all of Wehner's sputtering yield data are for clean and freshly exposed surfaces.

TABLE 8.2

PROTON SPUTTERING YIELDS

Metal/Ion	Threshold Energy in eV			
	He (calc)	Hg (calc)	Hg (Meas)	Protons (est)
Al	127	136	120-140	500
Si	60	61	60-70	240
Fe	205	75	60-70	800
Cu	244	74	50-70	980
Pt	850	67	70-90	3400

The question of yield as a function of energy is perhaps more difficult particularly at energies far above threshold. Goldman and Simon[12] deal with particle energies in the region of 500 keV. They postulate a ln E/E energy dependence and derive a theoretical yield for deuterons on copper of 6.5×10^{-4} (by extrapolation, about 0.2 at 1 keV). At 1.5×10^{8} cm sec^{-1} or 11.25 keV, the yield would be about 0.02. It seems obvious that their work cannot be applied for energies near threshold.

Keywell[13] has made measurements to about 5 keV for He/Ag. He obtained yield values which varied from about 3.5 per incident He at 6 keV to about 1.0 at 1 keV. His curves indicate a rise in yield proportional to $\sqrt{E}$ while Wehner's results show a rapid increase in the vicinity of threshold and a more or less linear relationship up to about 400 eV.

In the theory of Goldman and Simon for high speed ions, it is assumed that the mean free path of the incident ions is much longer than that of the knock-on particles. Therefore, only a small number of the latter particles can diffuse to the surface, which accounts for the relatively low calculated yield at 500 keV compared to that at say 100 eV. From their argument it may be that a maximum

in the yield would show up at the energy where the range of the incident particles is equal to the range of the emerging particles.

The mean free path λ for primary production is given by the above authors as

$$\lambda = (n_o \sigma)^{-1}$$

where n_o is the particle density in the medium and σ the cross section. They calculate $\lambda = 0.86 \times 10^{-4}$ cm for 500 keV deuterons on copper. Since the range is inversely proportional to the incident particle energy, 1 keV ions would have a range of about 10^{-7} cm or about equal to that of the knock-on particles.

Figure 8.1 shows Wehner's experimental result (c) extrapolated to H/Al (c') using the hard sphere formula for the fraction of energy exchanged.

$$\frac{\Delta E}{E} = \frac{\mu}{(1+\mu)^2} \quad \text{and} \quad \mu = \frac{M_2}{M_1}$$

where M_2 is the mass of the struck atoms and M_1 the mass of the striking ion. Curve (A) gives Keywell's experimental results and curve (E) the values calculated from the Goldman and Simon theory using their ln E/E energy dependence.

It has been pointed out recently[14][15][16] that previous experiments which reported values of sputtering coefficients for various types of ions disagree by orders of magnitude. One of the reasons for these large discrepancies is the difficulty of controlling the experimental conditions. For 10 keV protons on silver Moore et al[14] report a value of about 0.03 atom/ion and for 6 keV helium ions Keywell[13] obtained a coefficient of 4.5 whereas if Keywell's expression for the sputtering coefficient (which agrees with his data) is used a value of 2.7 for protons on silver is obtained. Keywell did not separate the neutral particles from his ion beam and this may account for the larger values. Measurements made by Weiss and his coworkers[16] of the neutral hydrogen beam accompanying a 10 keV ionized beam indicates a sputtering coefficient of about two.

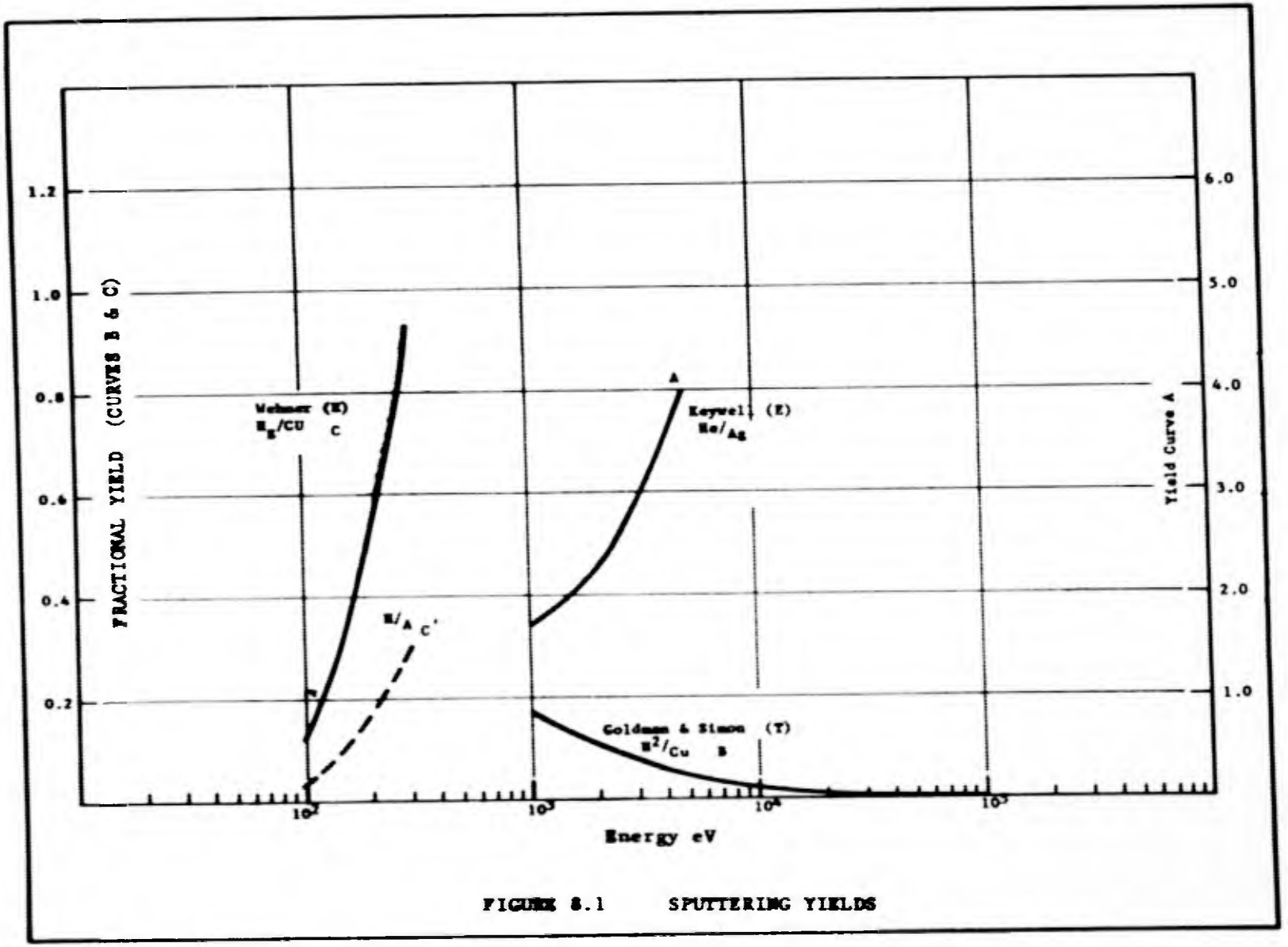

FIGURE 8.1 SPUTTERING YIELDS

Yonts et al[17] using the Oak Ridge "Calutron" obtained a coefficient of about 0.05 for 10 keV deuterium ions on copper with a decrease to about 0.02 at 40 keV. It appears therefore that for protons of 11 keV which may correspond to the burst condition, Moore's value may be at least of the correct order of magnitude. Unfortunately there is no theory available at present which will allow extension or extrapolation of the experimental results to other than the measured values.

However, there is the likelihood of a maximum in the region of interest (at least for the higher energies corresponding to a disturbed sun). It is possible that under average solar wind conditions no sputtering will take place at proton velocities below about 5×10^7 cm sec^{-1} and that with a suitable coating either of a heavy metal (W) or a refractory (SiO_2) little effect would be found below about 10^8 cm sec^{-1}.

8.3 SOLAR WIND EFFECTS

Since available experimental evidence as to solar wind particle densities and velocities, and as to sputtering yield values are uncertain, no reliable calculation of solar wind effects can be made. However, if the values often used are applied to natural phenomena, such as meteorites, apparently paradoxical results obtain. The effects of solar winds on meteorites, solar mass, and the earth's magnetic field are discussed below. The effect of solar wind on a possible lunar atmosphere is discussed in Section 7.

The very inconclusive nature of present solar wind speculations coupled with the possibly severe damage to space vehicle components at least under burst conditions, make measurements of solar wind densities and velocities an experiment of prime importance in cis-lunar vehicles.

8.3.1 Effects on Micrometeorites

Pressure Effects

The existence near the earth of micrometeorites in certain size ranges appears to be forbidden by light pressure and solar wind. Although the magnitude and existence of solar winds is not firmly established, the light pressure effect can hardly be questioned.

Light Pressure

The radiation pressure due to sunlight is related to distance from the sun by the inverse square law exactly as the gravitational attraction. We can then establish a relationship between the density and diameter of particles such that anywhere in the solar system the light pressure will equal the gravitational attraction. These particles will then be the smallest particles at any given density which can remain in the solar system. If we represent the light pressure at any distance R from the sun by

$$\text{Light pressure: } \frac{K}{(4\pi)} \cdot \frac{1}{R^2} = \frac{C}{R^2}$$

we can equate the light pressure on a particle to the gravitational force on the particle by:

$$\left(\frac{C}{R^2}\right) \frac{\pi d^2}{4} = \frac{\gamma M}{R^2} \cdot \frac{\pi \rho d^3}{6}$$

or

$$\rho d = \frac{3}{2} \cdot \frac{C}{\gamma M}$$

The radiation pressure due to light for a perfect absorber is equal to the radiation density. At one Astronomical Unit from the sun, the light pressure will be:

$$\text{L.P.} = \frac{1.92 \times 4.18 \times 10^7}{3 \times 10^{10} \times 6 \times 10} \text{ dynes/cm}^2 = 4.5 \times 10^{-5} \text{ dynes cm}^2$$

$$= C/(1 \text{ A.U.})^2 \quad \text{where A.U. is expressed in cm.}$$

An astronomical unit is 1.5×10^{13} cm and so

$$C = 4.5 \times 10^{-5} \times (1.5 \times 10^{13})^2 \approx 10^{22} \text{ dynes} \cdot \text{cm}^{-4}$$

$$\gamma M = 6.67 \times 10^{-8} \times 1.9 \times 10^{33} = 1.27 \times 10^{26} \text{ dynes} \cdot \text{gm}^{-1}\ \text{cm}^{-2}$$

and

$$\rho d = \frac{3}{2} \times \frac{10^{22}}{1.27 \times 10^{26}} \approx 1.2 \times 10^{-4} \text{ gms} \cdot \text{cm}^{-2}$$

or d(minimum) = $(1.2 \times 10^{-4}/\rho)$ cm.

Therefore, if we have particles with a density of one, their diameters must be 1.2 microns or greater if they are to remain in the solar system. Dust-balls or puff-balls with densities as low as .05 have been postulated as making up a large part of the meteorite population. For such particles a minimum diameter of 24 microns is established by light pressure. At the other extreme, iron particles with a density of 8 could exist with diameters as small as 1.5×10^{-5} cm or 0.15 microns. However, at these diameters, the size of the particle is smaller than the wave length of light, and one cannot consider it to be subjected to light pressure as calculated above.

Solar Winds Pressure

Solar winds with more or less steady values of 10^3 protons-cm^{-3} at velocities of 10^7 cm - sec^{-1} and gusts up to 10^5 protons-cm^{-3} with velocities of 1.5×10^8 cm - sec^{-1} in the region of the earth have been postulated. The pressure resulting from such solar winds will be equal to ρv^2 and so the steady wind and gust values will be:

$$\text{Steady} = 10^3 \times 1.6 \times 10^{-24} \times 10^{14} = 1.6 \times 10^{-7} \text{ dynes/cm}^{-2}$$

$$\text{Gust} = 10^5 \times 1.6 \times 10^{-24} \times (1.5)^2 \times 10^{16} = 3.6 \times 10^{-3} \text{ dynes/cm}^2$$

The steady wind pressure will not place any new limitation on particles since the solar light pressure is greater by two orders of magnitude.

The pressure due to gusts presents another situation. Since these pressures are not constantly applied, they do not straightforwardly counterbalance gravity as above, but a very simplified view of the possible effect can be considered. The energy of a particle in an elliptical orbit is given by

$$1/2\ Mv^2 - \frac{\gamma Mm}{R} = U = \frac{\gamma Mm}{2a}$$

where 2a is the major axis of the orbit.

If the total energy, U, of the particle becomes zero, the eccentricity becomes equal to 1 and the orbit will become parabolic. (For elliptical orbits the energy must be negative.) The solar wind particles, if absorbed, will transfer their energy to the meteorite and therefore increase the magnitude of the major axis. If we let a_o (the original semi-major axis) be equal to one astronomical unit, we can determine the time over which the high gust of solar wind must exist to reduce the energy of a particle to zero, and therefore change the orbit from elliptical to parabolic.

$$\Delta E = 1/2 \rho_{sw} V^3_{sw} A_m \Delta t = \frac{\gamma M \cdot \rho_m V_m}{2 a_o}$$

where ρ_{sw} = density of solar wind

ρ_m = density of meteorite

V_{sw} = velocity of solar wind

A = cross section of meteorite

V_m = volume of meteorite

$a_o = 1.5 \times 10^{13}$ cm.

M = mass of sun = 1.9×10^{33} gms.

From this

$$t = \frac{\gamma M \rho_m \cdot \pi d^3/6}{a_o \rho_{sw} V_{sw}^3 \pi d^2/4} = \frac{2}{3} \frac{\gamma M \rho_m d}{a_o \rho_{sw} V_{sw}^3}$$

For $\rho_{sw} = 10^5 \times 1.6 \times 10^{-24} \simeq 1.6 \times 10^{-19}$ gms - cm^{-3}

and $V_{sw} = 1.5 \times 10^8$ cm - sec^{-1}

we get

$$\Delta t = \frac{2 \times 6.67 \times 10^{-8} \times 1.9 \times 10^{33} \rho_m d}{3 \times 1.5 \times 10^{13} \times 1.6 \times 10^{-19} \times 3.375 \times 10^{24}}$$

$$= \frac{2 \times 6.67 \times 1.9}{3 \times 1.5 \times 1.6 \times 3.375} \times 10^7 \rho_m d \text{ seconds}$$

$$\approx 10^7 \rho_m d \text{ seconds.}$$

We can then set up a table as follows:

ρ (gm/cm^3)	d. (microns)	t (sec.)
.05	1	50
.05	10	500
.05	100	5000
1.0	1	1000
1.0	10	10,000
8.0	0.1	800
8.0	1	8000
8.0	10	80,000

So even for an iron particle of 10 microns diameter, the solar wind gusts would be required only for a total of one day to change the particle orbit to parabolic.

The average burst length for solar disturbance is about one hour. If we assume that they occur once each year we can establish a lifetime for meteorites in the solar system as related to density and diameter.

ρ(gm/cm^3)	d(microns)	Lifetime (years)
.05	1	disappear 1st burst
.05	10	" " "
.05	100	2
.05	1000	20
.05	10,000(1 cm)	200
1.0	1	disappear 1st burst
1.0	10	3
1.0	100	30
1.0	1000	300
1.0	10,000(1 cm)	3000
8.0	1	3
8.0	10	30
8.0	100	300
8.0	1000	3000
8.0	10,000(1 cm)	30,000

From this it would appear that if such solar wind gusts actually exist even very large meteorites could not remain in the solar system. A 1.3 cm diameter meteorite with a density of 1 would have zero magnitude if it entered the earth's atmosphere. About 4.5×10^5 such meteorites strike the earth each day.

The above argument is, of course, a very simple approach to the effect of "wind bursts" on the elliptical orbits of meteorites about the sun, in that it essentially assumes that the impulses are always applied perpendicular to the instantaneous velocity vector of the particle. Perhaps a more detailed investigation of this effect is warranted.

Sputtering

A second effect of the solar wind on meteorites will be the sputtering out of atoms of the meteorite material due to the impacts of high velocity protons. The energy of the protons involved in the solar wind will be:

At $V = 10^7$ cm - sec^{-1}

$$1/2\ mv^2 = \frac{1.6 \times 10^{-24} \times 10^{14}}{2 \times 1.6 \times 10^{-12}} \text{ electron volts}$$

$$= 50 \text{ electron volts}$$

At 1.5×10^8 cm - sec^{-1} the energy will be

$$50 \times 225 = 11{,}250 \text{ electron volts}$$

Opik[18] estimates that about 5 atoms are sputtered off for each proton striking a particle. This is a fairly catastrophic estimate since the rate of erosion of meteoritic material becomes quite high. For example, the impact rate of protons in our steady wind is

$$10^3 \times 10^7 = 10^{10} \text{ cm}^{-2} \text{ sec}^{-1}$$

and therefore the number of atoms sputtered per second from a meteorite of diameter d will be

$$\bar{N}_s = 10^{10} \times 5 \times \frac{\pi d^2}{4} \text{ atoms - sec}^{-1}$$

Since the surface area of the meteorite is πd^2 and the area per atom is about 10^{-16} cm^2 the time to sputter a layer one atomic diameter (10^{-8} cm) will be

$$T = \pi d^2 \times 10^{16} \Big/ \frac{5 \times 10^{10}\ \pi d^2}{4} \text{ seconds}$$

$$= 8 \times 10^5 \text{ seconds.}$$

Therefore the diameter of the meteorite is decreased by 2×10^{-8} cm in 8×10^{5} seconds, and this rate of decrease is independent of the size of the meteorite. Then the original diameter of a meteorite whose present diameter is d will be given by

$$d_o = d + \frac{2 \times 10^{-8}\, t}{8 \times 10^{5}} \text{ cm.}$$

where t is the lifetime of the meteorite in seconds.

If we take 300 million years as the lifetime of present day meteorites (this may be a considerable overestimate) we will get:

$$d_o = d + \frac{2 \times 10^{-8} \times 3 \times 10^{8} \times 3 \times 10^{7}}{8 \times 10^{5}}$$

$$= (d + 225) \text{ cm.}$$

This means that no meteorite now existing could have started life with a diameter smaller than 225 cm.

If the higher solar wind velocity of 1.5×10^{8} cm - sec^{-1} and densities of 6×10^{2} - cm^{-3} are used

$$\text{Impact rate} = 10^{11} \text{ - } cm^{-2}\ sec^{-1}$$

$$T = 8 \times 10^{4} \text{ seconds}$$

$$d_o = d + \frac{2 * 10^{-8}}{8 \times 10^{4}}\, t \text{ (sec)} = d + 7.5 \times 10^{-6}\, t \text{ (years)}$$

or $d_o = (d + 2250)$ cm for $t = 3 \times 10^{8}$ years

If the same values of atoms sputtered per incident atom are applied to the bursts of solar wind, one can estimate the erosion

due to these bursts. Actually, the number of atoms sputtered should increase with increasing energy of the incident proton. However, retaining the value of 5 we will get the time to sputter off one atomic layer to be

$$T = d^2 \times 10^{16} \quad 5 \times 10^5 \times 1.5 \times 10^8 \times d^2/4$$

$$\simeq 500 \text{ seconds.}$$

If we also assume as before, that the duration of such bursts is about one-hour per year we will then have the diameter of a meteorite decreased by

$$7 \times 2 \times 10^{-8} = 1.4 \times 10^{-7} \text{ cm/year.}$$

Then for a 300 million year old meteorite the erosion due to these large bursts would be

$$1.4 \times 10^{-7} \times 3 \times 10^{-8} = 42 \text{ cm.}$$

Of course, as shown previously small particles would have been driven out of the solar system by these bursts.

Since the steady wind erosion is fantastically large, one might assume that for the 11 Kev protons of the bursts the sputtering ratio is 5 to 1, and that this ratio varies linearly with energy of incident particle. Then the steady wind value would be reduced by a factor of 225 and so

$$d_o = \left(d + \frac{225}{225} \right) \text{ cm or } (d + 1.0) \text{ cm.}$$

which is not too serious. The burst erosion is still quite enormous.

If sputtering values are estimated from Wehner's[11] experimental work, perhaps a somewhat simplified view can be taken.

The absolute minimum energy required to sputter off an atom from a material is given by the molecular heat of vaporization of the material, and will vary with the target material. The average number of atoms sputtered out of a surface per incident particle will then be given by

$$\bar{N}_s = k\,(\Delta E - E_T)$$

where k is a constant to be obtained experimentally

E is the energy transferred from the incident particle to a molecule in the lattice

E_T is the threshold energy, or the molecular heat of vaporization of the target material.

It is not here assumed that the sputtered molecule is a directly struck surface molecule, but rather that a three-body collision is required. This would appear to be required since in atomic dimensions the surface is a plane, and the momentum of the struck molecule will be into the material rather than out of it.

If the impact of the particles are hard-sphere collisions the average energy transferred from the incident particle to the target particle will be

$$\Delta E = \left[U/(U+1)^2\right] E_i$$

where U = ratio of masses of incident and target particles

E_i = incident particle energy.

Then we have

$$\bar{N}_s = K\left[\frac{U E_i}{(U+1)^2} - E_T\right]$$

so that the number of molecules sputtered per collision from a given target material will be approximately proportional to the mass of the incident particle for a fixed value of E_i. For sputtering from iron and copper with Mercury ions Wehner has found that N_s for 50 volt ions is in the order of .01. He has carried out experiments with other target materials and the order of magnitude of the results are not changed. See Section 8.2.1. He has also used argon ions on iron, for example, and the relationship expressed above holds at least roughly. For 50 volt protons on iron the sputtering rate would then be about 1/10 that of mercury on iron, or about .001. The value may very well be zero because of threshold considerations. On silicon this value should not be radically different. If we accept the above value, the erosion rate due to the steady solar wind will be:

$$10^{10} \times 10^{-3} = 10^{7} \text{ molecules} - \text{cm}^2 - \text{sec}^{-1}.$$

and the time to sputter one molecular layer from a sphere will be

$$4 \times 10^{16}/10^{7} \approx 4 \times 10^{9} \text{ seconds.}$$

Then the original diameter of a meteorite of present diameter d would be

$$d_o = d + \frac{2 \times 10^{-8}\, t}{4 \times 10^{9}} \text{ cm}$$

where t is again the lifetime of a meteorite. Taking 3×10^{8} years as the lifetime we get

$$d_o = d + \frac{2 \times 10^{-8} \times 3 \times 10^{8} \times 3 \times 10^{7}}{4 \times 10^{9}} \text{ cm}$$

$$= d + 4.5 \times 10^{-2} \text{ cm}$$

which is at least not obviously unreasonable.

The energy of the burst protons is considerably higher or about 11 KeV. Although perhaps it is not justified, Wehner's value of the sputtering yield of 0.5 at 400 eV may be extrapolated to this higher energy. For protons the mass relationship will cause a reduction by a factor of 10 but the higher energy will give an increase by a factor of 30 (assuming a linear relationship with energy as indicated from experiments in the low energy range). The yield per incident proton would then be about 1.5 and

$$d_o = d + 10^{-11}\ t \text{ cm (t in sec).}$$

For bursts of one hour per year

$$d_o = d + 3.6\times10^{-8}\ t \text{ (t in years)}$$

For an assumed lifetime of 3×10^{8} years

$$d_o = d + 10 \text{ cm.}$$

However the values of the sputtering coefficient found from experiments at higher energies which are mentioned in Section 8.2.1 indicate that the above figures may be much too high. If the value of 0.03 found by Moore is used

$$d_o = d + \frac{2\times10^{-8} \times t}{0.89 \times 10^{5}} = d + 2.2\times10^{-13}\ t \text{ cm.}$$

or for bursts of one hour per year during a lifetime of 3×10^{8} years

$$d_o = d + \underline{2.2\times10^{-13} \times 3.6\times10^{3} \times 3\times10^{8}}$$

$$= d + 0.24 \text{ cm.}$$

8.3.2 Solar Mass and Energy Loss Due to Proton Emission

Mass Loss

It is perhaps instructive to compute the fraction of the mass represented by the flux of solar protons. We assume two cases:

1. Quiet sun

$$600 \text{ cm}^{-3} \text{ at } 10^8 \text{ cm sec}^{-1}$$

2. Bursts

$$10^5 \text{ cm}^{-3} \text{ at } 1.5 \times 10^8 \text{ cm sec}^{-1}$$

For the quiet sun we use Reiffel's values although they are probably too high. The solar flux density at the sun's surface will be

$$600\times10^8 \times \frac{(92.9)^2}{(0.432)^2} = 6\times10^{10} \times 4.6\times10^4 = 2.8\times10^{15} \text{ cm}^{-2} \text{ sec}^{-1}$$

or

$$2.8\times10^{15} \times 1.6\times10^{-24} \times 6.2\times10^{22} = 2.8\times10^{14} \text{ gm sec}^{-1}.$$

Therefore over a period comparable to the age of the solar system the sun would lose

$$2.8\times10^{14} \times 3.2\times10^7 \times 5\times10^9 = 4.5\times10^{31} \text{ gm.}$$

This represents a mass loss of

$$\frac{4.5\times10^{31}}{2\times10^{33}}$$

or about 2% of the sun's mass.

For bursts we have a proton flux of

$$1.5\times10^{8} \times 10^{5} = 1.5\times10^{13} \text{ cm}^{-2} \text{ sec}^{-1}.$$

However we assumed previously that the bursts would occur for only one hour per year. The total mass in this case becomes

$$4.5\times10^{31} \times \frac{1.5\times10^{13}}{6\times10^{10}} \times \frac{3.6\times10^{3}}{3.2\times10^{7}} = \frac{2.43\times10^{48}}{1.9\times10^{18}} = 1.3\times10^{30} \text{ gm.}$$

or somewhat less than 1/10 the quiet sun value.

The above figures may be compared with an estimated increase in solar mass due to the Poynting-Robertson effect of 10^{6} gm sec^{-1}, or much less than the loss due to proton ejection.

Energy Loss

Under quiet conditions the sun is losing energy in the form of proton mass at the rate of

$$2.8\times10^{14} \times 10^{21} = 2.8\times10^{35} \text{ erg sec}^{-1}$$

Using a figure for the solar constant of 2 calories per minute at the earth, the loss will be

$$1.4\times10^{6} \times 4.6\times10^{4} \times 6\times10^{22} = 3.9\times10^{33} \text{ erg sec}^{-1}$$

where

$$2 \text{ cal min}^{-1} = \frac{2 \times 4.2 \times 10^{7}}{60} = 1.4\times10^{6} \text{ erg sec}^{-1}$$

4.6×10^{4} is the solid angle factor and the solar surface is taken as 6×10^{22} cm^{2}.

On this basis the sun would lose energy about 100 times faster through the escaping protons than through its electromagnetic radiation. This fact would seem to argue strongly for at least a lower particle density.

Non-Uniform Distribution of Proton Flux

It is possible that the protons are emitted non-isotropically and perhaps the flux will be a function of the periferal velocity. In this case, the particle number would be proportional to cos ϕ, where ϕ is the angle from the plane of the equator. The fraction of the solid angle then will be

$$\int_0^2 \int_0^{\pi/2} \frac{2R^2 \cos^2\phi \, d\phi \, d\theta}{4\pi R^2} = \frac{\pi}{4}$$

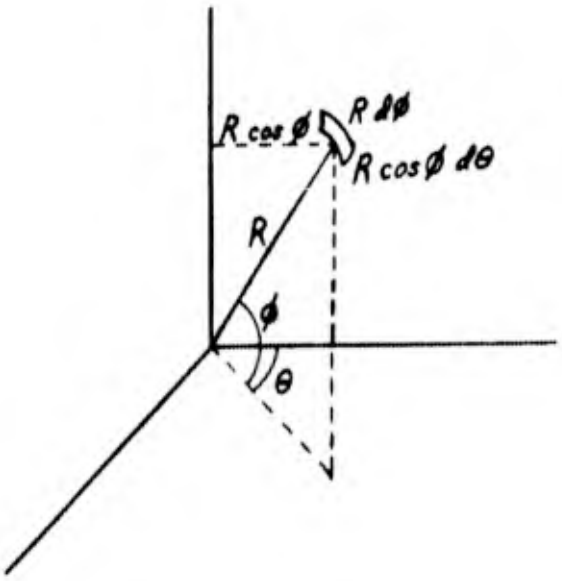

or a reduction of only about 25% from isotropism.

If both the number and velocity are proportional to cos ϕ, or a $\cos^2\phi$ dependence, the solid angle becomes equal to 2/3. Therefore it seems that non-uniform emission will not result in appreciably lower flux densities than for isotropic emission.

8.3.3 Interaction with Magnetic Field

An additional argument against high particle densities and velocities may be presented from consideration of the energy density of the solar plasma required to equal that of the earth's field. Setting these two quantities equal to one another

$$\frac{NmV^2}{2} = \frac{H^2}{8\pi}$$

Assuming a dipole field, the distance at which the solar wind can perturb the earth's field is

$$R = r_o \, (H_o^2/4\pi \, NmV^2)^{1/6}$$

For $N = 10^3$ protons cm^{-3} and $V = 10^8$ cm sec^{-1}, $R = 2.9 \, r_o$.

However the outer radiation band reported by Van Allen extends from about 3 r_o to 4 r_o. Therefore at this energy density the solar plasma could completely destroy the outer Van Allen band. The maximum values for the solar wind of 10^5 protons cm^{-3} and 1.5×10^8 cm sec^{-1} during bursts would have even more disastrous results since it could extend to about 1.1 r_o and penetrate completely the inner radiation band. The presently considered cosmic-ray albedo neutron source mechanism for the inner Van Allen belt is too slow to allow for disruptions as frequently as would be caused by these solar bursts.

REFERENCES

1. Section 3
2. Missiles and Rockets, p. 37, May 18, 1959
3. Freden and White, Univ. of Calif. Lawrence Radiation Lab. UCRL-5581-T, May 26, 1959
4. Unsöld and Chapman Obs. 69, p. 119 (1949).
5. Biermann, Astrophysik 29, p. 274 (1951)
6. Wurm, Handb. d. Phys. Vol. LII, p. 506, Springer, Berlin (1959)
7. Block, Symp. Electromag. Phenomena in Cosmical Physics, Cambridge, (1958)
8. Kozyrev, Izvestia Crimean Astro. Obs. 16, 148 (1956)
9. Blackwell, Obs. 76-77, p. 187 (1957)
10. Reiffel, Armour Res. Found. Report No. ARFDA-6.
11. Wehner, Phys. Rev. 93, 633 (1954)
12. Goldman and Simon, Phys. Rev. 111, 383 (1958)
13. Keywell, Phys. Rev. 97, 1611 (1955)
14. Moore et al, Annals New York Acad Sci. 67, 600 (1957)
15. O'Brianin et al, J. Chem. Phys. 29, 3 (1958)
16. Weiss et al, J. Chem. Phys. 29, 7 (1958)
17. Yonts et al, private communication
18. Öpik I.A.J. 4, 84 (1957) Structural Damage & Other Effects of Solar Plasmas
19. Watson, "Between the Planets", Harvard 1956

SECTION 9

LABORATORY EXPERIMENTS

9.1 INTRODUCTION

Probably a certain amount of laboratory investigation with the object of the simulation of lunar features or surface composition would be valuable. An interesting series of measurements was carried out many years ago by R. W. Wood[1]. The moon was photographed in the wavelength region of 3160 to 3260 Å and also in the visible.

A dark spot bordering Aristarchus appeared in the ultraviolet photographs but not with yellow light. Wood was able to demonstrate that a thin, invisible film of sulfur deposited on volcanic rock had similar properties while certain other materials which were tested had such dissimilar ultraviolet reflection that it appears certain that the cause of the discoloration could not be attributed to them.

Orlova[2] has compared the reflection of light from certain kinds of rocks with that from the moon. While none of the terrestrial materials seemed to be exactly comparable to the lunar surface, volcanic tuff and slag appeared to correspond more nearly in reflective properties than other terrestrial substances. Sytinskaia[3] has compared the brightness-color diagrams for various terrestrial ores and rock types with that of the moon. He found that only melted meteorites gave at all comparable diagrams and concludes that the lunar surface is covered by a layer of material resulting from the volatilization of impacting meteorites.

The above investigations are only examples of the kind of experiments that can be performed in the laboratory. They are most valuable perhaps in the negative sense; that is, when it can be demonstrated that certain circumstances are not possible or unlikely. It is in general not possible to provide positive evidence for specific compositions or conditions. However such experimentation could be extremely important in pointing the way to significant experiments with research vehicles or in actual manned exploration. No doubt a wide variety of biological investigations in a simulated lunar environment also are possible.

In the following section a simple experiment is described which reproduces some of the characteristics of the lunar craters.

9.2 LUNAR CRATER SIMULATION

Perhaps if any feature of the moon's surface distinguishes it from the terrestrial landscape it is the presence of the craters. Some authorities believe that the moon has not been geologically active for millions of years. Although a few relatively recent craters of probable meteoric origin are known, the geological history of the earth makes unlikely the finding of primeval features except in deep ocean areas[4].

Although the origin of the craters is not known, they have been variously described as resulting from volcanic action[5] meteorite impact[6] or from defluidization[7]. Actually the lunar features are quite varied and it is possible that all of these processes have played a part in the formation of the lunar surface.

Experimental Results

Following a suggestion of Dr. Ralph Havens, a brief experimental investigation was undertaken to simulate crater formation in the laboratory. Gaydon and Learner[8] have used somewhat similar means for producing model craters and their method was also used. In our experiment a small quantity of water was placed in a shallow pan and the pan filled with a fine powder. Care was taken to wet only a small volume of the powder at the bottom of the pan and no liquid was allowed to penetrate to the surface. The surface was smoothed without packing and the pan then placed under a bell-jar which was slowly evacuated. In a few minutes jets of vapor were observed to break through the surface, forming craters

very much reminiscent of those of lunar photographs

The particle size and composition of the dust were found to be rather critical in producing craters which had the desired appearance. Several materials were tried and best results were obtained with a combination of 120 mesh carborundum and 400 mesh glass frit. In fact ordinary soil and dust from the machine shop worked reasonably well and typical shallow craters could be produced. However it was not possible to study these matters at any length and it is probable that a more suitable experimental combination could be found.

Although it is not suggested that the analogy to the lunar craters can be defended in a very precise way, it must be admitted that this simple experiment can reproduce many of the characteristics observable in lunar photographs. The experimentally produced formation of Figure 9.1 shows for example some of the features often associated with walled plains:

1) little or no external wall

2) ghosts of smaller craters in the central plain

3) rows of craters along the rim.

These formations were produced by allowing the water vapor to form many small craters which eventually coalesced to form a larger relatively level area.

In Figure 9.2 individual external-walled craters will be noticed. The tendency to form hexagonal rims and terraces as on the moon can be seen. The apparent color differentiation of the outer slope due to gravitational separation of particle size is also apparent. Using a modification of the Gaydon and Learner method, if the air supply can be cut off at the right instant, a definite central protrusion can be produced. However precise control of the air supply is difficult and no real success was obtained in producing the relatively high and angular peaks characteristic of the central mountains in lunar craters. When air was allowed to enter rapidly and to erupt suddenly through the dust layer a radial pattern of lighter dust which had some of the characteristics of a ray system was formed.

A detailed analysis of the relationship between the blow holes produced experimentally and the actual lunar craters has not been attempted. In fact without more precise information about lunar geology any closer analogy is unwarranted. However the fact that many of the observed characteristics of the lunar landscape can be reproduced in such a simple way certainly merits further investigation.

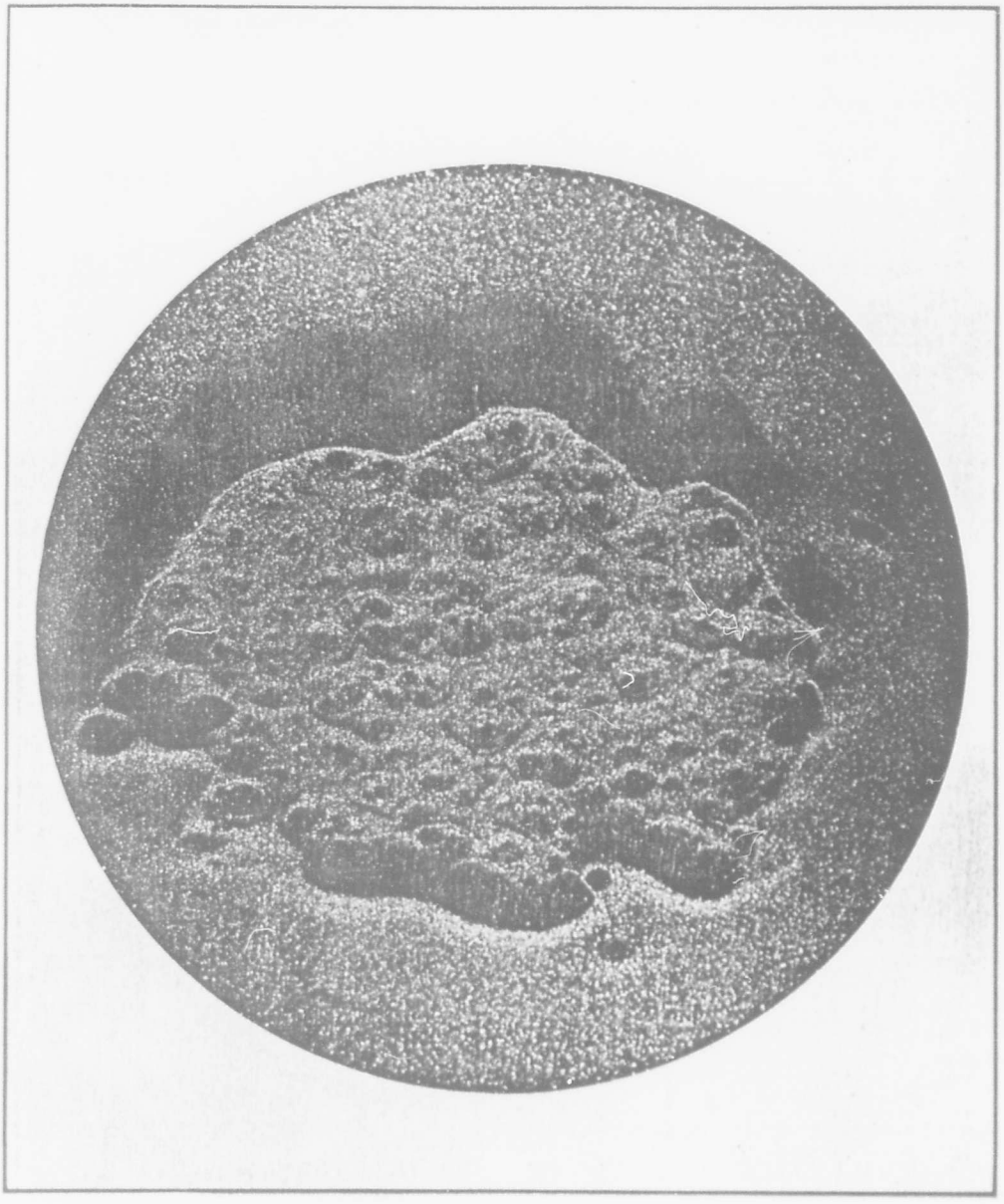

FIGURE 9.1 SIMULATED WALLED-PLAIN

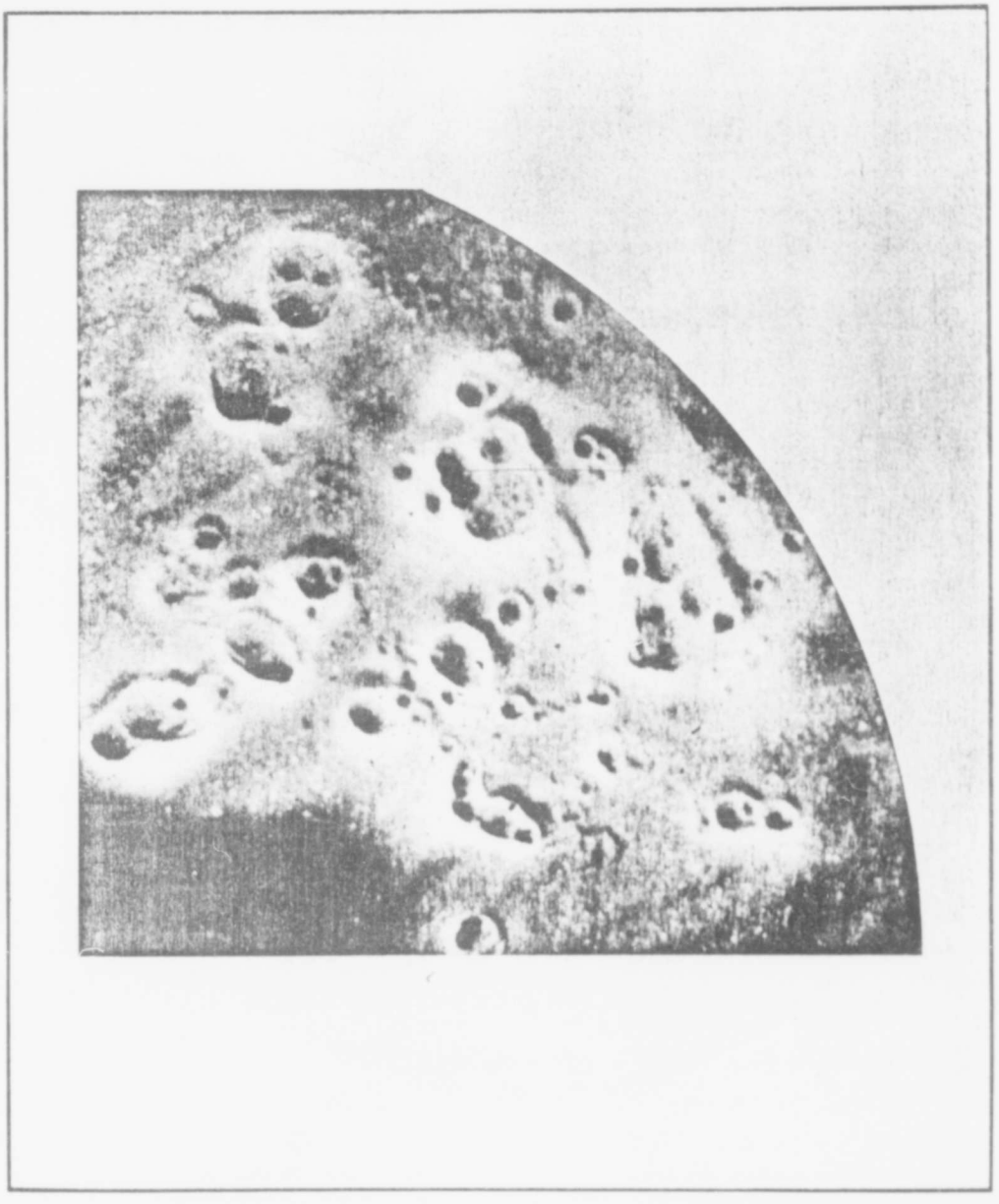

FIGURE 9.2 SIMULATED LUNAR CRATERS

1. R. W. Wood, Astrophys. J., 36, 75 (1912).

2. H. C. Orlova, Vestinik Leningrad Univ., Ser. Mat. Mekh. Astron. No. 1, 152-7 (1957).

3. N. N. Sytinskaia, Leningrad Univ. Scientific Notes, No. 190, (1957) Series of Math. Sciences, No. 29, Works of Astronautical Observatory, Vol. 17, p. 74-87.

4. Observatory (discussion Bondi, Davies & Hey) 76/7, 220 (1956/7)

5. A. Dauvillier, Le Volcanisme Lunaire et Terrestre, Paris (1958).

6. H. C. Urey, The Planets, Their Origin and Development, Yale Univ. (1952).

7. J. Green, Lunar and Planetary Exp. Coll. 1, 1-13, (1959).

8. A. G. Gaydon and R. L. M. Learner, Nature 183, 37 (1959).

APPENDIX A

EVIDENCE OF LUNAR GAS EMISSION*

Study of the lunar surface may, logically, be divided into four chronological sections with the second ending around 1902 at which time Simon Newcomb wrote: "A world which has no weather and on which nothing ever happens - such is the moon." The first era had ended in 1860 with the publication of James Clerk Maxwell's "Kinetic Theory of Gases." During that first era, the question of a lunar atmosphere was an open one. Observations by well known astronomers had limited its density to a thousandth that of the earth's but also had provided plausible, positive observations favoring the existence of such a thin atmosphere.

The photographic plate and the new, large refracting telescopes provided excellent photographs during the second interval. Some of them compare well with the better ones of today. This period witnessed violent discussion concerning the mound and craterlet, Linné. During the four decades both amateur and professional astronomers made many lunar observations. There were a good many announcements of changes on the moon's surface. Except for Linné, any permanent changes well may be dismissed as illusory, or at best as unproven. There are, however, some transitory changes such as occasional haze within the ring plain Plato and

---

*The contents of this appendix are taken from a paper "Obscurations of Lunar Features", presented by Dr. Dinsmore Alter to a National Academy of Sciences Synposium in Washington, D. C. on April 27, 1959.

the monthly variation in one of the black spots of Hercules, for which evidence strongly supports reality. Each such reported case must be considered independently.

The third era was that in which the attitude of nearly all professional astronomers was well characterized by Newcomb's statement. It appeared to them that the surface of the moon offered so little of new, valuable material that it was a waste of time and equipment to study it. Very few of them made more than token observations, although several groups did excellent photographic work (App. B).

The fourth era began after World War II, and study of the moon by various methods has accelerated greatly during the last few years. One of the problems now being studied is outgassing, which ties back to the crater Linne observations of 1866.

That crater was discovered by Riccioli during the seventeenth century. Lohrman, Maedler and Schmidt all observed it as a crater. Schmidt drew it as a crater in eight out of eleven drawings which he made between 1840 and 1843. However, in 1866 he announced that the crater no longer remained and that only the bright mound was observable. During 1867, numerous observers could find only the mound. Late in that year, Schmidt announced that he could observe a mountain in the center of the mound. During 1868 Knott, Buckingham and Key observed a shallow depression at the center. Later a craterlet was detected by Secchi who estimated its diameter as barely half a mile. Still later Huggins

measured the diameter as two miles. Since that time, it has been observed more or less easily through large telescopes when near the terminator.

In the present program pairs of photographs have been made of the lunar surface. One plate from each pair is a Kodak II-O which uses only light of shorter wave length than, roughly, 4900 A, in the blue-green. The other plate is either a I-N or a IV-N which is sensitive beyond 9500. With it is employed a Pyrex filter with its 10% cutoff near 7200. Therefore, it photographs only in the infrared. The blue-violet plates do not show the craterlet on the mound, although it is sometimes conspicuous in the infrared. Plates, like those of the Lick series, made largely in the green and the yellow would show it.

Disturbances in the earth's atmosphere cause the blue-violet photographs to show less lunar detail than do the infrared ones. Each astronomer must himself decide whether a pair of plates exhibits a true haze over any lunar feature. To do this he should compare the loss in neighboring features with that in the one which is being studied. If the feature shows significantly greater loss, a haze becomes a probable explanatory hypothesis. In such a pair for Linné* the difference appears

---

*The plates discussed here, and the Kozyrev spectrograms are not reproduced in this report. The loss of detail due to the reproduction methods would obscure the features of interest.

great enough to demand a belief that it is due to the moon itself, not to our atmosphere. One hypotheses which is not open to serious objections is that a thin haze exists and that it is more easily penetrated by red than by blue light. This haze need not be primarily gaseous, since the lunar surface must, in general, be covered by a fine dust. Although the thickness of the dust layer is controversial, a layer only a few millimeters thick can produce a haze. An outgassing, even though the density of the gas at the orifice of a craterlet is very low with respect to that of the earth's atmosphere, can stir up a thin dust cloud.

Seeing conditions at Mt. Wilson on the morning of October 26, 1956 were unusually good. Four pairs of plates were secured of the area from Ptolemaeus through Tycho. The appearance of obscuration on the western floor of Alphonsus was evident on the blue plates. Its reality was checked on all four pairs by using Arzachel as a control. Such obscurations are most easily observed under a low sun. Scattering of sunlight by a gas is almost independent of the solar altitude but the illumination of a surface feature seen through it, rather closely follows the cosine law.

The color index photography program of the moon was started in April of 1954 because of one of the Moore-Chappell series of Lick plates. This unusually beautiful picture exhibits the floors of

Ptolemaeus and of some other nearby objects as "milky". The appearance is almost like that suggested by some descriptions of visual observations of Plato when near the terminator. The milkiness is especially interesting at a bay which extends from the southwestern part of the floor, where a haze appears to pass over a shaded area and to mitigate the blackness. This bay is only about forty miles from the obscuration area of Alphonsus. No one can determine with certainty whether the milkiness of this plate represents a real lunar condition or is merely a freakishness of photography.

Publication of the Alphonsus results led Dr. N. A. Kozyrev of the Pulkova Observatory to make a spectrographic study of the region. For this work he used the 50-inch reflector of the Crimea Observatory with a prism spectrograph. On the night of 1958 November 3 he was observing with phase conditions almost the same as they had been when a haze first was observed in 1956. The slit of his spectrograph was extended east and west across the central peak of Alphonsus. Each line of a spectrogram must exhibit the radiation profile along its trace on the lunar surface. The line is strengthened where the moon is bright and the intensity fades to practically zero at the shadows. The same thing holds true for the continuum. The lunar spectrum must be the solar spectrum, modified by any color exhibited by the moon, by any absorbing gases and by any luminescence.

Unfortunately the accounts in our newspapers suffered both from omission of pertinent data and language difficulties. It would have been far better if the word "eruption" had not been used. Technically, it is correct but the image which it brings to mind is not. The "eruption" was a half-hour long discharge of gas from the craterlet atop the high central mountain of Alphonsus.

The following is quoted from a letter written by Dr. Kozyrev. The letter was accompanied by glossy paper prints of the three most important spectrograms.

"Spectrogram 1: Nov 3 0^h-1^h U.T. You will notice that the central peak is redder than the neighboring (floor of Alphonsus) and has a normal appearance of the spectrum.

"Spectrogram 2: 3^h-3^h30^m U.T. The spectrum of the central mountain shows a bright gaseous emission. The most prominent emission bands are the 4756 A (which has not yet been identified) and the Swan band group of the molecule C_2 at 4735, 4713 and 4696 A. In addition one may see other lines; their identification has not yet been made.

"Spectrogram 3: During the guiding of the Spectrogram 2 I noticed a marked increase in the brightness of the central region and an unusual white color. All of a sudden the brightness started to decrease. At this instant the exposure was stopped and a new one started from 3^h30^m to 3^h40^m. The result was a normal spectrum with only a slight suspicion of a Swan band."

There is no question about the emission shown in the continuum. However, the prints which have been available do not show the Swan spectrum. These prints have gone through several stages before preparation of the transparency which was examined and any Swan bands which showed in the originals well may have been completely masked. The Swan bands are found in cometary spectra. They are due to the effect of solar radiation in exciting the carbon molecules to luminescence. Although the presence of these bands would be important, Kozyrev's observation of the brightening and his securing a spectrum with any luminescence pattern is even more so. It well may be true that the original negatives would show the Swan spectrum.

Kozyrev's results started quite a number of observations of the Alphonsus area and there have been some interesting, confirmatory observations. On November 19, Dr. H. P. Wilkins in northwest Kent in England reported that using a 15½ inch reflector, "the central peak appeared bright but a faint dusky reddish patch, about 2 miles in diameter, was distinctly seen immediately to the south". He reports also that on the same night J. Wall and F. D. Brewin also saw the dusky patch with a 12 inch telescope.

Later that night, although still on the 18th by Pacific Standard Time, two physicists from San Diego, Drs. H. F. Poppendiek and W. H. Bond, who are amateur astronomers, observed the moon with a 6-inch reflector.

They had not heard about the Kozyrev observations. At about eight P.M. they observed a bright cloud obscuring the peak in Alphonsus and watched it for nearly half an hour. Two weeks later they checked and found nothing. It is interesting that Wilkin's observation of a dusky cloud preceded their observation, exactly as Kozyrev observed a reddishness to the peak about three hours before he saw the bright cloud.

One other observation made on that night must be included. Mr. Raymond J. Stein, supervisor of the Newark Museum, observed the moon from the roof of the museum, using a 4-inch reflector. Seeing conditions were unusually good. He reports: "At 22:00 U.T. I suddenly noticed that a portion of the shadow covering the floor of the neighboring crater Alpetragius had faded. Just a few minutes previously, the shadow had covered about two-thirds of the crater floor causing the peak of the high central mountain to stand out in bold relief as a bright spot against a black background. Now the mountain peak was but several magnitudes brighter than the background. Approximately one-half of the total shadow had faded, almost disappearing completely. I definitely did not see a glow, nor can I say that haze was apparent. A portion of the shadow merely vanished and seemed to be replaced by a much lighter shade. At 22:05 U.T. the shadow gradually darkened until in approximately 20 seconds, it had repossessed the area it had originally occupied." Alpetragius is just outside the wall of Alphonsus on the east.

When all data from every source are considered it seems to be definitely true that at least some residual outgassing still takes place on the moon It is possible that there is even more action, but as present it seems best to accept only that to which one is forced and to leave more interesting speculations to the future when more data may be available The outgassing does, however, demonstrate the need for certain systematic programs of lunar observation Whatever facts can be learned from stations on the earth will aid space research and cost little in comparison to those learned by means of rockets Our lunar programs are seriously handicapped by lack of sufficient systematic data

APPENDIX B

APPLICATION OF PHOTOGRAPHY TO LUNAR OBSERVATIONS, WITH NOTES CONCERNING THE HISTORY OF THE ART

B 1 EARLY PHOTOGRAPHY

Probably it is legitimate to consider the first inventive steps toward our photography of today as belonging to the 16th century, although possibly they should be turned backward even to the Arabian Alhazen at the beginning of the eleventh century. Certainly, the beginnings consist of the invention and improvement of the camera obscura which had a long and useful history even before the use of light sensitive salts.

Commonly the invention is stated as that of Baptista Porta in 1553. However, an unpublished manuscript by Leonardo da Vinci, who died in 1519, describes and pictures the camera. Roger Bacon, also, in 1267 makes reference to it although he may never have constructed one.

In 1568, Barbaro suggested the use of a convex lens and a diaphragm to secure sharper images. Danti in 1573 made use of a mirror to secure erection of the image. Risner proposed the use of a portable box in place of the fixed room then in use. Kepler inserted a concave lens behind the convex one to give larger images. This is exactly what

Galilleo was doing at about the same time to secure a direct view of distant objects. Zahn in 1665 introduced additional lenses and shielding side wings to increase the brilliancy of the images. There was much use of the portable camera to assist in sketching.

The light sensitivity of silver salts was observed during the sixteenth century, but it was not known that the effect was due to light instead of heat. This fact was learned early in the 18th century by Schulze in Germany. Late in that century Scheele and Wedgwood in England experimented with silver nitrate on paper and other substances. In none of his work was any means known of fixing the images and they had little value at the time.

Useful recording of pictures through the effects of light on silver salts developed through the work of J. Nicephore Niepce as an aid to lithography. Successful work by him and his nephew attracted the attention of the painter Daguerre, who had experimented with silver salts. In 1826, Daguerre proposed a partnership to Niepce who had been handicapped by the call of his nephew to army service. Three years later, the partnership was formed. They found advantages of silver iodide over the nitrate. During the experimentation Daguerre learned that if a metal plate which was coated with silver iodide was exposed at a camera focus and then fumed with mercury vapor he could obtain an image. The results were published and were presented to the French Academy on 19 August 1839.

The process was a great success although at first the sensitivity of the coated metal was low. Soon they increased it hundredfold. Portraiture by it became a fad and today most families still have from one to dozens of such reversed portraits of their ancestors and collateral relatives. The first step in the manufacture of a Daguerretype was to silver plate a copper plate. Next this plate was highly buffed. After the buffing it was exposed to iodine vapor to produce the silver iodide. By 1840, the plate was resensitized by exposure to bromine. It now was ready for exposure to the light image. Latitude was small, and it was necessary to time the exposure accurately. The next step was development of the picture by mercury vapor. One wonders how much mercury poisoning there may have occurred among those early photographers. The final step was fixing with thiosulphate of soda. The picture now was stable but its quality was improved by toning in a solution of gold chloride. Those of us who used the printing out papers which were almost universal at the beginning of this century will remember that we very carefully washed out all the excess silver, then toned with gold and fixed the picture as a final step. One excellent paper (Aristo Platino) required additional toning with platinum chloride. The fixing process was discovered by the astronomer, Sir J. J. F. Herschell in 1819.

B.2 DEVELOPMENT OF LUNAR PHOTOGRAPHIC TECHNIQUES

The daguerreotype brought about the first astronomical photograph, one of the moon, made in 1840 by Dr. J. W. Draper. His pictures were of poor quality and the diameter of the image was only about an inch. Ten years later Dr. W. C. Bond, first director of the Harvard College Observatory, used the fifteen inch refractor there to secure excellent daguerreotypes of the moon. These were shown in London at the great exhibition of 1851 and there attracted the attention of Warren De la Rue who at 36 already had made a large fortune as a paper manufacturer. The wet plate, or collodian process, was announced in that same year. It was invented by an English architect named Scott Archer. At first it was necessary to prepare his plates immediately before exposure. Later modifications made it possible to keep them for some time before use. In 1864, W. B. Bolton and B. J. Sayce prepared plates using a dry emulsion of collodion. The gain in convenience was great but the sensitivity was not improved in their first plates.

The last of the major inventions was that of Dr. R. L. Maddox in 1871. He followed the previous procedure but substituted silver bromide for the iodide and held it as an emulsion in gelatine instead of collodion. His dry plate was the prototype of the plates in use today. Much improvement was made by quite a number of experimenters

during the next dozen years. In 1877, the first commercial dry plates were placed on the market by three manufacturers. By 1879, rather rapid ones were available and exposures as short as one two-hundredth of a second could be made. This ended the period of general amateur experimentation in improvement of plates.

During the 1880's various dyes were introduced and the first isochromatic and orthochromatic plates were produced by an extension of their spectral sensitivity toward the red. In 1906, this extension was completed throughout the red and provided the introduction of the first panchromatic plates. This advance was of extreme importance to astronomy. By 1925, infrared plates were usable to greater wavelengths than 9000. The first infrared plates were very unstable and were slow. Great improvements have been made, both in stability and in sensitivity Today, the astronomer or other scientist has a fairly good range of speed, graininess and contrast from which to select the plate most useful in his work. Perhaps directly and indirectly, Dr. C. E. K. Mees of the Eastman Kodak Company has contributed most to the qualities of the plates which are used by astronomers today.

B.3 EARLY LUNAR PHOTOGRAPHY

The interest which Bond's lunar photographs aroused in De la Rue initiated the first use of photography as a tool in astronomical research. His wealth made it possible for him to secure the best of instrumental aid. In 1853, he made exquisite lunar photographs, using the new glass plate method. He had recognized the chromatic advantages of the reflector and used one of thirteen inch diameter in his first work. By 1857, he had installed the driving clock which is essential in astronomical photography and that same year completed his observatory, to be devoted to photographing astronomical objects. The famous physicists Foucault and Fizeau had used the daguerreotype process in 1845 to photograph the sun but apparently nothing further had been done. De la Rue's photographic observations of the sun are among the greatest series of science. In that same year cooperation began between him and the Royal Society. Before his death cooperative, photographic, solar observations extended around the earth.

In the United States lunar photography was much developed by Dr. Henry Draper, son of the man who photographed the moon in 1840, and by Lewis M. Rutherford. During the seventies photography was invoked in an attempt to determine the truth concerning the apparent changes in the craterpit on the bright mound, Linne, in Mare Serenitatis. Nothing definite could be learned. The telescopes were not large and

the plates were not sensitive for light waves longer than about 5000. The question concerns obscuration by gas or dust. Red and especially infrared waves are needed. The Linne question at last may have been partially settled in 1957 and 1958.

Professor N. P. Shaler of Harvard used photography for a rather systematic study of the lunar surface. His results and their discussion comprise a volume published near the start of the century. W. H. Pickering, also of Harvard, made a long series of exquisite observations mostly from the Mandeville station in Jamaica.

The 36-inch Lick Observatory refractor was used in the 1890's to secure perhaps the best lunar pictures to that time. The long focus revealed more details than previously had been possible. The Paris Observatory, using its 23.6 inch refractor, also contributed its share. None of these pictures exhibited all the data which could be observed visually. They did, however, have two great advantages because they recorded all data which were within their scope and because the truth of their record was incontrovertible, not marred by preconceived ideas or by faulty imagination. Soon lunar photography lagged. It was believed little more could be learned.

B.4 TWENTIETH CENTURY LUNAR PHOTOGRAPHY

During recent decades lunar photographs have been made sporadically at nearly all large observatories. Undoubtedly no publication has been made of many excellent ones. Any listing certainly is incomplete. For example, some excellent lunar photographs have been published from the French Pic du Midi Observatory. However, rumor states that there has been large scale consistent observation there.

One of the best small groups of photographs was made by Dr. F. G. Pease on September 17, 1919, using the 100" telescope at Mt. Wilson. The moon was at last quarter that morning and three pictures of the group were skillfully joined to produce a beautiful montage which has been published many times. Even today, with modern plates, its quality scarcely has been excelled.

Previous to World War II, the late Dr. Fred Wright of the Carnegie Institution made an extensive series, using that same telescope. The material, apparently, is now being prepared for publication by his daughter, Miss Helen Wright and the astronomer, Dr. Gerard Kuiper. Probably it will form part of a promised photographic atlas.

One of the most important series of lunar photographs is that which was made by the late Dr. J. H. Moore, former director of the Lick Observatory, and Mr. J. F. Chappell, the observatory photographer. They

used the 36" refracting telescope and secured the whole of the lunar disk on each plate which was exposed. The rather small number of exposures extended over approximately ten years, 1938 - 1948. Due to the difficulties incident to chromatic aberration in a visual refractor, it was impossible for them to make use of either violet or infrared light. Their plates had maximum sensitivity in the yellow green and were controlled by a transmittin filter for that region.

B.5 SPECIAL METHODS FOR LUNAR PHOTOGRAPHY

Moore and Chappell introduced a necessary systematic practice to the art. Photographs of much research value must conform to at least three conditions:

(1) Transparency of the air must be good.

(2) Seeing condition, or steadiness of the image, must be unusually good. Except for a small amount of experimental work, the majority of nights which are very satisfactory to the spectroscopist are useless for lunar and planetary photography.

(3) The telescope must be large enough that its resolving power permits a record of small details on nights of unusually good seeing. The standard statement concerning resolving power is based on the diameter of the objective or mirror. The equation used is that of Dawes for the minimum separation at which a double star can be resolved.

(There is no need here to go into theory of diffraction rings.) If s is the separation of the stars and d the diameter of the mirror or objective in inches

$$s'' = \frac{4'' \cdot 5}{d}$$

One mile of the lunar surface subtends a little less than one second of arc as viewed from the earth. Therefore, even under the most perfect seeing conditions, a telescope of 18" diameter would be required to reveal a crater a quarter of a mile in diameter. Of course, even greater resolving power would be desirable.

(4) Moore and Chappell used only the best nights. On nights when the "seeing" was unusually steady, and the moon available, the regular observer would notify them. They would spend approximately an hour making from three to five exposures. The regular program was then resumed. A rather few plates, therefore, told enough of the story that Dr. Alter spent fully 700 hours studying them before exposing his own first plates.

In this type of photographic work an additional factor must be considered in determining resolving power. The "grain" of the photographic plates varies greatly. Fast plates have coarse grain. Usually, slow plates have fine grain and some plates, such as process plates and lantern

slides, have negligible grain so far as lunar photography is concerned. This is not true of most of the plates used at the telescope. Kodak I-N plates, exposed at the Cassegrain focus of the 60" at Mt. Wilson, do show granular difficulties on nights when the seeing is exceptionally steady. If exposed at the much shorter Newtonian focus the graininess would be serious. Long focus telescopes have greater practical resolving power in lunar photographic research than do shorter ones of the same objective or mirror diameter.

It would be natural to expect telescopes of long focus and of great diameter to give the best results. The layman expects the 200" Hale reflector at Palomar Mountain to reveal more detail than would be possible with any other.

"Bad seeing", i.e., unsteadiness of the image, is due to mixing currents or "waves" of air at different temperatures. It follows different patterns. Some comes from air near the telescope. Some comes from greater altitudes. Sometimes the waves are "short". At other times they are "long". If the distance between shiftings of light in a given direction is less than the diameter of objective or the mirror, it is impossible to obtain a "perfect picture", no matter how short the exposure time may be. If such "short" waves are near the telescope, one part of the lunar disk may be in sharp focus but another part out of focus at the same instant. If the waves are much larger than that diameter, the whole image may be shifted with little distortion and a very short exposure at the proper instant can produce valuable results.

As we go to larger telescopes we decrease the frequency of instants when the atmospheric waves may be considered as "long". This limits greatly the size of telescope which it is efficient to use for such work. The instants when the whole aperture of the 200" could be used efficiently must be extremely rare and perhaps never occur. Such rare instants do exist for the 100", as is proved by the Pease photographs, but possibly are too infrequent to justify scheduling the telescope for such work. Definitely for the 60" there are quite a number of desirable nights per year. Perhaps one clear night out of five is usable to obtain lunar negatives of research quality, and one out of ten is excellent.

A 36" telescope would give a definitely improved ratio of "good" nights. Its theoretical resolving power would reveal craters an eighth of a mile in diameter. Of course, the larger telescope could be "stopped down" and used, but that involves the use of a far more expensive instrument and one which on that same night could have been used on a program which took advantage of its full light gathering power.

The astronomer planning any definite program of lunar photography must consider several preeminent factors:

(1) Observing conditions, both with respect to transparency and seeing.

(2) A telescope of at least 36" diameter is needed. Probably it would be poor procedure to have one of much more than twice that diameter.

(3) The long Casseg-ain focus, or the still longer Coude focus, is essential because of plate graininess. If necessary a proper form of enlarging lens could be employed at the Newtonian focus.

(4) The observatory must be so located that it is practicable to carry out the Moore-Chappell procedure and to notify the observer whenever the conditions are right. If he cannot reach the telescope within 15 or 20 minutes of notification the plan fails. Also the observatory program must be such that the director is willing to permit such interruption of other work.

(5) A very highly specialized form of camera, probably costing between two and three thousand dollars, is needed.

(6) The cost of photographic plates will be large and the supply must be assured before the program is operative.

(7) Probably it would be foolish to consider a less than two year program.

Any special plan to be executed would add other conditions to these general ones.

The best known recent series of lunar photographs is probably that of Dr. Dinsmore Alter.

This series was started in 1954 following a long study of the Moore-Chappell photographs.

One of the Lick photographs, made 1937 October 26 at phase $22^{d}.07$ and at colongitude $173^{\circ}.8$, showed the floor of Ptolemaeus with a milky appearance as though it were covered by a thin fog. This appearance was especially strong at the southern "shoreline" of the comparatively flat floor. It brought to mind visual observations (made by experienced amateurs) of the floor of Plato, which has been reported sometimes as milky near sunrise and sunset.

The initial plan was to obtain data on this phenomenon by means of photographs in blue-violet and in red and infrared. Permission was obtained to use the 60-inch reflector at Mount Wilson for this purpose and, special 5 x 7 camera was built in the Griffith Observatory shops. The first 35 plates were exposed on April 9, 10 and 11. Pairs of plates were exposed, using Kodak 103a-O Bkd, without a filter, to obtain the blue-violet pictures and 103a-E with a Pyrex C. G. 2-64 to secure the red. The seeing during the three nights varied from about 2 to better than 3 on the Mount Wilson scale. This is their usual quality of seeing and is entirely satisfactory for spectroscopic work. Colongitude 360° was passed on April 10. The phases were, therefore, shortly after sunrise on Ptolemaeus.

These first plates demonstrated the greatest difficulty to be encountered in the work. Not only does the lack of steadiness of the terrestrial atmosphere affect very much the quality of all photographs of celestial objects but the effect is considerably greater for blue than for red light.

Possibly a blue plate exposed under the somewhat unusually good seeing 4 would equal a red one exposed under seeing 3. As steadiness improves, this color difference lessens and at rare conditions of seeing 6 would not be large. However, during 4½ years of this program Dr. Alter never rated it better than 5. If one is examining plates for effects caused by an obscuring medium it becomes almost impossible to demonstrate beyond reasonable doubt that they exist. Always the blue plate shows less detail at each point of the image than does the red one. The only argument that the observer can use is that the obscuration at some given feature is greater than at other features and that consequently it is probable that a medium exists at that point. Nights like October 26, 1956 are rare and even they give results which may not convince those who have held definite, theoretical, contrary views concerning the nonexistance of such media.

At about 0300 P.S.T. on that date seeing became unusually good with a basic 4, varying upward for short intervals to fully 5. Ptolemaeus, Alphonsus and Arzachel were near the sunset terminator. When the sun is low at a given point one finds the best possible condition to aid in search for obscuration by a gaseous medium. Rayleigh scattering is almost independent of the sun's altitude but the illumination of a lunar plain follows the sine law of altitude. The floor under a low sun is far less bright than under a high sun. Infrared radiation passes through a gaseous mass more freely than do blue and violet.

Under these conditions the haze effect should show more plainly on the shorter wave plate. On the morning of October 26, Dr. Alter secured four pairs of plates. Each pair demonstrated quite well the probable existence of an absorbing gaseous layer on the western floor of Alphonsus. The results have been published as one of a series of seven papers on 'The Nature of the Lunar Surface", in Publications of the Astronomy Society of the Pacific. Kozyrev was continuing this work, using a spectrograph, when he made his startling recent observations. (Appendix A).

APPENDIX C

VISIBILITY OF TRACKING BALLOONS

C.1 REFLECTION FROM SPECULAR SPHERICAL REFLECTORS

The intensity of reflected light from spherical specular reflectors between the earth and the moon will depend upon the diameter of the reflector and its distance from the earth. When the reflector is in opposition, the reflected intensity can be calculated quite simply as shown in Fig. C-1. For a convex spherical mirror all of the light from a distant source which is incident upon the mirror surface within an angle of 45° from the direction to the source is reflected into a solid angle of 2π. The total incident light so received is given by

$$F_t = F_o \pi R_p^2$$

where F_t = total incident light

F_o = solar light flux at balloon surface

R_p = projected radius = $R_s \cos 45^{\circ}$

From this the intensity of reflected light received at a surface a distance d from the balloon is:

$$F_E = F_o \pi (R_s \cos 45^{\circ})^2 / 2\pi d^2 = F_o R_s^2 / 4d^2 \qquad \text{(C-1)}$$

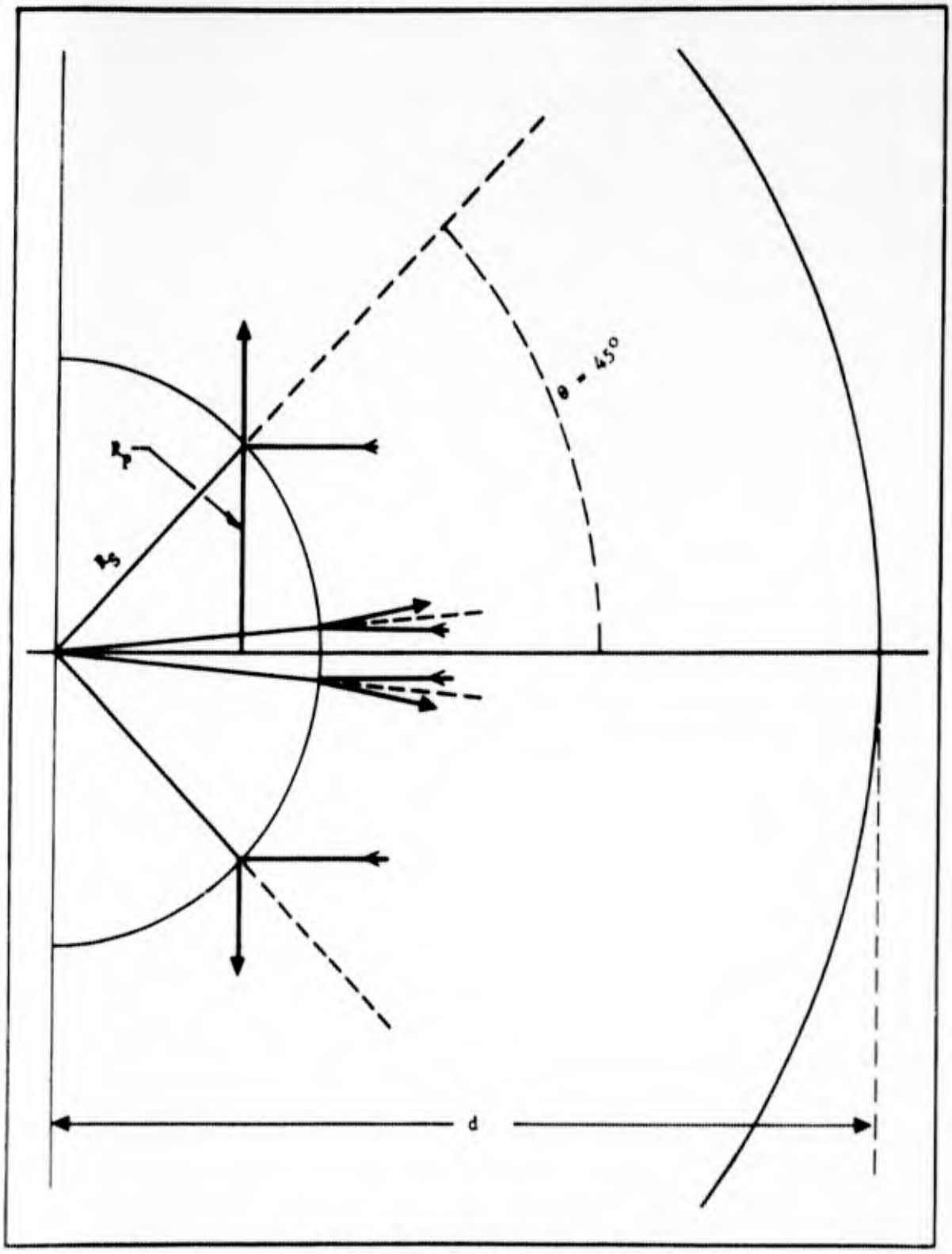

FIG. C-1 SPHERICAL REFLECTOR (OPPOSITION)

where F_E is the reflected flux at the earth's surface. In the above relation, the fact that the focal point of the mirror (for a small angular aperture) is R/2 behind the surface is ignored.

The above value is strictly correct only for exact opposition, and may be obtained in another manner. In Fig. C-2, it is seen that the light from a distant source reflected into a region of radius R_E at a distance d, will be equal to that incident upon a region of the mirror surface bounded by one-half the angle subtended at the mirror by the receptor. All light incident upon the mirror outside of this area will be reflected at an angle sufficiently great to miss the earth. The radius of the projected area on the mirror from which light is reflected to the earth is then

$$R_p = R_s \cdot R_E/2d$$

and so the intensity of the reflected light at the earth's surface will be:

$$F_E = F_o \pi (R_S \cdot R_E/2d)^2 / \pi R_E^2 = F_o R_S^2/4d^2$$

If the sun and reflector are not in opposition, and the sun has an elevation angle of θ with respect to the earth, the light flux reflected from the reflector to the earth can be calculated as shown in Fig. C-3. Consider the light incident upon a circular strip of width $R_s d\theta$ centered about an angle of $\theta/2$ with respect to the Z axis (or source direction). The area of this strip as seen in the

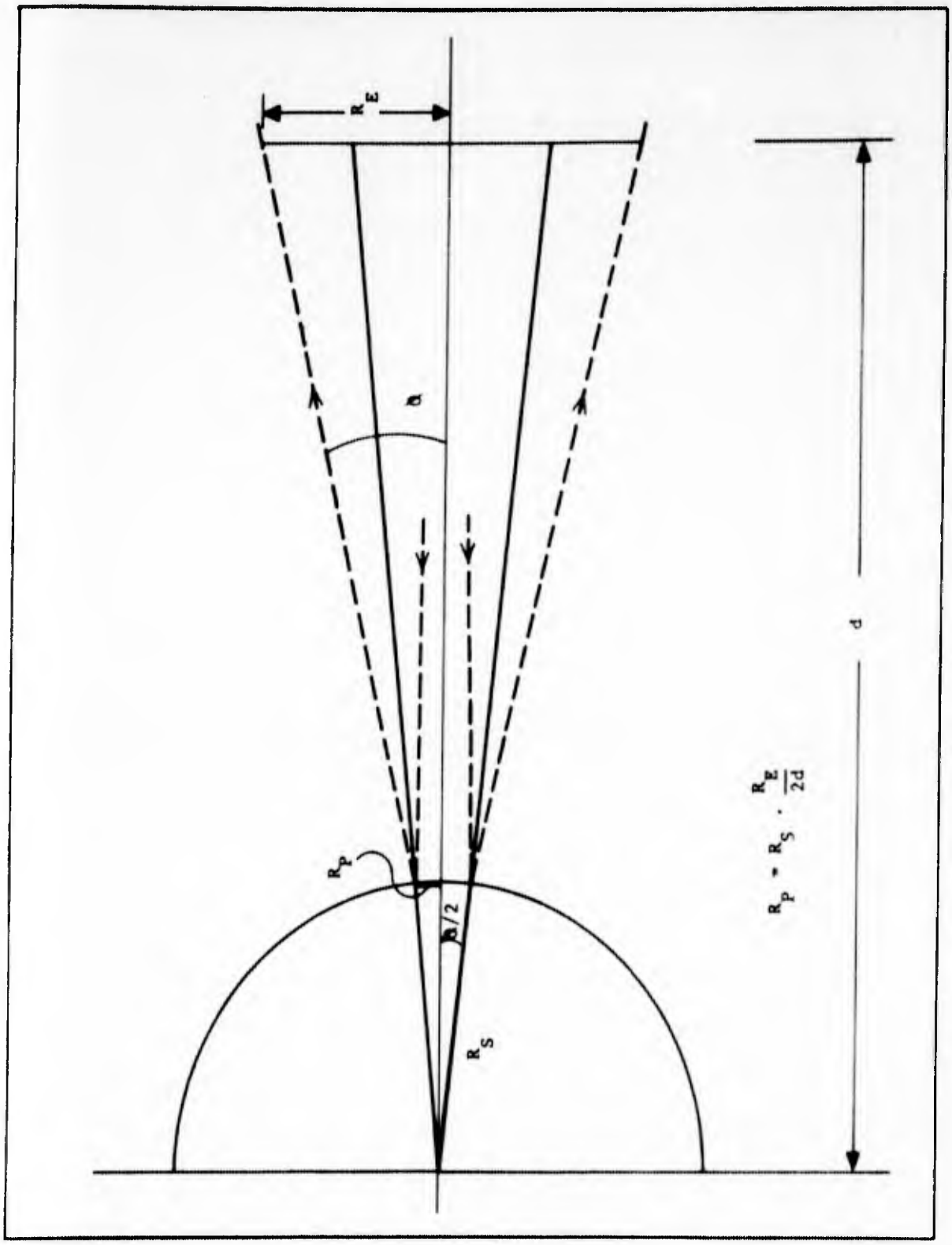

FIG. C-2 FLUX FOR OPPOSITION

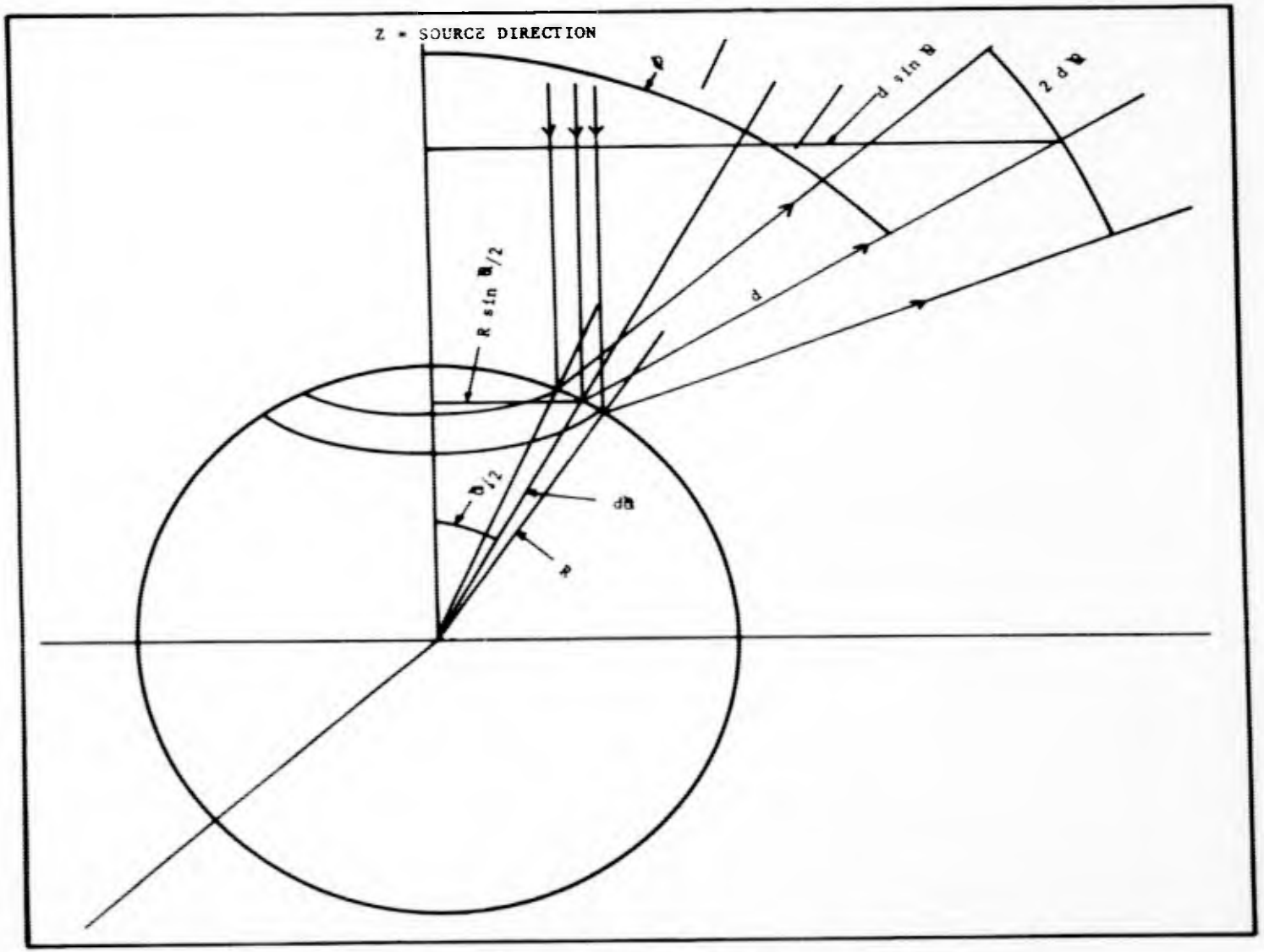

FIG. C-3 SPHERICAL, SPECULAR REFLECTOR - SUN ELEVATED

figure will then be

$$A_s = 2\pi R_s^2 \sin \theta/2 \, d\theta$$

The incident light per unit area on this strip will then be given by $F_o \cos \theta/2$ when F_o is the light flux/unit area from the source. The total light incident upon the strip in question will then be

$$E = 2F_o \pi R_s^2 \sin \theta/2 \cos \theta/2 \, d\theta \qquad (C-2)$$

All of this light will be reflected into a region bounded by two cones as shown, and the angle between the two conical surfaces will be equal to $2d\theta$. At a distance d, from the surface, all of the light reflected from the circular strip will impinge upon an area equal to

$$A_E = 2\pi d^2 \sin \theta 2d\theta \qquad (C-3)$$

Therefore the intensity of the reflected light as received on this area will be

$$\begin{aligned} I &= \left[2F_o \pi R_s^2 \sin \theta/2 \cos \theta/2 d\theta\right] \Big/ 2\pi d^2 \sin \theta 2d\theta \\ &= \left[F_o R_s^2 \sin \theta/2 \cos \theta/2\right] \Big/ 2d^2 \sin \theta \\ &= F_o R_S^2 / 4d^2 \end{aligned} \qquad (C-4)$$

since $\sin \theta/2 \cos \theta/2 = 1/2 \sin \theta$.

The light flux received from a spherical specular reflector is therefore independent of the phase angle of the source, reflector and receiver system.

C.2 CONVEX SPHERICAL DIFFUSE REFLECTOR

The light received at the surface of the earth from a convex spherical diffuse reflector in cis-lunar space can be calculated as shown in the following.

Let the sub-solar point be the pole (Fig. C-4) and ϕ the angle between the polar axis and an arbitrary point (P) on the surface. The light flux incident on unit area of the spherical surface at P is then readily seen to be J cos ϕ, where J is the solar light flux at the Earth-Lunar distance. In this calculation, the incident light is assumed to be parallel. An element of area ds at the point P will be given by

$$ds = R^2 \sin\phi \, d\phi \, d\theta \qquad (C-5)$$

with θ being the azimuth angle as shown. In this picture the terminator is quite accurately at $\phi = \pi/2$; and so the total light incident upon the illuminated hemisphere is readily attained by integration:

$$E_{total} = JR^2 \int_0^{2\pi} \int_0^{\pi/2} \cos\phi \sin\phi \, d\phi \, d\theta$$

$$= 2\pi \, JR^2 \, (\sin^2\phi) \Big|_0^{\pi/2} = J\pi R^2 \qquad (C-6)$$

as would be expected from simple considerations.

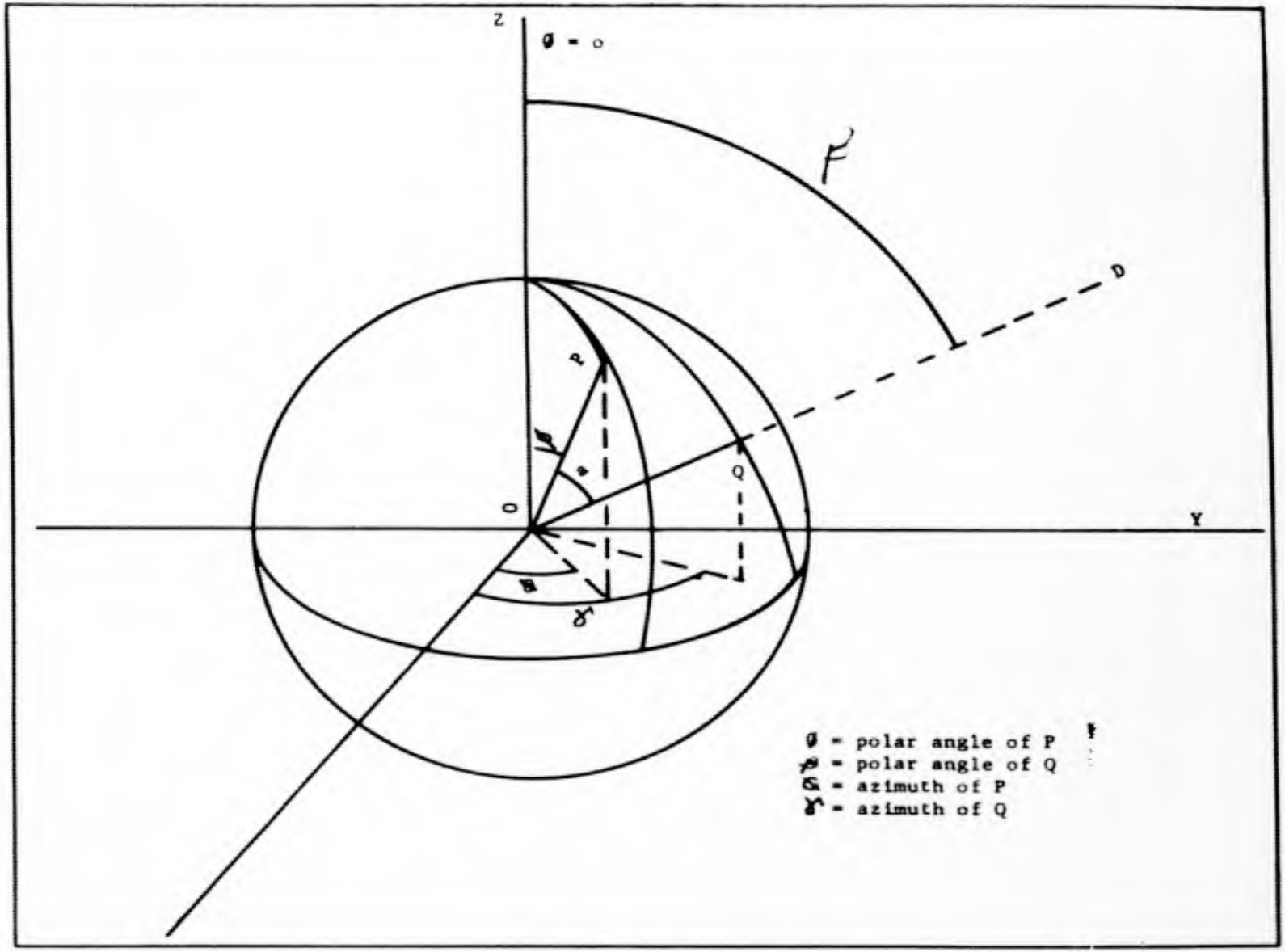

FIG. C-4 ANGULAR RELATIONSHIPS

Since the surface is a diffuse reflector, the amount of light reflected from unit area at point P into unit solid angle in the direction D is equal to

$$E_{\omega D} = \frac{1}{\pi} J \cos\phi \cos\alpha \qquad (C\text{-}7)$$

where α is the angle between OP and OD, the direction to the receiver.

The light reflected into unit solid angle in the direction of the receiver at D from an element of area at P is then

$$E_{\omega D} = \frac{1}{\pi} JR^2 \cos\phi \sin\phi \, d\phi \, d\theta \cos\alpha \qquad (C\text{-}8)$$

Let the radius, R, be unity and $\cos\alpha$ is the projection of OP on OQ. If components of OP and OQ are x, y, z and x', y', z', respectively,

$$x = \sin\phi \cos\theta \qquad x' = \sin\beta \cos\gamma$$

$$y = \sin\phi \sin\theta \qquad y' = \sin\beta \sin\gamma$$

$$z = \cos\phi \qquad z' = \cos\beta$$

and

$$\cos\alpha = xx' + yy' + zz'$$

$$= \sin\phi \cos\theta \sin\beta \cos\gamma + \sin\phi \sin\theta \sin\beta \sin\gamma \cos\phi \cos\beta$$

$$= \sin\phi \sin\beta (\cos\phi \cos\gamma + \sin\phi \sin\gamma) + \cos\phi \cos\beta$$

$$= \sin\phi \sin\beta \cos(\gamma - \theta) + \cos\phi \cos\beta$$

The light reflected into unit area at distance d and in the direction OD from the visible portion of the illuminated hemisphere is then (for $d \gg R$):

$$E_D = \frac{JR^2}{\pi d^2}\left(\sin\beta \iint \cos\phi \sin^2\phi \cos(\gamma - \theta)\, d\phi\, d\phi + \cos\beta \iint \cos^2\phi \sin\phi\, d\phi\, d\theta\right) \qquad (C\text{-}9)$$

Special Cases.

Two special cases can be solved quite readily. These are for full phase and quadrature. A simplification can be made without loss of generality by defining the coordinates such that the source and receiver (Sun and Earth) are contained in the yz plane. Then γ becomes $\pi/2$ and the term $\cos(\gamma - \theta)$ becomes $\cos(\pi/2 - \theta) = \sin\theta$.

Full Phase.

For the full phase situation β is zero and the general expression above (C-9) reduces to

$$E_{DF} = \frac{JR^2}{\pi d^2} \int_0^{2\pi} \int_0^{\pi/2} \cos^2\phi \sin\phi\, d\phi\, d\theta \qquad (C\text{-}10)$$

the limits being readily established since the illuminated and visible portions of the hemispheres are identical. Integrating this expression we obtain

$$E_{DF} = \frac{JR^2}{d^2} \cdot 2 \left(-\frac{\cos^3\phi}{3}\right)\Bigg|_0^{\pi/2} = \frac{2JR^2}{3d^2} \qquad (C\text{-}11)$$

as the reflected light flux (per unit area) at the surface of a receiver at distance d.

Quadrature

For quadrature the angle β is $\pi/2$ and (C-9) then reduces to

$$E_{DF} = \frac{JR^2}{d^2} \int_0^{\pi} \int_0^{\pi/2} \cos\phi \sin^2\phi \sin\theta \, d\phi \, d\theta \qquad \text{(C-12)}$$

The limits on ϕ are established by the fact that only the upper hemisphere is illuminated. The limits on θ are fixed by the portion of the sphere which is visible from a distant point along the y axis. Then the light flux at the receiver from the quadrature (half moon) will be:

$$E_{DQ} = \frac{JR^2}{d^2} \cdot 2 \left(\frac{\sin^3\theta}{3}\right) \Big|_0^{\pi/2} = \frac{2JR^2}{3\,d^2} \qquad \text{(C-13)}$$

so that the light received from the balloon at quadrature will be $1/\pi$ that received at full phase.

Gibbous Phase

While the full phase and quadrature cases fall out quite simply the evaluation of light received from the reflector in the gibbous phase ($0 < \beta < \pi/2$) and the crescent phase ($\pi/2 < \beta < \pi$) is somewhat more difficult. For simpler calculation, rotate the coordinate system until the source and receiver are in the xz plane with the x component of OD being positive (Fig. C-5). The components of OP and OQ now become

$x = \sin\phi \cos\theta$ $\qquad$ $x' = \sin\beta$

$y = \sin\phi \sin\theta$ $\qquad$ $y' = 0$

$z = \cos\phi$ $\qquad$ $z' = \cos\beta$

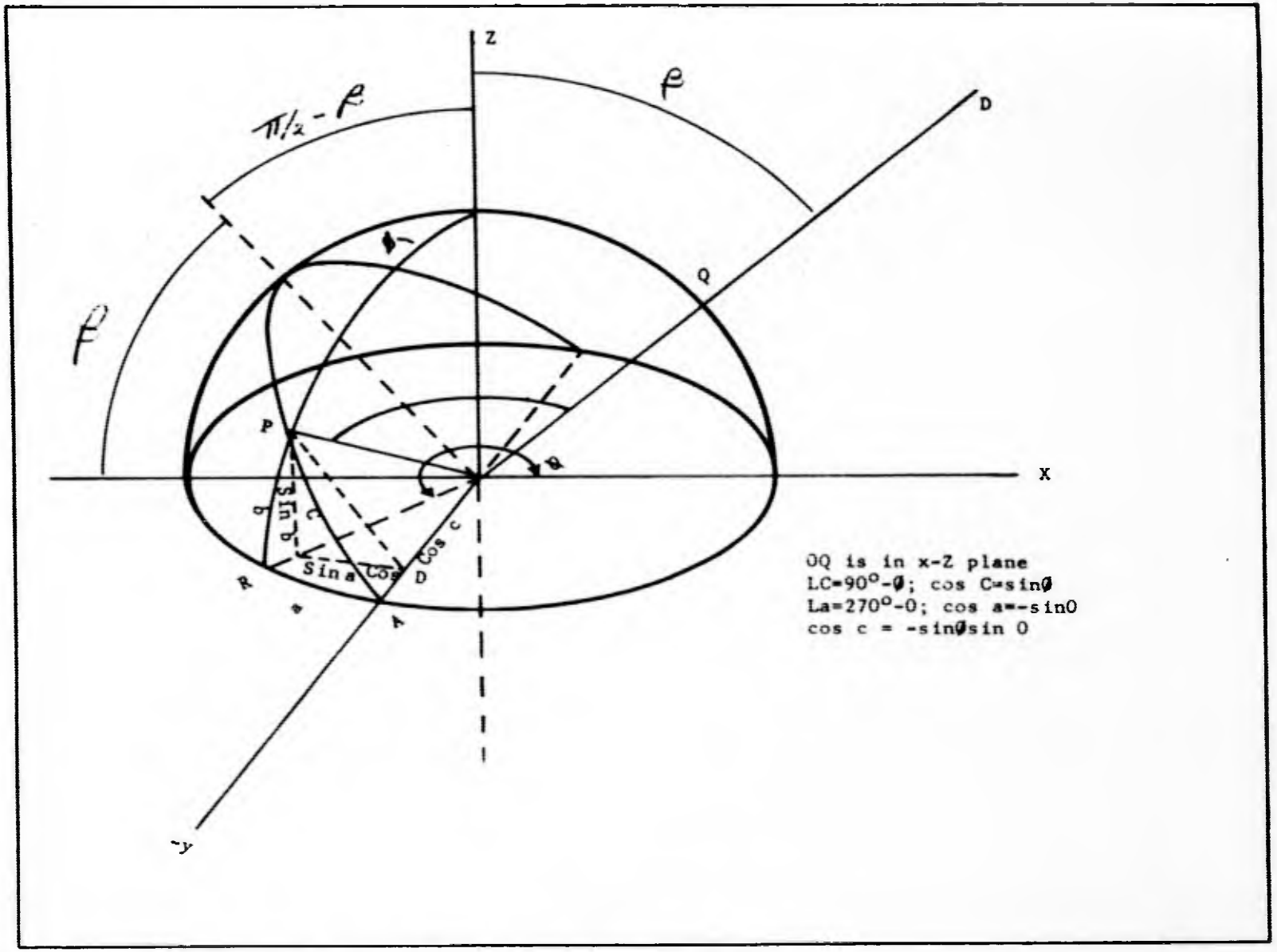

FIG. C-5 ANGULAR RELATIONSHIPS - GIBBONS PHASE

Then, considering the unit sphere as before, $\cos\alpha$ will be given by

$$\cos\alpha = xx' + yy' + zz' =$$

$$\sin\phi \cos\theta \sin\beta + \cos\phi \sin\beta \qquad \text{(C-14)}$$

and (C-9) can be rewritten as

$$E_D = \frac{JR^2}{d^2} \left(\sin\beta \iint \sin^2\phi \cos\phi \cos\theta \, d\phi \, d\theta + \cos\beta \iint \cos^2\phi \sin\phi \, d\phi \, d\theta\right) \qquad \text{(C-15)}$$

although it must be noted that the limits of integration will not be the same as for (C-9).

To establish a relationship between the value of ϕ, at the limit of visibility from D, and the angles β and θ refer to the figure and note that again using the unit sphere

$$\cos c = \text{projection of OP on OY} = \cos b \cos a$$

$$b = 90^\circ - \phi \text{ so } \cos b = \sin\phi$$

$$a = 270^\circ - \theta \text{ so } \cos a = \sin\theta$$

from which, since $\cos c = \cos b \cos a$

$$\cos c = \sin\phi \sin\theta$$

From the law of sines (referring to the triangle)

$$\frac{\sin b}{\sin\beta} = \frac{\sin c}{\sin \pi/2} \quad \text{or} \quad \sin b = \sin\beta \sin c$$

If we now start with the relations:

$$\cos c = -\sin\phi \sin\theta$$

$$\sin b = \cos\phi = \sin\beta \sin c = \sin\beta \left(1 - \cos^2 c\right)^{1/2}$$

$$= \sin\beta \left(1 - \sin^2\phi \sin^2\theta\right)^{1/2}$$

Then squaring, we get

$$\cos^2 \dot{\phi} = 1 - \sin^2 \dot{\phi} = \sin^2 \beta \, (1 - \sin^2 \dot{\phi} \sin^2 \theta)$$

$$= \sin^2 \beta - \sin^2 \beta \sin^2 \theta \sin^2 \dot{\phi}$$

so

$$\sin^2 \dot{\phi} \, (1 - \sin^2 \beta \sin^2 \theta) = 1 - \sin^2 \beta = \cos^2 \beta$$

from which

$$\sin \dot{\phi} = \frac{\pm \cos \beta}{(1 - \sin^2 \beta \sin^2 \theta)^{1/2}} \qquad \text{(C-16)}$$

From this we can obtain a relation for $\cos \dot{\phi}$;

$$\cos^2 \dot{\phi} = 1 - \frac{\cos^2 \beta}{1 - \sin^2 \beta \sin^2 \theta} = \frac{1 - \sin^2 \beta \sin^2 \theta - \cos^2 \beta}{1 - \sin^2 \beta \sin^2 \theta}$$

$$= \frac{1 - \sin^2 \beta \sin^2 \theta - (1 - \sin^2 \beta)}{1 - \sin^2 \beta \sin^2 \theta}$$

$$= \frac{1 - \sin^2 \beta \sin^2 \theta - 1 + \sin^2 \beta}{1 - \sin^2 \beta \sin^2 \theta}$$

$$= \frac{\sin^2 \beta \, (1 - \sin^2 \theta)}{1 - \sin^2 \beta \sin^2 \theta} = \frac{\sin^2 \beta \cos^2 \theta}{1 - \sin^2 \beta \sin^2 \theta}$$

Therefore

$$\cos \dot{\phi} = \pm \frac{\sin \beta \cos \theta}{(1 - \sin^2 \beta \sin^2 \theta)^{1/2}} \qquad \text{(C-17)}$$

The choice of sign for these quantities when used as the limits of integration must be determined. For the situation illustrated in Fig. C-4 (gibbous phase) ϕ and β will lie between ϕ and $\pi/2$, and θ between $\pi/2$ and $3\pi/2$. Then since both sin ϕ and cos ϕ must be positive the proper signs will be

$$\sin \phi = \frac{+ \cos \beta}{(1 - \sin^2 \beta \sin^2 \theta)^{1/2}}$$

$$\cos \phi = \frac{- \sin \beta \cos \theta}{(1 - \sin^2 \beta \sin^2 \theta)^{1/2}}$$

since cos θ will be negative.

We can then proceed to evaluate (C-15) as follows: The total energy received in a unit area at D from the gibbous reflection will be:

$$E_{DG} = \frac{JR^2}{\pi d^2} \int_{-\pi/2}^{\pi/2} \int_{0}^{\pi/2} \sin \beta \sin^2 \phi \cos \phi \cos \theta + \cos \beta \cos^2 \phi \sin \phi) \, d\phi \, d\phi$$

$$+ \int_{\pi/2}^{3\pi/2} \int_{0}^{\phi} \sin \beta \sin^2 \phi \cos \phi \cos \theta + \cos \beta \cos^2 \phi \sin \phi) \, d\theta \, d\phi \qquad \text{(C-18)}$$

For the sake of convenience let us evaluate the two integrals separately. The first integral is readily treated, the first integration leading to:

$$E_{DG}(I) = \frac{JR^2}{\pi d^2}\left[\sin\beta \int_{-\pi/2}^{\pi/2} \cos\theta\, d\theta \left(\frac{\sin^3\phi}{3}\right)\Bigg| + \cos\beta \int_{-\pi/2}^{\pi/2} d\theta \left(\frac{-\cos^3\phi}{3}\right)\Bigg|_0^{\pi/2}\right] \qquad (C\text{-}19)$$

$$= \frac{JR^2}{3\pi d^2}\left[\sin\beta \int_{-\pi/2}^{\pi/2} \cos\theta\, d\theta + \cos\beta \int_{-\pi/2}^{\pi/2} d\theta\right]$$

$$= \frac{JR^2}{3\pi d^2}\left[\sin\beta\,(\sin\theta\Big|_{-\pi/2}^{\pi/2} + \cos\beta\,(\theta)\Big|_{-\pi/2}^{\pi/2}\right]$$

$$= \frac{JR^2}{3\pi d^2}\left(2\sin\beta + \pi\cos\beta\right) \qquad (C\text{-}20)$$

In the first step in integrating the second integral we set the limits for ϕ as given in (C-16) and (C-17).

$$E_{DG}(II) = \frac{JR^2}{3\pi d^2}\left[\sin\beta \int_{\pi/2}^{3\pi/2} \cos\theta\, d\theta \frac{\cos^3\beta}{(1-\sin^2\beta\,\sin^2\theta)^{3/2}} + \cos\beta \int_{\pi/2}^{3\pi/2} d\theta\right.$$

$$\left. + \frac{\sin^3\beta\,\cos^3\theta}{(1-\sin^2\beta\,\sin^2\theta)^{3/2}} + \cos\beta \int_{\pi/2}^{3\pi/2} d\theta\right] \qquad (C\text{-}21)$$

If we now let $u = \sin\beta \sin\theta$

$$du = \sin\beta \cos\theta \, d\theta$$

C-21 can be written as (the limits referring to θ)

$$E_{DG}(II) = -\frac{JR^2}{3\pi d^2}\left[\cos^3\beta \int_{\pi/2}^{3\pi/2} \frac{du}{(1-u^2)^{3/2}} + \cos\beta \sin^2\beta \int_{\pi/2}^{3\pi/2} \frac{du}{(1-u^2)^{3/2}}\right.$$

$$\left. - \cos\beta \int_{\pi/2}^{3\pi/2} \frac{u^2 du}{(1-u^2)^{3/2}} + \cos\beta\,(\theta) \Big|_{\pi/2}^{3\pi/2}\right] \qquad \text{(C-22)}$$

from which

$$E_{DG}(II) = \frac{JR^2}{3\pi d^2}\left[(\cos^3\beta + \cos\beta \sin^2\beta - \cos\beta) \frac{\sin\beta \sin\theta}{(1-\sin^2\beta \sin^2\theta)^{1/2}} \Big|_{\pi/2}^{3\pi/2}\right.$$

$$\left. + \cos\beta \sin^{-1}(\sin\beta \sin\theta \Big|_{\pi/2}^{3\pi/2} + \pi \cos\beta\right]$$

$$= \frac{JR^2}{3\pi d^2}\left[-2\beta \cos\beta + \pi \cos\beta\right] \qquad \text{(C-23)}$$

Since $\cos^3\beta + \cos\beta \sin^3\beta - \cos\beta$

$= \cos^3\beta + \cos\beta(1-\cos^2\beta) - \cos\beta = 0$

Then the light received at the point D from the gibbous reflector is the sum of D17 and D19.

$$E_{DG} = \frac{2JR^2}{3\pi d^2} \left(\pi \cos\beta - \beta \cos\beta + \sin\beta \right) \qquad (C\text{-}24)$$

Crescent Phase

Referring to Fig. (C-5), the limits for ϕ can be established again for the crescent phase in the same manner as for the gibbous reflector. The terms for $\sin\phi$ and $\cos\phi$ are the same as given in (C-16) and (C-17). For the crescent phase, β will lie between $\pi/2$ and π, ϕ between 0 and $\pi/2$ and in the quadrant visible from D θ varies from $-\pi/2$ to $+\pi/2$. Since again both $\sin\phi$ and $\cos\phi$ must be positive we must now use

$$\sin\phi = \frac{-\cos\beta}{(1-\sin^2\beta \sin^2\theta)^{1/2}} \qquad (C\text{-}25)$$

and

$$\cos\phi = \frac{+\sin\beta \cos\theta}{(1-\sin^2\beta \sin^2\theta)^{1/2}} \qquad (C\text{-}26)$$

as $\cos\beta$ will be negative, and $\sin\beta$ and $\cos\theta$ will be positive throughout the range considered. For the crescent phase we obtain the value for light received at D by subtracting the value of the integral of C-15 over the region of the visible illuminated quadrant beyond the horizon from the value of the integral over the whole quadrant. Then

$$E_{DC} = \frac{JR^2}{d^2}\left[\int_{-\pi/2}^{\pi/2}\int_{o}^{\pi} \sin\beta \sin^2\phi \cos\phi \cos\theta + \cos\beta \cos^2\phi \sin\phi)\, d\theta\, d\phi\right.$$

$$\left.\int_{-\pi/2}^{\pi/2}\int_{\phi}^{0} \sin\beta \sin^2\phi \cos\phi \cos\theta + \cos\beta \cos^2\phi \sin\phi)\, d\theta\, d\phi\right] \quad (C\text{-}27)$$

The first integral was evaluated above (C-20)

The second integral becomes:

$$E_{DC(II)} = \frac{JR^2}{\pi d^2}\int_{-\pi/2}^{\pi/2} \sin\beta \cos\theta \left(\frac{\sin^3\theta}{3}\right)\Bigg|_{\phi}^{0} + \cos\beta \left(\frac{-\cos^3\phi}{3}\right)\Bigg|_{\phi}^{0} d\theta$$

$$= \frac{JR^2}{3\pi d^2}\int_{-\pi/2}^{\pi/2}\left[+\frac{\sin\beta \cos\theta \cos^3\beta}{(1 - \sin^2\beta \sin^2\theta^{3/2}} + \frac{\cos\beta \sin^3\beta \cos^3\theta}{(1 - \sin^2\beta \sin^2\theta)3/2} - \cos\beta\, d\theta\right.$$

$$\left.= \frac{JR^2}{3\pi d^2}\int_{-\pi/2}^{\pi/2} + \frac{\cos^3\beta\, du}{(1 - u^2)^{3/2}} + \frac{\cos\beta \sin^2\beta\, du}{(1 - u^2)^{3/2}} - \frac{\cos\beta\, u^2\, du}{(1 - u^2)^{3/2}} - \cos\beta\, d\theta\right.$$

and again the limits refer to θ and not to u.

Then

$$E_{DC}(II) = \frac{JR^2}{3\pi d^2}\left[\left(+\cos^3\beta + \cos\beta \sin^2\beta - \cos\beta\right)\frac{\sin\beta \sin\theta}{(1 - \sin^2\beta \sin^2\theta)^{3/2}}\Bigg|_{-\pi/2}^{\pi/2} + \cos\beta \sin^{-1}\left(\sin\beta \sin\theta\Big|_{-\pi/2}^{\pi/2} - \cos\beta\,(\theta)\Big|_{-\pi/2}^{\pi/2}\right)\right]$$

$$= \frac{JR^2}{3\pi d^2}\left(2\beta\cos\beta - \pi\cos\beta\right) \qquad \text{(C-28)}$$

The value for the crescent reflector is then the difference between C-20 and C-28

$$E_{DC} = \frac{JR^2}{3\pi d^2}\left(2\sin\beta + \pi\cos\beta - 2\beta\cos\beta + \pi\cos\beta\right)$$

$$= \frac{2JR^2}{3\pi d^2}\left(\pi\cos\beta - \beta\cos\beta + \sin\beta\right) \qquad \text{(C-29)}$$

which is the same as for the gibbous phase. This relation holds for all phases as the full and quadrature cases are special values of the crescent and gibbous.

APPENDIX D

THE MAGNETIC FIELD OF THE EARTH, THE SUN AND THE MOON

D.1 GEOMAGNETIC FIELD

Extrapolation of the known facts concerning the earth's field probably should provide the main basis for a discussion of fields exterior to the earth. a first approximation the magnetic field of the earth may be considered to originate in uniform magnetization of the whole volume or from a dipole with a strength of 8.1×10^{25} gauss cm^3 located at the center. The axis of the field is inclined at an angle of 11.4^{o} to the axis of rotation and the vertical magnetic intensity at the earth's surface varies from about 0.3 gauss at the equator to about 0.6 at the geomagnetic pole[1].

Superimposed on the steady field are transient components amounting to not more than a few percent of the total intensity which may be separated from the main field by the method of spherical harmonic analysis[2]. This part of the field appears to be due to current systems in the upper atmosphere or even at appreciable distances from the earth.

Except for the small external part, the field seems to be of internal origin, exhibiting little correlation with geographic structure. A second outstanding feature is the slow change with a period of the order of hundreds of years (the secular variation)[3]. Local anomalies of

of considerable extent are not uncommon. The largest, at Kursk, USSR results in a field several times greater than the normal value. Geometrically, it is in the form of strips roughly 250 km long. Anomalies generally are believed to consist of deposits of ferromagnetic material, probably magnetite.. Other large ferruginous deposits are known which produce negligible magnetic affects. These latter are evidently sedimentary and have been laid down in such a way that the ferromagnetic substances are more or less aligned in the field of the earth. Generally speaking, the local anomalies are presumed to be due to thermal remanence or induction in the earth's field[4].

In order to explain the observed phenomena, theories have been proposed based on ferromagnetism, electrostatic and dynamic principles. However well they may explain the main field, they shed little light on the matter of a probable origin in the core or of the secular variation. The theory of Elsasser[5], [6] and Bullard [3] seems to show that magneto-hydrodynamic motions in a fluid, conducting core would under certain conditions, generate and sustain a magnetic field. This latter theory does not present a real explanation of the secular variation nor is it clear to what the cause of convection in the core may be attributed. It seems however to have gained the widest acceptance[7].

The field at a distance from the earth should be nearly the dipolar value and be given by

$$H = H_o \left(\frac{a}{r}\right)^3$$

where H_o is the field at the surface

r the radial distance

and a the radius of the earth.

In practice, exact calculations require more extensive computations. The quiet field has been measured to altitudes of 100-200 km. Heppner [8] et al found that up to 160 km the difference between measured and expected fields could be explained by local anomalies. The accuracy of the measurements was $\pm$ 5 γ in the above experiment.

In the last few years, more and more information has been obtained concerning the external components of the field. The current systems responsible for the observed effects cannot be defined uniquely by measurements at the earth's surface and therefore rocket or satellite measurements are necessary. Maple[9] et al and Singer[10] found a negative discontinuity in the field strength at 105 km of about 1%. This result appears to confirm the existence of an equatorial current sheet or "electrojet" flowing in an easterly direction. Cahill[11] has found, in a series of ROCKOON launchings, that the electrojet consists of two or more current layers and to be rather restricted in spacial extent.

Chapman[12] has made estimates of the expected fields due to

certain of these ionized layers in the upper atmosphere. Passage through an auroral arc for example may cause a field change of $\pm$ 0.27 gauss; i.e., from about 0.33 to 0.87 gauss. Other current systems may result in variations of the order of 100 γ. Measurements of this type will require instrumental accuracies of the order of $\pm$ 10 γ or one part in 10^4 at a maximum field intensity of about 0.5 gauss. Heppner[13] has made similar estimates for satellite altitudes of 1400 km. The expected field changes are of the order of 10 γ requiring an accuracy of perhaps one part in 10^5. All of the above figures neglect the effect of magnetic induction in the earth. However, this correction is probably small but should decrease the above values.

D.2 THE MAGNETIC FIELD OF THE SUN

From the Zeeman effect which is observed in the solar spectrum, the presence of magnetic fields on the sun has been known for many years and magnetic energy seems to play an important part in sunspot phenomena. The most recent measurements[14] indicate a general solar field of about 1 gauss and of opposite polarity to that of the earth. This field intensity is more than an order of magnitude less than previously reported[15].

It seems quite likely that the solar field will deviate considerably from the dipolar configuration due to outward streaming of ionized gases. The lines of force may be stretched out to produce an essentially radial field[16]. At the earth's orbit a solar field of 1 gauss could result in a field as large as 10 γ on this basis, compared with the dipole value of

0.001 γ. Alfvén[17] has raised objections to the use of Zeeman effect measurements and derives somewhat higher values for the solar field. His model also postulates a distortion of the field which results in its extension to distances of perhaps four times the orbital radius of the earth. At the earth, the intensities for the assumed configurations vary from 7 to 70 γ, and are comparable with those of the disturbed field.

Stellar fields of several thousand gauss have been measured but produce negligible effects at the earth because of the enormous distances. As in the case of the earth, no entirely acceptable theory seems to have been proposed. It may be that the fields are remnants of fields associated with the formation of the star or, more likely, have a magnetohydrodynamic origin in the turbulent gases of the interior.

In this connection, the so-called "fundamental" theories perhaps should be mentioned. These theories state that magnetism is a property of massive rotating bodies and give the magnetic dipole moment M as

$$M = \beta \frac{G^{1/2} U}{C}$$

where $\beta \approx 1$

G is the gravitational constant,

C the velocity of light

and U the angular momentum.

Blackett[18] has pointed out that the theory is in agreement with measurement for the star 78 Virginis, the earth and for the sun (if the older value of

50 gauss is used). Unfortunately, it has not been confirmed either by careful laboratory investigation or by measurement of the earth's field[19]. While serious difficulties are encountered in connection with this theory, it is mainly of interest because it does in principle, permit generalized application to any astronomical body.

D.3 THE MAGNETIC FIELD OF THE MOON

Since the moon appears to have no liquid core[20], a self-excited dynamo theory of the magnetic field cannot be applied. Furthermore, its low density (3.33) indicates that no appreciable fraction can be iron, making ferromagnetism unlikely as a source. Because these theories seem to be the most successful in explaining the fields of the earth and the sun, the existence of a lunar field of any appreciable intensity is doubtful.

Even with a field comparable to that of the earth, direct measurement from terrestrial locations would not be possible because of the extremely low intensity ($\sim 10^{-6}$ gauss). Recently, however, Kopal[21] reports measurements of Kozyrev as evidence for no appreciable magnetic field on the moon. His interpretation is based upon the disappearance at sunset of luminescence which is presumed to be due to charge particles from the sun.

Vestine[22] has discussed in some detail the various possibilities for the existence of a lunar field and has provided estimates of the field strengths which can be expected. He shows that if the moon were originally part of the earth as has been hypothesized, and has a composition similar to that of terrestrial rocks, a field as large as 40 γ might result. This field would be that due to thermoremanent magnetization in the field of

the earth. It is possible that the same conditions would obtain if the moon and the earth merely were much closer at one time[20]

The same author shows that the magnetic energy trapped within a cloud of gaseous material condensing to form the moon would not result in a field since even if the lunar conductivity were higher than that of terrestrial rock, the time of decay would be small. He states also that lack of information as to the magnetic properties of meteorites prevents a conclusion based on Urey's[23] theory of lunar accretion from smaller meteoritic masses. However, it seems certain that in this case the moon would have been at some time above the Curie point, and probably in any case could have only a remanent field. Vestine also suggests the possibility that a remanent magnetization may have resulted from toroidal fields produced by thermoelectric action in a molten moon He estimates a possible field as great as 100 δ for this case.

Perhaps as postulated by Urey[23] the iron on the moon is distributed throughout in masses the size of iron meteorites On the surface therefore, there may be local concentrations of iron He estimates that an iron meteor as large as 100 miles in diameter fell in the Mare Imbrium[24]. Such a collision would form a ferromagnetic area possibly 850 km in diameter (somewhat less than the diameter of the mare), and several times the extent of the largest known terrestrial anomaly. Considering it to be a dipole with a surface field intensity

of the same order as the lunar field it would be detectible as approximately 10% change in field strength at a distance of 1000 km.

D.4 INSTRUMENTATION

Methods which have been used for making magnetic field measurements may be divided into three general classes: (1) astatic, induction, and spin system devices. Blackett has discussed the limitations of the first two methods and has been able to construct instruments which have characteristics near the theoretical limits.

An astatic magnetometer consists of two equal and oppositely directed bar magnets attached to a vertical rod and suspended by a fiber. The vertical gradient of horizontal field produces a deflection proportional to the field difference between the top and bottom magnets. It is clear that while sensitivities as high as 10^{-10} gauss have been realized, such a system at least in its usual form is not suited for use in a lunar vehicle.

Blackett[19] has also provided an analysis of the rotating coil magnetometer in which it is shown that extremely high sensitivities are in principle possible. With small coils and speed of rotation of the order of 10 revolutions per second the limit may be of the order of 10^{-7} gauss. With the use of high permeability cores the sensitivity should be greater than this figure but probably the signal to noise ratio will be limited to

about the above order of magnitude by the characteristics of the amplifier. Since the induced voltage is proportional to the sine of the angle which the axis of the coil makes with respect to the field, more than one instrument will be required to completely determine the field intensity.

A magnetometer of the rotating coil type was used in the Farside experiment. This instrument consists of a rotating coil of wire surrounding a high permeability core, and is in principle a small dynamo. The voltage induced in the coil is proportional to the speed of rotation and the geometry of the coil. The voltage E_G developed across the coil is given by $E_G = \phi\, 2\pi f\, H_o/10^8$, where ϕ is a function of the geometry and $2\pi f$ is the angular velocity. In sensitive instruments the voltage may be amplified and in this case the limiting sensitivity is determined by the thermal noise generated in the coil and the noise figure of the amplifier. The thermal noise voltage $E_T^2 = 4KTR\Delta f$. For $R = 2 \times 10^4$ and $\Delta f = 100$, E_T equals about 0.1 microvolt.

The magnetometer used in the Farside experiment[27] employed a coil of fine wire containing a Mu-metal core connected to a transistor amplifier. The unit weighed less than a pound and was sensitive to 10^{-5} gauss. The voltage developed across the coil by the rotation of the vehicle (10 cycles/sec) was amplified, rectified and applied to a trigger circuit to give an output pulse rate proportional

to field strength.

A sensitive magnetometer which has been used in rocket exploration is the so-called flux-gate magnetometer. This device consists of two small Mu-metal core coils within an alternating field produced by a concentric driving solenoid. The induced fields in the smaller coils are balanced in a bridge circuit Due to the non-linearity of the magnetization characteristic of the Mu-metal a steady field will give rise to harmonics of the driving frequency in a pick-up coil. These harmonic voltages are proportional to the field intensity and may be filtered and amplified. Such an instrument was used by Maple[9] et al to measure the field discontinuity due to the equatorial electrojet current. Their instrument was sensitive in the region of 10^{-4} gauss. The minimum detectible field according to Blackett is of the order of 10^{-7} gauss. The flux-gate instrument requires rather exact adjustment and calibration and local fields must be carefully balanced out.

In the above instruments the field strength indication is a function of the position of the instrument in the field. Therefore a single instrument will determine the field only with respect to a particular orientation of the rocket. To measure the vector magnitude of the field, three instruments are necessary.

The limitations of induction instruments have led to the development of devices in which the field strength indication is orientation-independent. These magnetometers take advantage of the fact that nuclear and atomic spin moments may be aligned by external means. In the transition from oriented to non-oriented states, electromagnetic radiation which is a function of the magnetic field intensity is emitted.

One such device is the proton precession magnetometer[26]. This instrument has been employed in rocket measurements and its constructional simplicity as well as high accuracy appear to be of advantage. This magnetometer consists of a container of proton-rich substance (water or kerosene for example) within a solenoidal coil. A current flowing in the coil produces a strong field which causes the proton spin moments to become oriented. This field is then turned off and the spins precess about the earth's field. In doing so they resonate at the Larmor frequency, $f = gH$ where g is the gyromagnetic ratio. For protons in the field of the earth, this frequency lies in the audio range and is about 2000 cycles per second. A voltage of this frequency is induced in the coil and in practice an electronic means for switching the coil from the polarizing current to an amplifying circuit is provided. The accuracy of the instrument has been given as approximately $\pm$ 10 γ. The lower limit of field strength measurement is probably near 100 gamma. The signal amplitude is pro-

portional to $\sin^2\phi$, where ϕ is the angle between the axis of the sensing coil and the earth's field. It therefore requires the use of two sensing coils placed at right angles to one another in order to obtain a signal at all times during the rocket flight.

Varian Associates[27] have under development for the Naval Research Laboratory another magnetometer which uses the principle of spin orientation. This instrument uses an optical method for producing the necessary population differences. Although the important principles have been demonstrated, it is understood that no usable instruments are presently available, at least for rocket exploration purposes. However it appears that the basic ideas are quite promising and that sensitivities several orders of magnitude greater than for proton precession magnetometers are possible.

In this new system a beam of circularly polarized sodium resonance radiation is used to "optically pump" atoms of an alkali vapor in argon from the -1/2 magnetic sublevel of the ground state to the first excited state. Because of collisions with the "buffer gas", argon, the excited atoms return to both sublevels without preference as to which level, resulting eventually in all of the atoms being in the +1/2 sublevel and a net magnetic moment along the beam direction. The intensity of the light transmitted through the vapor can be monitored by means of a photocell. Any change in the

relative populations, as for example by radio frequency resonance between the magnetic sublevels, will modulate the intensity of light received by the photocell.

In the system described[27], a second polarized light source and photocell are placed at right angles to the first beam so that the two intersect. In the same region a weak r-f magnetic field is also applied. If there is a static magnetic field present and if the frequency of the r-f field corresponds to the Larmor frequency, then the intensity of the light beam is modulated at the Larmor frequency. By sweeping the r-f frequency the resulting resonance lines have been found to be extremely sharp, with a width of perhaps 10^{-5} gauss or 10^{-7} gauss in the most favorable instance. For sodium the resonance frequency is about 0.7 Mc/gauss.

In all cases the actual level structure is more complicated than outlined above and makes an exact description difficult For potassium the level separations result in a resonance frequency of 1 MC per gauss. Further refinement of the basic device has been suggested and includes use of a single light source and elimination of the r-f generator. This is accomplished by connecting an amplifier between the photocell and light source.

REFERENCES

1. Chapman and Bartels, "Geomagnetism", Vol. I and II, Oxford University Press, 1940.

2. H. Vestine, Laporte, Lange and Scott, "The Geomagnetic Field, Its Description and Analysis", Carnegie Institute of Washington, Pub. 580, (1947).

3. E. Bullard, "The Interior of the Earth" in "The Earth as a Planet" Ed. by G. P Kuiper, Chicago (1954).

4. S. K. Runcorn, "The Magnetism of the Earth's Body" in Handbuch der Physik, Springer-Verlag, Berlin, 1956.

5. W. M. Elsasser, Rev. Mod. Phys., 22, No. 1, (1950).

6. W. M. Elsasser, Rev. Mod. Phys., 28, p. 135, (1956).

7. T. G. Cowling, "Magnetohydrodynamics", Interscience, 1957.

8. Heppner, Stolarik and Meredith, Journal Geophys. Res. 63, p. 277 (1958).

9. Maple, Bowen and Singer, Jour. Geophys. Res. 55, 115, (1950).

10. Singer, Maple and Bowen, Jour. Geophys. Res. 56, 265, (1951).

11. L. J. Cahill, Jour. Geophys. Res. 64, 489, (1959).

12. S. Chapman, "Rocket Exploration of the Upper Atmosphere" Ed. by R. L. F. Boyd and M. J. Seaton, Pergamon, London (1954).

13. J. P. Heppner, in book "Scientific Uses of Earth Satellites", by J. A. Van Allen, University Mich., Ann Arbor (1956).

14. H. W. Babcock and H. D. Babcock, A. J. 121, 349 (1955).

15. H. Alfvén, "Cosmical Electrodynamics", Oxford, 1950.

16. E. N. Parker, Phys. Rev. 110, 6, 1445 (1958).

17. H. Alfvén, Tellus 8, 1 (1956): See also H. W. Babcock, Nature 533 (1956).

18. P.M.S. Blackett, Nature, 159, 658 (1947).

19. P.M.S. Blackett, Phil. Trans. Roy. Soc. London, Ser. A, 245, 213 (1952).

20. H. Jeffreys, "Dynamics of the Earth-Moon System" in "The Earth as a Planet", Ed. by G. P. Kuiper, University of Chicago, (1954).

21. Z. Kopal, "Prospecting the Moon Without Rockets", The New Scientist, 1052, (1958).

22. E. H. Vestine, Rand Corp. Research Memo RM-1933, ASTIA, AD133008, 9 July (1957).

23. H. C. Urey, "The Planets, Their Origin and Development", Yale University, (1952).

24. H. C. Urey, Proc. Lunar and Planetary Exploration Colloquim 1, 1 (1958).

25. Farside Report, Aeronutronic Publication No. C-125

26. A. L. Bloom and L. E. Johnson, Elec. Ind. & Tele-Tech, Aug. (1957).

27. Varian Asso. Tech. Proposal 592 "Research on Alkali Vapor Resonance" Mar. 7, 1957.

B Series

1-75 AFSWC (SWOI), Kirtland AFB, NMex

UNCLASSIFIED